DISSERTATION

CONTRIBUTION OF AGRICULTURAL FIRE AND WILDFIRE SMOKE $PM_{2.5}$ CONCENTRATION IN RURAL REGIONS OF THE US AND THE ASSOCIATED HEALTH IMPACTS

Submitted by

Olivia Sablan

Department of Atmospheric Science

In partial fulfillment of the requirements

For the Degree of Doctor of Philosophy

Colorado State University

Fort Collins, Colorado

Fall 2025

Doctoral Committee:

Advisor: Jeffrey R. Pierce
Co-Advisor: Emily V. Fischer

Bonne Ford
Sheryl Magzamen
Jeffrey L. Collett Jr.

ABSTRACT

CONTRIBUTION OF AGRICULTURAL FIRE AND WILDFIRE SMOKE IN US RURAL REGIONS $PM_{2.5}$ CONCENTRATION AND ASSOCIATED HEALTH IMPACTS

Exposure to landscape fire smoke is a growing public health concern. Fine particulate matter ($PM_{2.5}$) from these fires has been associated with various adverse health outcomes, yet many rural and underserved regions lack adequate monitoring to support meaningful epidemiologic analysis. This dissertation quantifies the smoke exposure in New Mexico and southern Florida. We also conduct an epidemiological analysis with health data in New Mexico to determine the sensitivity of different inputs.

In Chapter 2, we used public low-cost PurpleAir sensors, regulatory monitors, and 29 PurpleAir sensors deployed for this study to quantify $PM_{2.5}$ from agricultural fires. We found satellite imagery is of limited use for detecting smoke from agricultural fires in Florida due to the cloud cover, overnight smoke, and the fires being small and short-lived. For these reasons, surface measurements are critical for capturing increases in $PM_{2.5}$ from smoke, and we used multiple smoke designation methods. During the study period, median 24-hour $PM_{2.5}$ concentrations increased on smoke-impacted days compared to unimpacted days, with smoke observed. We contrasted the region near the Everglades Agricultural Area (EAA) with large populations of low-income and minoritized groups to the more affluent coastal region. The inland region experienced more smoke-impacted monitor days than the Florida east coast region, and there was a higher study-average smoke $PM_{2.5}$ concentration in the inland area. These findings highlight the need to increase air quality monitoring near the EAA.

In Chapter 3, we use Emergency Department (ED) visits in an epidemiological analysis to better understand the uses of four smoke exposure estimates in NM during summer 2022: 1) $PM_{2.5}$ from the EPA regulatory-grade monitors, 2) $PM_{2.5}$ from both the US Environmental Protection Agency (EPA) regulatory-grade monitors and low-cost PurpleAir observations, 3) modeled 24-hour average wildfire smoke $PM_{2.5}$ from the Community Multiscale Air Quality Modeling System (CMAQ), and 4) CMAQ daily 1-hour maximum wildfire smoke. We found significant associations with all-respiratory related ED visits, including pneumonia and heart failure. However, the magnitude and significance of associations varied across the four smoke-exposure products. We found modeled CMAQ output was less suitable for this epidemiological study, while the smoke exposure estimate that leveraged both regulatory and PurpleAir measurements provided more precise exposure estimates, highlighting the importance of low-cost sensors in rural regions. Our findings emphasize the need to critically assess the inputs used in epidemiological studies for accurate and meaningful results.

In Chapter 4, we compared the use of ED visits to Syndromic Surveillance (SS) reports from 2019-2022 in New Mexico. Previous epidemiological studies used hospitalizations and Emergency Department (ED) visits to understand the impact of smoke exposure on human health. However, there is typically a substantial delay for these health datasets to be received by state health agencies. Syndromic Surveillance (SS) is a real-time, voluntary reporting system chief complaints and/or discharge diagnoses from the ED, which has been used in fewer epidemiological studies of wildfire smoke exposure. We conducted a time-stratified case crossover study to compare association between wildfire smoke exposure and ED visits versus SS from 2019-2022 in New Mexico. We found some consistency in our results for all respiratory-related, asthma, and all-cardiovascular related ED visits versus SS reports; however, there were meaningful differences in significance and magnitudes of several odds ratios in comparing the two types of outcomes. The “air quality related” SS data query may be useful for studying the impact of wildfire smoke exposure. We found significantly increased odds with this query in our study, with comparable results to all respiratory-related SS reports. Overall, we hypothesize that SS could be a valuable tool for allocating resources in New Mexico during an intense, local wildfire event. Future research work should be conducted to further our understanding of the use of SS in epidemiological studies of wildfire smoke exposure.

ACKNOWLEDGEMENTS

I could not have asked for a better advising team than Dr. Jeff Pierce and Dr. Emily Fischer. They have cultivated the scientist in me and pushed me to be the best possible version of myself. They inspire and excite me, and I am forever grateful for the opportunity to be mentored by them. Dr. Bonne Ford was instrumental in my success at CSU. She not only taught me how to use Python with her brilliant tutorials, but she taught me how to tell the story behind my science, to tailor my communication of scientific findings to each audience, and to be confident in myself as a woman in science. I cannot thank her enough. I want to thank Dr. Sheryl Magzamen for being an honorary advisor and guiding me through conducting a study in another field. I would also like to extend a thanks to Dr. Jeff Collett for serving as a member of my committee and always bringing knowledge and kindness to the table.

To my friends at CSU Atmospheric Science who have supported me and made my time here in Fort Collins unforgettable, Emily Lill, Ivy Glade, Tyler Barbero, En Li, Andrey Marsavin, Madison Shogrin, Milena Guajardo, the Pierce Group, the Fischer Group, and so many others, you mean so much to me! To my friends beyond atmospheric science, Lucy Guiberson, Anisa Guajardo, Cameron Freeman, Peter Kessinger, and more, thank you for everything.

Finally, thank you to my family. You have always stood by me and encouraged me to do hard things. Your phone calls, visits, postcards, and texts are appreciated more than you know. I am excited to be the first Dr. Sablan in our family.

The following acknowledgements are adapted from three individual articles presented in Chapters 2-4. The research in Chapters 2 was based upon work supported by the National

Aeronautics and Space Administration Health and Air Quality Applied Sciences Team Grants (NASA HAQAST) 80NSSC21K0429 and 80NSSC21K0514. Research reported in this publication was partially supported by the National Institute on Aging of the National Institutes of Health under award number R01AG083925. Additionally, for Chapter 2, I would like to thank the community members who hosted PurpleAir sensors and made this work possible. The research in Chapters 3 and 4 was supported by the National Science Foundation GeoHealth INTERN Grant ICER-211941 and NASA HAQAST Grant 80NSSC21K0429. The work in Chapters 3 and 4 could not have been possible without the New Mexico Department of Health (NMDOH). Dr. Chelsea Eastman Langer and Stephanie Moraga-McHaley at the NMDOH were amazing hosts for my 3-month stay in New Mexico. Their support, enthusiasm, and commitment were essential to the success of this project. Another thanks to Colin Hawkinson for data support and so much more during and after my stay in New Mexico.

DEDICATION

In memory of Dr. Eric Sullivan (1975-2023), who taught me how to code and so much more.

TABLE OF CONTENTS

CHAPTER 1

INTRODUCTION[1]

This introduction serves as brief background on the topic matters discussed at length in Chapters 2 - 4. First, we give an overview of agricultural fires and wildfires in the US, as the following chapters investigate these fire types in two regions, New Mexico and southern Florida. We then provide a short background on our motivation for studying landscape fires in each region. We also discuss the epidemiological analysis used to determine health outcomes associated with wildfires smoke exposure. Lastly, we outline the following chapters and reference the peer-reviewed journal articles which the chapters were adapted from.

1.1 Overview of the impacts of agricultural fires and wildfires

Fires are a major source of primary fine particulate matter ($PM_{2.5}$) emissions in the United States. While landscape fire smoke is a global concern, this dissertation focuses on the United States, where large wildfires in the west are increasing rapidly in frequency and intensity (Abatzoglou et al., 2021; Dennison et al., 2014), and agricultural burning remains a relevant source of emissions despite alternative practices (McCarty, 2011). In 2017, wildfires and agricultural fires together accounted for approximately 30% of all primary $PM_{2.5}$ emissions nationwide (US EPA, 2017). As the climate continues to warm, the frequency, size, and intensity of wildfires are projected to increase, further increasing $PM_{2.5}$ levels and impacting human health (Buchholz et al., 2022; Burke et al., 2023; Childs et al., 2022; Ford et al., 2018; Volckens, 2024). At the same time, agricultural burning continues to be practiced across parts of the US, including

[1] Adapted from the introductions of the three journal articles presented in Chapters 2-4 of this dissertation. See individual chapters for full citations (Sablan et al., 2025, *GeoHealth*; Sablan et al., under review, *GeoHealth*; Sablan et al., in prep).

the Southeast (e.g., Florida, Georgia), Southern Plains (e.g., Texas, Louisiana), and Great Plains (e.g., Kansas, Minnesota) (Baucum & Rice, 2009; Boopathy et al., 2002; Brey et al., 2018; Pinakana et al., 2023; Sablan et al., 2024). Thus, agricultural fires further contribute to primary $PM_{2.5}$ emissions along with wildfires.

Rural populations are exposed to agricultural fire smoke and wildfire smoke, but most studies focus on populated, urban regions (e.g., Gupta et al., 2018; Liang et al., 2021; Wallace et al., 2022). $PM_{2.5}$ from wildfire smoke has been linked to a suite of associated health outcomes in more densely populated regions of states like California and Colorado (e.g., Abdo et al., 2019; Alman et al., 2016; Heft-Neal et al., 2023; Holstius et al., 2012; Magzamen et al., 2021). However, far fewer studies focus on rural smoke exposure, and rural populations may experience different vulnerabilities and health impacts than urban populations (Chakraborty et al., 2022; Jbaily et al., 2022). Agricultural burning often occurs in rural regions, and the impacts of agricultural fires on $PM_{2.5}$ concentrations and on human health are less studied (H. Nowell et al., 2022; Pennington et al., 2023; Stem et al., 2024). In order to investigate health impacts of agricultural smoke, the contribution of $PM_{2.5}$ from smoke must be quantified first. Smoke exposure in rural regions of the US remains less studied than more populated regions.

In this dissertation, we studied landscape fire smoke in two rural regions of the US: southern Florida and New Mexico. We studied smoke from agricultural-sugarcane burning in Florida and wildfire smoke in New Mexico. In Section 1.2, we will discuss the purpose of agricultural fires in southern Florida and the challenges quantifying smoke $PM_{2.5}$. We will then give an overview of the recent wildfire seasons in New Mexico in Section 1.3., followed by details on the epidemiological study we conducted and the data inputs that were tested in Section

1.4. We then present an outline of the chapters in this dissertation and the corresponding peer-reviewed manuscripts in Section 1.5.

1.2 Quantifying smoke from southern Florida sugarcane burning

In southern Florida, agricultural burning is primarily used in sugarcane harvesting to remove the unwanted outer leaves of the plant (Baucum & Rice, 2009). Florida is the largest producer of sugarcane in the U.S., with nearly half of the state's prescribed and agricultural burn authorizations being agricultural burns used to ease the sugarcane harvesting process (Florida Department of Agriculture and Consumer Services, 2024). The Everglades Agricultural Area (EAA) in southern Florida, where the majority of the sugarcane is grown, has higher percentages of people who identify as non-White and people living in poverty compared to the coastal regions of south Florida (US Census Bureau, 2023). Air pollution disproportionately affects low income and minoritized groups in the US (Chakraborty et al., 2022; Jbaily et al., 2022; Mohai et al., 2009). Therefore, it is important to investigate disparate impacts of smoke exposure in this region, which we will demonstrate in Chapter 2.

Quantifying agricultural fire smoke exposure remains a major challenge in southern Florida, where regulatory monitoring is sparse. There is only one regulatory $PM_{2.5}$ monitor near the EAA, despite thousands of agricultural burn authorizations issued annually (Florida Department of Agriculture and Consumer Services, 2024). Sugarcane burns are small, short-lived, and sometimes occur overnight making them hard to detect with sparse monitoring networks or satellite observations, which will be discussed further in Chapter 2. Recent studies have investigated sugarcane burning in the US (Nowell et al., 2022; Pennington et al., 2023; Stem et al., 2024), but quantification of smoke remains a challenge with the limited network of monitors. In Chapter 2, we deploy low-cost sensors in southern Florida to supplement regulatory monitors and better quantify agricultural fire smoke.

1.3 Wildfire smoke in New Mexico

New Mexico (NM) is impacted annually by both local wildfires and smoke transported from fires in other states (Brey et al., 2018). More recently, smoke from several large wildfires, including Arizona's Telegraph Fire and numerous California wildfires, was transported to New Mexico. This caused a state-wide increase in $PM_{2.5}$ concentrations, which is discussed more in Chapters 3 and 4. In 2022, NM experienced the state's largest wildfire, Calf Canyon/Hermit's Peak. This fire burned 1,382 km^2 in northern NM, becoming the largest wildfire in state history (Tunby et al., 2023). In the same wildfire season, the Black Fire burned 1,316 km^2 in the southwest (Hulburd, 2022). The 2022 wildfire season was anonymously intense, but in the future, NM is expected to continue to experience a longer, more intense, and more destructive wildfire season. Additionally, fires in other western states are also expected to increase in duration and frequency, further contributing to $PM_{2.5}$ concentrations in NM through long-range transport (Dennison et al., 2014; Ford et al., 2018).

In New Mexico, quantifying wildfire smoke $PM_{2.5}$ is challenging, as discussed at length in Chapter 3. The regulatory monitors are located in more populated areas (i.e., Albuquerque, Santa Fe, Las Cruces); however, wildfires usually occur in more remote areas, and the smoke may be transported across both types of area (Brey et al., 2018). Low-cost sensors, like the PurpleAir $PM_{2.5}$ sensors, fill in many monitoring gaps in NM. For example, the regulatory monitoring network was insufficient for capturing the smoke from the Calf Canyon/Hermit's Peak wildfire as we will show in Chapter 3, but the PurpleAir network provided measurements at locations much closer to the fire to allow for more accurate smoke exposure estimates. Despite leveraging regulatory and low-cost monitors, measuring smoke $PM_{2.5}$ in NM is difficult.

1.4 Sensitivity of data inputs to an epidemiological study in NM

The case-crossover study design has been widely used to evaluate the health effects of smoke exposure (Alman et al., 2016; Gan et al., 2017; Hahn et al., 2021; Magzamen et al., 2021; Stowell et al., 2019); however, the sensitivity of several data inputs has not been explored. In a case-crossover study, the patient is used as their own control; therefore, we compare the smoke $PM_{2.5}$ concentrations on the day of the patient's health event to the smoke $PM_{2.5}$ concentrations on days when the patient did not have a health event. This study design is valuable because it controls for individual-level confounders (e.g., age, sex, race). Selection of an appropriate referent period, or the time period which the exposure event is compared to, is an essential component of the study design framework (Janes et al., 2005b, 2005a). In Chapters 3 and 4, we investigated using different smoke exposure estimates, referent or comparison windows, and health datasets in studying the associated health outcomes with NM wildfire smoke, which has not been explored previously. Exploring these data input dependencies is important for identifying key uncertainties with assessing the impact of smoke on human health.

1.5 Dissertation chapters and goals

The goal of this dissertation is to quantify the contribution of smoke on $PM_{2.5}$ concentrations from agricultural burns and wildfires in two regions of the US: New Mexico and Florida. We also aim to gain insight into the dependencies of inputs to epidemiological studies in studying NM wildfire smoke exposure. Through this dissertation, we improve understanding of the health and environmental impacts of $PM_{2.5}$ from fires in the U.S. through two case studies in distinct regions.

Chapter 2, with Appendix A as supplementary material, is published as:

Sablan, O., Ford, B., Gargulinski, E., Henery, G., Nowell, H. K., Rosen, Z., Slater, K., Soja, A. J., Wiese, L. K., Williams, C. L., Magzamen S., Fischer, E. V., Pierce, J. R., (2025). Characterizing particulate matter impacts of smoke from 2022-2023 agricultural burning in south Florida. *GeoHealth*.

Chapter 3, with Appendix B as supplementary material, is currently in review as:

Sablan, O., Ford, B., Hawkinson, C., Hu, L., Langer, C. E., Maichak, C., Maji, K. J., Moraga-McHaley, S., Russell, T. G., Uejio, C. K., VanSickle, M., Fischer, E. V., Pierce, J. R., Magzamen, S., Health impacts of wildfire smoke exposure in New Mexico during 2022 and sensitivity to exposure estimate and referent period. *GeoHealth*.

Chapter 4, with Appendix C as supplementary material, is currently in preparation for submission:

Sablan, O., Ford, B., Hawkinson, C., Hu, L., Langer, C. E., Maichak, C., Maji, K. J., Moraga-McHaley, S., Russell, T. G., Uejio, C. K., VanSickle, M., Fischer, E. V., Pierce, J. R., Magzamen, S., Investigating smoke-related emergency department visits and syndromic surveillance reports in New Mexico 2019-2022.

Finally, Chapter 5 summarizes this work and looks ahead to future research directions.

CHAPTER 2

CHARACTERIZING PARTICULATE MATTER IMPACTS OF SMOKE FROM 2022-2023 AGRICULTURAL BURNING IN SOUTH FLORIDA[2]

2.1 INTRODUCTION

While wildfire smoke has been extensively studied, the impact of prescribed and agricultural smoke to air quality and human health remain less understood. Fine particulate matter ($PM_{2.5}$) is a major air pollutant regulated by the US Environmental Protection Agency (EPA) under the National Ambient Air Quality Standards due to its adverse effects on human health (US EPA, 2024b). A significant source of $PM_{2.5}$ in the US is smoke from landscape fires, including agricultural burns, wildfires, and prescribed fires, which collectively accounted for 55% of total primary $PM_{2.5}$ emissions nationally in 2020 and 57% in 2017 (US EPA, 2017, 2020). $PM_{2.5}$ from wildfire smoke has been extensively studied and linked to increased risks of cardiorespiratory-related emergency department visits (Alman et al., 2016; Gan et al., 2020; Hahn et al., 2021; Rappold et al., 2011) and hospitalizations (Gan et al., 2017; Magzamen et al., 2021; Stowell et al., 2019), adverse pregnancy outcomes (e.g., low birth weight) (Abdo et al., 2019; Holstius et al., 2012), and cognitive decline (B. Zhang et al., 2023). Research on the air quality impacts of agricultural and prescribed fires in the US has recently increased (Liu et al., 2016; Pennington et al., 2023; Sablan et al., 2024; Travis et al., 2023). Gaps in knowledge remain due to the challenges of monitoring these smaller, shorter-duration burns, which often occur in rural areas with sparse regulatory and low-cost monitoring networks.

---

[2] Adapted from Sablan, O., Ford, B., Gargulinski, E., Henery, G., Nowell, H. K., Rosen, Z., et al. (2025). Characterizing particulate matter impacts of smoke from 2022-2023 agricultural burning in south Florida. GeoHealth.

Florida is the leading sugarcane producer in the US, with nearly half of the state's prescribed and agricultural burn authorizations being agricultural burns used to ease the sugarcane harvesting process (Baucum & Rice, 2009). Sugarcane burning involves the controlled burning of fields to remove the outer foliage of the plant, allowing easier access to cut the sugarcane stalks. Although there are environmentally-friendly and health-conscious methods of harvesting sugarcane (e.g., mechanical sugarcane harvesting), the use of fire is a cost-effective and efficient method (Bordonal et al., 2018). Open Burned Authorizations must be obtained from the Florida Forest Service to burn sugarcane, and the authorizations show an average of about 50 acres burned per fire during 2020-2023. Fires are brief, typically lasting 15 to 20 minutes, but smoldering afterward can continue to produce smoke. The resulting smoke from sugarcane agricultural fires is an environmental and public health concern. Several recent studies have investigated sugarcane burning in the US (Nowell et al., 2022; Pinakana et al., 2023; Stem et al., 2024). By building on this foundational research, studies like ours aim to advance knowledge of sugarcane burning impacts on air quality.

In addition to exposure to smoke from agricultural sugarcane burning, southern Florida experiences smoke from prescribed fires, wildfires, and long-range transported smoke from other regions (Brey et al., 2018). Prescribed fires are conducted on publicly managed land (e.g., national preserves, national and state parks, wildlife management areas) as well as private land and often occur during the same period as agricultural fires. For example, during the 2022-2023 Florida sugarcane burning season, there were several wildfires that occurred in southern Florida, including the Mile 31 (National Centers for Environmental Information, n.d.-a), Cypress Camp Trail (National Centers for Environmental Information, n.d.-b), and Sandy wildfire (InciWeb, 2023). Additionally, long-range transported smoke from landscape fire activity in other regions (e.g., Mexico, Cuba) can impact southern Florida. In this study, we remove long-range transported smoke from our smoke estimates; however, prescribed fire smoke is not removed, as it occurs concurrently with sugarcane burning and is challenging to distinguish. This overlap of smoke from multiple fire types makes it challenging to isolate and quantify the contribution of agricultural smoke in Florida.

Air pollution disproportionately affects low income and minoritized groups in the US (Chakraborty et al., 2022; Jbaily et al., 2022; Mohai et al., 2009). The Everglades Agricultural Area (EAA), where the majority of the sugarcane is grown in Florida, has higher percentages of people who identify as non-White and people living in poverty compared to the coastal regions of south Florida (Figure 2.1). This area also has a lower population than the surrounding regions, with fewer regulatory monitors than the more populated coast. There was only one regulatory-grade $PM_{2.5}$ monitor in the EAA region during 2022-2023. We deployed $PM_{2.5}$ monitors to investigate potential disparities.

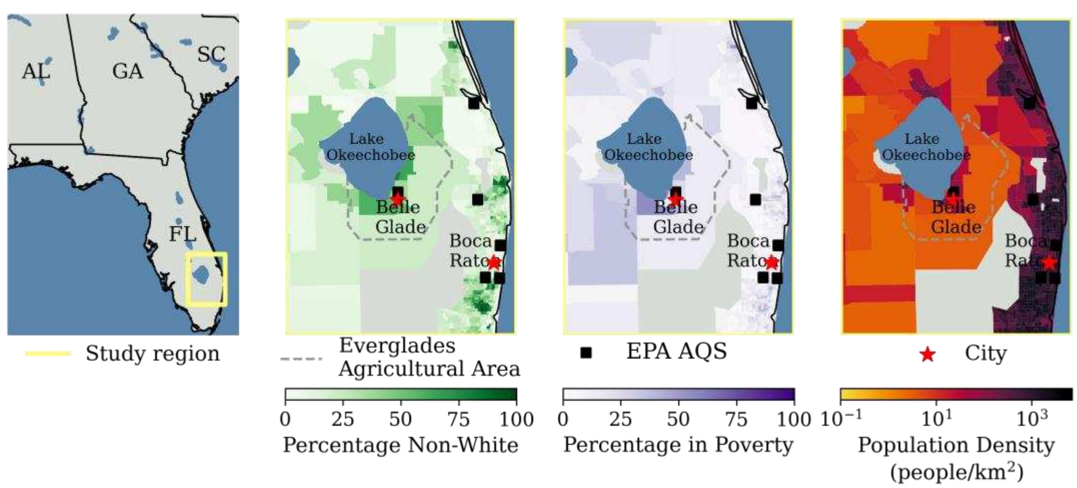

Figure 2.1. Demographics by census tract from the American Community Survey 2019 and EPA AQS $PM_{2.5}$ monitor locations. a) Map of southeastern US with the study region highlighted in a yellow box, b) Percentage of people who identified as non-white, c) Percentage of people in poverty. Poverty is computed by the US Census Bureau using income and family size in

conjunction with defined Poverty Thresholds. d) Population density (people per km^2) using a logarithmic scale. Gray areas have no reported population information. The Everglades Agricultural Area is outlined in a gray-dashed line, and two major cities are identified with red stars.

This study aims to quantify the contribution of sugarcane burning to $PM_{2.5}$ concentrations in southern Florida. By using a network of low-cost PurpleAir sensors to supplement the region's regulatory monitors and existing public PurpleAir network, we measured $PM_{2.5}$ during the 2022–2023 burning season. Our analysis works to isolate $PM_{2.5}$ from agricultural-fire smoke from other sources, including long-range transported smoke and anthropogenic sources. Given the higher percentages of low-income and minoritized populations living near the sugarcane growing region (Figure 2.1), our goal was to assess potential disparities in smoke exposure between the inland region, where sugarcane is grown, and the more affluent coastal areas. Previous work demonstrates that smoke from small landscape fires in this region can result in meaningful health impacts (Pennington et al., 2023). Our study seeks to fill in measurement gaps in assessing smoke exposure, which can provide a better understanding of the health impacts.

2.2 METHODS

We deployed low-cost $PM_{2.5}$ sensors (PurpleAir) to southeastern Florida to determine the impact of smoke from sugarcane burning on $PM_{2.5}$ concentrations for October 2022 - May 2023. We supplemented the regulatory monitors from the US Environmental Protection Agency Air Quality System (EPA AQS) (Figure 2.2). We used these in situ data alongside satellite observations from the National Oceanic and Atmospheric Administration Hazard Mapping System (NOAA HMS) (https://www.ospo.noaa.gov/products/land/hms.html) smoke plumes to attribute $PM_{2.5}$ concentrations to smoke from burning. We used the Moderate Resolution Imaging Spectroradiometer (MODIS) burned area product (MCD64A1) and Burned Area

Authorizations from the Florida Forest Service to determine the extent and timing of the sugarcane burning. We used the MODIS cloud fraction (MYD08_M3 v6.1; MOD08_M3 v6.1) for quantifying the cloud coverage in Florida to determine when fires or smoke may be missed by satellites. To investigate environmental conditions, we used the Modern-Era Retrospective Analysis for Research and Applications, Version 2 (MERRA-2) planetary boundary layer height reanalysis and the Automated Surface/Weather Observing Systems (ASOS/AWOS) wind speed data (https://www.weather.gov/asos/). We discuss these data in the following sections.

2.2.1 In situ $PM_{2.5}$ measurements

We used in situ measurements from the EPA AQS and PurpleAir sensors in southeastern Florida to study $PM_{2.5}$ emitted from sugarcane burning smoke. At the time of this study, there were six regulatory monitors in southeastern Florida within 50 km of the Everglades Agricultural Area (EAA) (Figure 2.2). Five of these monitors are stationed near the coast, approximately 25 - 50 km from burned areas (gray dots in Figure 2.2), where there is a higher population density. One regulatory monitor (AQS Site ID: 12-099-0008) was stationed in the city of Belle Glade, within the EAA. Before October 2021, this site was considered a non-regulatory monitor but has since been replaced with a regulatory monitor (Teledyne T640 at 5.0 LPM).

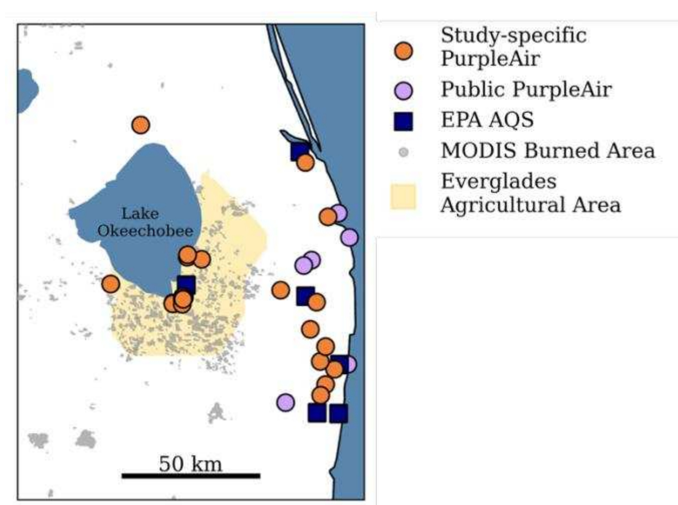

Figure 2.2 Locations of in situ $PM_{2.5}$ monitors, including the PurpleAir deployed specifically for this study (orange), the Public PurpleAir (purple), and the EPA AQS (navy) with the Moderate Resolution Imaging Spectroradiometer (MODIS) burned area product. The Everglades Agricultural Area (EAA) is highlighted in yellow.

We supplemented the EPA AQS monitor by deploying 29 PurpleAir $PM_{2.5}$ sensors. PurpleAir sensors are low-cost devices (~$300 USD) that use light scattering techniques to estimate $PM_{2.5}$ mass (µg m^{-3}). They include two Plantower sensors (channels A and B), which measure at 680 ± 10 nm. PurpleAir sensors also include a BOSCH BME280 to measure pressure, temperature, and humidity. They have been evaluated in the laboratory as well as in the field, and perform with high precision, but lower accuracy (Barkjohn et al., 2021; Jaffe et al., 2023; Malings et al., 2020; Tryner et al., 2020). Accuracy often decreases with increased temperature and humidity; however, we applied a correction factor to mitigate these issues (Barkjohn et al., 2021; full description in Section 2.1.1). The accuracy of PurpleAir measurements also decreases with increasing particle size. PurpleAir sensors perform best for particles between 0.3 and 1 µm, with limited ability to detect particles in the largest reported size range (2.5 - 10 µm) (Kuula et al., 2020; Molina Rueda et al., 2023). In this study, we aim to quantify smoke particles. Smoke that is measured is often aged (4-8 hours), and is typically around ~0.3 µm (June et al., 2022), which is on the low end of the PurpleAir measurement range. Additionally, in regions with high ambient relative humidity, the hygroscopic growth of smoke particles can further increase their size and scattering properties, potentially causing inaccuracies in PurpleAir estimates.

2.2.1.1 PurpleAir field deployment

PurpleAir sensors are commercially available and can be installed by the public. There were 6 public PurpleAir monitors in southeastern Florida at the time of this study (Figure 2.2). All 6 of these sensors were installed near the coast and outside of the EAA. To increase spatial coverage of $PM_{2.5}$ monitoring in southern Florida, we partnered with volunteers throughout the region to host PurpleAir sensors (Figure 2.2). Due to the EAA being largely rural, we prioritized widespread placement. Previous studies have observed primary burning from October- March (H. Nowell et al., 2022); however, participants hosted monitors from September - June to capture the entirety of the burning season and gather non-smoke $PM_{2.5}$ concentrations outside of the burn season. During this period, the study region was affected by smoke from sources other than agricultural fires. This includes prescribed fire smoke, wildfire smoke, and smoke transported from other regions. As discussed below, we isolated the effects of smoke from agricultural sugarcane burning.

2.2.1.2 PurpleAir data quality procedures

PurpleAir calibrates the Plantower lasers in production; however, to use PurpleAir in a research context requires further corrections and validation. We tested the accuracy of the sensors in Fort Collins, CO from July-September 2022 against a Federal Equivalent Method (FEM) monitor (GRIMM EDM 180, Ainring, Germany). Sensors were co-located (< 5 m) with the GRIMM monitor for a period of 14 days. The 24-hr average corrected $PM_{2.5}$ concentrations during testing ranged from 2 to 29 μg m^{-3}. The 24-hr average temperature from the BOSCH BME280 ranged from 13 - 42 °C, and the percent relative humidity ranged from 12 - 69%. We performed these tests to identify issues in individual PurpleAir sensors prior to deployment. We corrected the raw $PM_{2.5}$ estimates with the Barkjohn et al. (2021) correction factor (discussed below). The average Pearson correlation coefficient during our testing between the two corrected PurpleAir channels within each individual sensor was 0.96, and the mean absolute difference was 0.59 μg m^{-3} (Figure A1.1). The correlation on average between the GRIMM monitor and the uncorrected PurpleAir measurements was 0.85 and the mean absolute difference was 3.62 μg m-

^{3}. After applying the correction factor to the PurpleAir estimates, the Pearson correlation on average was 0.64, and the mean absolute difference decreased to 2.03 µg m^{-3} (Figure A1.2). We identified one sensor to be unsuitable for deployment (R^2 = 0.03, mean absolute difference = 3.5, mean bias = -37.7%).

Due to an influx in available volunteers to host monitors in Florida, we also conducted brief quality testing prior to deployment with 6 sensors that were not included in the test above. We could not compare the $PM_{2.5}$ estimates to the FEM during this testing period, so we compared to the average $PM_{2.5}$ across all 6 sensors. We tested these monitors indoors for one day, before deeming them field-ready. $PM_{2.5}$ concentrations during this testing period were much lower than our previous testing in Fort Collins, CO. The 24-hr indoor mean $PM_{2.5}$ concentrations ranged from 0-1 µg m^{-3}, with a standard deviation of 0.6 µg m^{-3}. Due to the low concentrations and few observations with a brief testing period, the agreement between channels (R^2 = 0.2) and comparison to the overall sensor average (R^2 = 0.8) is relatively low (Figure A1.3); however, the sensors performed with consistently high precision with a maximum difference of channel agreement of 0.13 µg m^{-3}.

Before analysis of the campaign data, we performed several quality checks of the raw PurpleAir data ("CF1") using the methods outlined in a previous study (Sablan et al., 2024). We took 10-minute averages of the $PM_{2.5}$ estimates and then removed data with the following conditions: (1) temperature > 65 ^{o}C (0.0092 % of observations), (2) relative humidity > 100% (0.0007 % of observations), (3) channel disagreement > 10% from the average of the two channels or 10 µg m^{-3} in the absolute difference between the channels (1.4 % of observations), and (4) measurements > 500 µg m^{-3} (0.0007 % of observations).

We applied the Barkjohn et al. (2021) correction factor to all the quality-checked 10-minute average PurpleAir data from the deployment in Florida. This correction factor was developed for the entire US and scales $PM_{2.5}$ based on measurement concentrations and relative humidity. The US EPA developed the correction factor using measurements from 53 PurpleAir sensors co-located with regulatory monitors across 16 states, including one site in Florida. At the co-located site in Florida, the average relative humidity (60%) was similar to this campaign (56%). Across all monitors in the study, the correction factor improved the root mean square error of the PurpleAir compared to the reference monitors by > 60%.

Additionally, we tested two other PurpleAir correction factors available on the PurpleAir website (https://map.purpleair.com/), the ALT [cf = 3] correction factor (Wallace et al. 2021), and the AQandU correction factor (Kelly et al., 2017; Sayahi et al., 2019). We compared the average $PM_{2.5}$ concentrations from the 14 PurpleAir sensors in Belle Glade and the EPA regulatory monitor (AQS Site ID: 12-099-0008) for the raw PurpleAir and the three correction factors. The Barkjohn et al. (2021) correction factor yielded $PM_{2.5}$ estimates closer to the EPA reported values for this field campaign (higher R^2; lower mean absolute difference) than other correction factors (Figure A1.4). While this comparison is limited by the lack of direct co-location between the monitors, it provides some indication of which correction factor may be most appropriate for this study.

All measurements were converted from UTC to Eastern Time (ET). We accounted for daylight savings during this campaign, and $PM_{2.5}$ concentrations were shifted an hour later after March 12, 2023.

2.2.2 Administrative burn permitting data

We investigated the timing of sugarcane burning in Florida by obtaining Open Burn Authorizations (OBAs) from the Florida Fire Service (Florida Department of Agriculture and Consumer Services, 2025). An OBA is required for agricultural burning, silvicultural burning (burning for land management), land clearing, pile burning, and acreage burning (Florida Department of Agriculture and Consumer Services, 2024). We received statewide OBAs for October 2020 - October 2023. Sugarcane agricultural burns accounted for 45% of all issued OBAs during this period, and most of the sugarcane burned areas are within or slightly west of the Everglades Agricultural Area (Figure A1.5). Sugarcane burns were ignited starting at 06:00 and continued until 16:00 ET (Figure A1.6); however, Florida regulations require most fires to be ignited at 09:00 ET or later. The burns must be completed two hours after sunset. There were other types of fires that occurred during the campaign, including several ecological prescribed fires conducted in February 2023 near the EAA (Figure A1.7).

2.2.3 Satellite products

We used the MODIS burned-area product to determine the extent of sugarcane burning. To designate smoke impacts, we used the NOAA HMS smoke plumes and fire hotspots. Satellite products can be useful for distinguishing the presence of smoke, although we found several drawbacks with using NOAA HMS in this region to study small agricultural fires (discussed further below and in Section 2.2.5). We used the MODIS cloud-fraction products from Aqua and Terra for investigating the potential for clouds to obscure satellite detection of smoke. Additionally, we used the MERRA-2 planetary boundary layer height reanalysis data and ASOS wind speed to understand smoke dispersion due to environmental factors in the region of study.

2.2.3.1 Burned area product

We used the MODIS/Terra+Aqua Direct Broadcast Burned Area Monthly L3 Global 500m SIN Grid V061 product (Giglio et al., 2021) to determine the extent of burning in southeastern Florida (Figure 2.2). The MODIS burned area product has been shown to underpredict burned area (Chang & Song, 2009; Mohler & Goodin, 2012; Scholtz et al., 2020; Zhu et al., 2017); therefore, we did not use this product as a method of quantification of the impact of agricultural fires, but instead used it to qualitatively highlight the region of burning.

2.2.3.2 Cloud fraction and wind data

To investigate the presence of clouds in Florida, we used the MODIS/Aqua Aerosol Cloud Water Vapor Ozone Monthly L3 Global 1Deg CMG (MYD08_M3) and the MODIS/Terra Aerosol Cloud Water Vapor Ozone Monthly L3 Global 1Deg CMG (MOD08_M3) data (Platnick, 2015). We took an area average of this product for our study region ($-81^{o} \leq x \leq -80W^{o}$; $25^{o} \leq x \leq 27^{o}N$) for each month to investigate seasonal variability. We conducted the same area averaging using planetary boundary layer height (PBLH) reanalysis from MERRA-2 Hourly 0.625 x 0.5 degree V5.12.4 (M2T1NXFLX) data (Global Modeling and Assimilation Office (GMAO), 2015). We obtained wind speed observations from the ASOS station in Clewiston, FL (-80.95^{o}W, 26.75^{o}N). Although this station is not within the EAA, it is the closest ASOS to the burning region in Florida. We used PBLH and wind speeds for investigating smoke dispersion.

2.2.3.3 NOAA HMS smoke and fire products

We used smoke plumes and fire hotspots from the NOAA HMS Fire and Smoke Product (Rolph et al., 2009; Ruminski et al., 2023). NOAA HMS uses satellite observations from geostationary and polar-orbiting satellite observations. Digitization of smoke plumes as polygons and automation of fire hotspot locations are quality checked by analysts. By taking into account multiple satellite observations, the HMS is a comprehensive dataset of smoke plumes and fire hotspots; however, relying on this product entirely may not be adequate to distinguish the presence of smoke in certain regions, as discussed in the next section. There are several limitations with the HMS product. HMS smoke polygons are only produced during the daytime. Satellite observations cannot be used overnight to digitize smoke plumes due to the lack of visible imagery. In regions where there is overnight smoke, there is no information provided regarding nighttime plumes. Additionally, when there is dense cloud cover during the day, smoke may be hidden or obscured and missed by HMS analysts. The source location of the smoke plume is not identified in the HMS dataset.

2.2.4 Smoke designation via multiple methods

Previous studies have used HMS smoke plume polygons to determine the presence of smoke either in the atmospheric column or at the ground (e.g., Brey & Fischer, 2016; Corwin et al., 2022; O'Dell et al., 2019; Sablan et al., 2024). However, there are several limitations of this product that are particularly important for agricultural burning in the study region. While HMS incorporates data from polar-orbiting and geostationary satellites, smaller fires often go undetected. Despite HMS using a suite of satellite observations, both polar-orbiting and geostationary satellites are not able to detect smaller fires: the two overpass times of polar-orbiting are not when burns typically occur (Al-Saadi et al., 2008; Huang et al., 2018; H. K. Nowell et al., 2018; Soja et al., 2009).

Additional challenges in this region include the daytime-only availability of HMS smoke polygons and frequent cloud cover that obscures satellite observations. The HMS product is limited to daytime observations, yet we observed smoke overnight in the EAA region, indicated by large increases in $PM_{2.5}$ concentrations (Figure A1.8; Figure 2.5). Cloud cover further inhibits satellite-based detection; during the burning season (October 2022 - May 2023), the mean cloud fraction from MODIS products was 0.5 over southeastern Florida (Figure A1.9). The highest monthly values were in April and ranged from 0.60 to 0.67, depending on the satellite and time of day. We provide results from using HMS smoke polygons alone to designate smoke; however, these values should be used as a comparison to other methods, and we do not suggest relying only on HMS smoke polygons alone to designate smoke in this region because of the issues described in this section.

The HMS product is, however, well-suited to identify the presence of large smoke plumes from fires upwind. Transported smoke from fires outside the study regions (e.g., Mexico, Cuba) reached Florida during our campaign. We used the size of the HMS smoke plumes to separate transported smoke from local-fire smoke. When smoke plumes had a total area > 15^{o} squared, we classified periods as impacted by smoke transported to Florida from other regions. This area threshold was determined by an analysis of historical HMS smoke plume areas in Florida.

Given the particular challenges associated with this region that is impacted by local agricultural burning at various times of day and frequently under cloud conditions, we conservatively designated the presence of smoke on a daily basis using multiple methods:

15 μg m^{-3}: A day at a specific monitor is designated as smoke-impacted when $PM_{2.5}$ concentrations $\geq$ 15 μg m^{-3} for at least one hour within that 24-hour period.

20 μg m^{-3}: A day at a specific monitor is designated as smoke-impacted when $PM_{2.5}$ concentrations $\geq$ 20 μg m^{-3} for at least one hour within that 24-hour period.

30 μg m^{-3}: A day at a specific monitor is designated as smoke-impacted when $PM_{2.5}$ concentrations $\geq$ 30 μg m^{-3} for at least one hour within that 24-hour period.

20 µg m^{-3} or HMS: A day at a specific monitor is designated as smoke-impacted when either $PM_{2.5}$ concentrations are ≥ 20 µg m^{-3} threshold for at least one hour within that 24-hour period *or* a NOAA HMS smoke plume polygon overlaps the monitor. A flowchart describing this method can be found in Figure A1.10.

Our analysis uses several $PM_{2.5}$ thresholds (1: 15 µg m^{-3}, 2: 20 µg m^{-3}, 3: 30 µg m^{-3}) to provide an estimated range of the impact of local agricultural burning on 24-hour average $PM_{2.5}$. We compared the number of monitor days identified by these ground-based thresholds to those identified using only the presence of HMS smoke plumes (Table A1.1). There were many monitor days where sites had overlapping HMS plumes, but the surface-concentration levels did not meet the smoke designation thresholds. There were also days on which there was not an overlapping HMS smoke plume, and the surface concentrations exceeded our thresholds, which are substantially higher than the average, non-smoke day concentrations. The multi-threshold approach is important because without reliable satellite-based methods, misclassification of $PM_{2.5}$ as smoke is possible, and we need to estimate the uncertainty in smoke impacts. In particular, there may be other sources of $PM_{2.5}$, particularly in the coastal region, that may cause $PM_{2.5}$ concentrations to exceed these thresholds. We provide results both with and without the removal of transported smoke in Table 1, but focus the following discussion on local smoke impacts, with transported smoke excluded.

We also used a combined technique using HMS smoke plumes and an hourly $PM_{2.5}$ threshold of 20 µg m^{-3}. We acknowledge that 20 µg m^{-3} may not be an absolute threshold for agricultural smoke in Florida, but in this study, the presence of smoke often pushed $PM_{2.5}$ concentrations above this threshold for one to several hours. This is further supported by previous studies (e.g., Nowell et al., 2022), which show that $PM_{2.5}$ concentrations in this region remain well below 20 μg m^{-3} in the absence of smoke. A monitor was designated to be smoke-impacted for the day when there was an HMS smoke plume over the monitor or when there was a one hourly average during 24-hours that reached or exceeded 20 μg m^{-3}. A monitor was designated to be smoke-free for the day when both of the following are true: 1) no HMS smoke plumes were observed over the monitor; and 2) all hourly average $PM_{2.5}$ concentrations remained < 20 μg m^{-3}.

Given the relatively small size of smoke plumes from agricultural fires in Florida, we categorized plumes as either from local fires or transported from upwind fires based on their area. Periods with transported smoke in the atmospheric column may coincide with local burning, further increasing surface $PM_{2.5}$ concentrations. However, transported smoke does not always reach the surface. To account for this, we provide estimates of the impact of local agricultural smoke both with and without the removal of days potentially influenced by transported smoke. Due to the challenges with HMS plumes over Florida, the number of days impacted by transported smoke is likely a lower bound. The threshold designation methods used may lead to a misclassification of $PM_{2.5}$ as smoke with lower thresholds might include contributions from other sources. In contrast, the higher threshold may miss lower-concentration smoke events, leading to an underestimation of smoke and its impacts. Additionally, the use of a higher threshold could overestimate median smoke concentrations on smoke-impacted days for the high threshold designation, while underestimating the lower threshold. However, the upper threshold may be an underestimate of the annual and seasonal contribution of smoke to $PM_{2.5}$ because there are fewer days classified as smoke-impacted.

2.2.5 Trajectory analysis to support tracking of smoke transport

To track the near-source transport of smoke from fires in Florida, we used the NOAA HYbrid Single-Particle Lagrangian Integrated Trajectory (HYSPLIT) model (Stein et al., 2015). This model is commonly used to compute the trajectory of air parcels. We calculated 12-hour forward trajectories initiated from all HMS fire hotspots in southern Florida (-81.5^o x -80^o; 26^o x 27.5^o) during the campaign (October 2022 - September 2023). The HMS fire hotspot product combines detections from the Geostationary Operational Environmental Satellite - R Series (GOES-R)/ Advanced Baseline Imager (ABI) Fire Detection product and the Joint Polar Satellite System (JPSS)/ Visible Infrared Imaging Radiometer Suite (VIIRS) products, and NASA's Earth Observing System (EOS) Moderate Resolution Imaging Spectroradiometer (MODIS) fire product. We used meteorological data from the NOAA High-Resolution Rapid Refresh (HRRR) model (Dowell et al., 2022), which provides conditions every 4 hours. The HYSPLIT model produces trajectory locations for every hour; however, we interpolated between the reported locations to provide 10-minute observations. This finer temporal resolution allows for tracing of short-lived plumes and more accurate determination of smoke transport, which may vary significantly on a sub-hourly basis due to shifting wind patterns and rapid changes in plume behavior. If a calculated trajectory intercepts the surface (z = 0), all subsequent locations for this trajectory were removed (Stein et al., 2015). We acknowledge regional differences in weather patterns (e.g., clouds) may make it more challenging to detect hotspots in certain areas, possibly leading to a bias in the HYSPLIT results as winds may, on average, be different under clear sky versus cloudy conditions.

2.3 Results

2.3.1 Duration of burn season in southern Florida

To determine the length of the current burning season in Florida, we obtained Open Burn Authorizations (OBAs) for sugarcane burning near the study region (≤ 27.5° N) from the Florida Fire Service (Figure 2.3). In recent years, the burning season has extended from October through May. Previous studies (and reports) also indicate the sugarcane burn season occurs in Florida from October – May (Baucum & Rice, 2009; McCarty, 2011; H. Nowell et al., 2022; "Sugar Field Burning," 2024). The number of acres burned during the season of study (2022-2023) was consistent with the previous two seasons. The majority of the burning during the three seasons occurred from December through March, with a monthly maximum of 71,200 total acres burned during December 2021. There is a seasonal average of 374,100 total acres burned. These seasonal averages are in line with Bacuum & Rice et al. (2009) who found a decrease in sugarcane acreage burned over time, with 454,400 acres during the 2000-2001 season and 400,000 acres during the 2008-2009 season. There is also variability in the total burning each season; 393,000 acres were burned in 2021-2022 while only 344,000 acres were burned over the course of the 2022-2023 burning season.

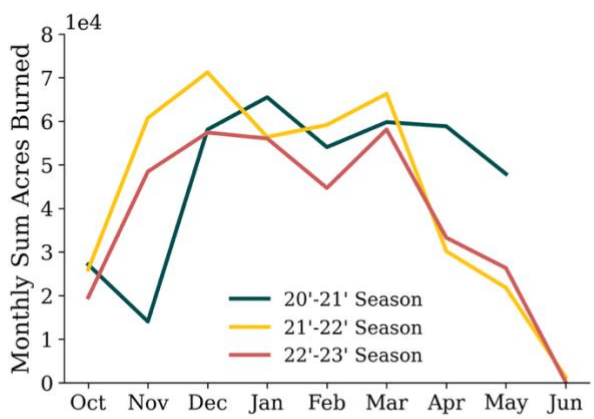

Figure 2.3. Monthly acres burned from sugarcane-agricultural fires from the Florida Fire Service Open Burned Authorizations (OBAs) for 2020, 2021, 2022, and 2023, separated into burning

seasons (October - June). There were no OBAs issued for July - September. There were 15 sugarcane agricultural fires away from the study region (> 27.5° N) that were not included in this analysis.

2.3.2 Impact of smoke on $PM_{2.5}$ concentrations

In this section, estimates of the impact of smoke on $PM_{2.5}$ are presented by number of days per monitor or "monitoring days" (Figure 2.4; Table 2.1). In Table 2.1, each designation method is compared (see Section 2.2.4). The median 24-hour $PM_{2.5}$ concentrations on smoke-free days ranged from 4.0 - 4.7 µg m^{-3} and from 6.3 - 11.6 µg m^{-3} for smoke-impacted days, and the percent of monitoring days deemed as smoke-impacted ranged from 4 - 28% (Figure 2.4). The median contribution of local agricultural fires to $PM_{2.5}$ ranged from 2.3 - 6.9 µg m^{-3} across all designation methods, with the inclusion of potential transported-smoke days. With the transported smoke removed, this range decreases to 1.4 - 5.1 µg m^{-3}. Transported smoke-days may also be impacted by local smoke; therefore, removing transported smoke days may also remove some local-smoke influence. The seasonal contribution of smoke to $PM_{2.5}$ was calculated by multiplying the median smoke contribution to $PM_{2.5}$ by the fraction of days affected by smoke for each monitor during the burning season (October - May), then dividing by the total number of monitor observation days during the season. The seasonal contribution ranges from 0.27 to 0.94 µg m^{-3}, including days potentially impacted by transported smoke. Under the assumption that agricultural burning is entirely during October - May (Figure 2.3), the median contribution of smoke to the 2022-2023 annual-average $PM_{2.5}$ was 0.13 - 0.43 µg m^{-3}, including transported-smoke days. If days potentially influenced by transported smoke are excluded, the annual contribution ranged from 0.06 - 0.16 µg m^{-3}.

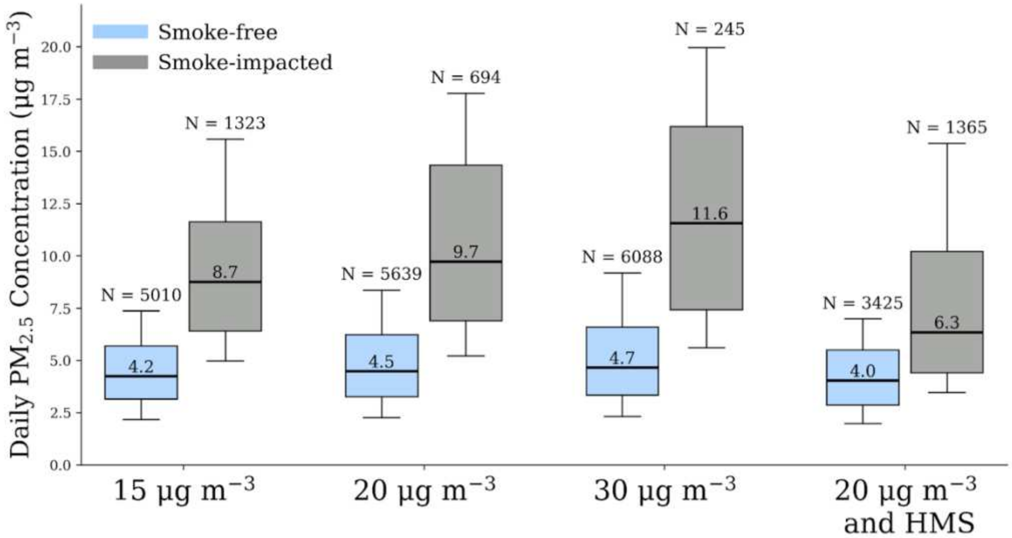

Figure 2.4. 24-hour average $PM_{2.5}$ concentration distributions for different smoke designation methods during the 2022-23 burning season for all sensors in southern Florida. Outliers have been excluded from the figure and the median for each category is shown above the bold line. The edges of the boxes represent the 1st and 3rd quartiles. The whiskers are 10th and 90th percentiles. Days impacted by transported smoke were not removed from the distributions

Table 2.1. Number of smoke-free and smoke-impacted days at each monitoring site, the $PM_{2.5}$ concentration (median (25th-75th)) for smoke-free and smoke-impacted days, the smoke contribution to $PM_{2.5}$, the seasonal and annual contributions of smoke $PM_{2.5}$ for each smoke designation method in μg m^{-3}. Designations with removal of transported smoke (determined from the NOAA Hazard Mapping System) smoke plumes are in gray rows. The "HMS only" smoke designations are included for completeness, but they are not the best estimate due to HMS limitations in the study region.

Smoke Designation Method	Number of smoke-free monitoring days	Number of smoke-impacted monitoring days	Conc. (μg m^{-3}) on smoke-free days median (25^{th} - 75^{th})	Conc. (μg m^{-3}) on smoke- impacted days median (25^{th} - 75^{th})	Smoke contribution to $PM_{2.5}$ on smoke-impacted days (μg m^{-3})	Seasonal contribution of smoke to $PM_{2.5}$ (μg m^{-3})	Annual contribution of smoke to $PM_{2.5}$ (μg m^{-3})
≥ 15 μg m^{-3}	5010	1323	4.2 (3.1 - 5.7)	8.7 (6.4 - 11.6)	4.5	0.94	0.43
	3745	743	4.0 (2.9 - 5.2)	7.0 (5.6 - 9.6)	3.1	0.51	0.16
≥ 20 μg m^{-3}	5639	694	4.5 (3.3 - 6.2)	9.7 (6.9 - 14.3)	5.2	0.57	0.26
	4096	392	4.1 (3.0 - 5.5)	7.8 (5.9 - 11.4)	3.6	0.32	0.10
≥ 30 μg m^{-3}	6088	245	4.7 (3.3 - 6.6)	11.6 (7.4 - 16.2)	6.9	0.27	0.13
	4340	148	4.3 (3.1 - 5.8)	9.4 (6.4 - 13.6)	5.1	0.17	0.06
≥ 20 μg m^{-3} and HMS	3425	1365	4.0 (2.9 - 5.5)	6.3 (4.4 - 10.2)	2.3	0.66	0.23
	3425	1063	4.0 (2.9 - 5.5)	5.4 (4.1 - 7.6)	1.4	0.32	0.10
Designation included for completeness, but not the best estimate due to HMS limitations in the study region:							
HMS only	3689	2644	4.2 (3.0 - 5.8)	5.9 (4.2-8.8)	1.7	0.70	0.33
	3689	799	4.2 (3.0 - 5.8)	4.8 (3.9 - 6.7)	0.6	0.11	0.04

Nowell et al. (2022) showed that sugarcane harvest activities contributed 1.4 μg m^{-3} to seasonal mean $PM_{2.5}$ from 2009-2018. They subtracted the mean $PM_{2.5}$ outside the harvesting season (April - September) from $PM_{2.5}$ concentrations measured at the regulatory site in Belle Glade during the harvest season (October - March). The upper end of our seasonal contribution to smoke was 0.94 μg m^{-3}. Differences in these estimates are likely due to variations in the smoke season length, different calculation methods, and potential seasonal cycles in non-smoke $PM_{2.5}$, which may have influenced the results. Despite inherent differences in methodology, the results are consistent and the growing bodies of research show that $PM_{2.5}$ concentrations increase with burning in this region of Florida.

3.3 Variability in the diurnal cycle of $PM_{2.5}$

Diurnal patterns of smoke $PM_{2.5}$ concentrations in the region were evaluated using the ≥ 20 μg m^{-3} threshold (Figure 2.5). Results for all other designation methods are provided in the Supplement (Figures A1.10 - A1.12). $PM_{2.5}$ increases related to agricultural burning occurred at varying times throughout the day (e.g., early morning, mid-morning, afternoon, evening, and overnight). As a result, when averaging across all hours for the entire campaign, there is not a distinct diurnal cycle.

On days designated as smoke-impacted, there is an increase in the hourly average 98th percentile of $PM_{2.5}$ at inland sites overnight on smoke-impacted days that does not occur on smoke-free days. This pattern is not evident at the coastal monitoring locations. Two inland local maxima in $PM_{2.5}$ occurred at 04:00 (91 μg m^{-3}) and 20:00 ET (51 μg m^{-3}; Figure 2.5). This particular timing may be a result of 1) fires smoldering overnight, 2) lower planetary boundary layer heights (PBLH) decreasing dispersion and transport of smoke away from local sources, and 3) lower wind speeds at night decreasing ventilation. Although authorized burns are generally limited to daytime hours (09:00 ET to two hours before sunset), residual smoldering can produce smoke well into the night, when stable atmospheric conditions can concentrate smoke near the surface. The PBLH in the study region during the burn season (October 2022 - May 2023) averaged 574.7 m from 23:00 - 07:00 EST. The PBLH increased to 1369.9 m at 14:00 ET. Average wind speeds in this region are also lower overnight; the average wind speed from 23:00 - 07:00 ET was 4.2 km hr^{-1}, with a maximum wind speed of 7.0 km hr^{-1} at 14:00 ET.

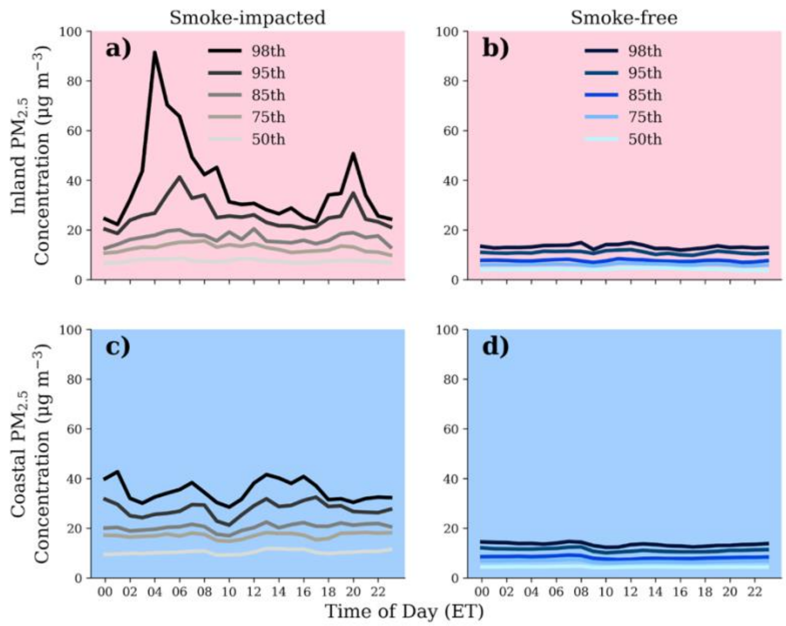

Figure 2.5. Hourly 50th, 75th, 85th, 95th, and 98th percentile $PM_{2.5}$ concentrations during October 2022 - May 2023 for a) inland monitors (> 50 km from the coastline; pink) on smoke-impacted days (classified using criteria of an hourly average $PM_{2.5}$ concentration ≥ 20 μg m^{-3}), b) inland monitor on smoke-free days, c) coastal monitors (<30 km from coastline; blue) on smoke-impacted days, and d) inland monitors on smoke-free days. Other smoke designation methods are shown in Figures A1.11-1.13.

Nowell et al. (2022) reported that seasonal-average $PM_{2.5}$ concentrations from the Belle Glade regulatory monitor maximized at 10:00 ET during October to March 2009-2019 and decreased after 19:00 ET. Note that this averaging included days with local burning and without. This pattern of elevated $PM_{2.5}$ concentrations in the late morning was observed both during the October-March harvest season and outside of it. In our study, smoke was observed at varying times throughout the day, with inland $PM_{2.5}$ increases overnight and in the early morning due to meteorological conditions and/or smoldering. These increases on smoke-impacted days were most evident in the 98th percentile of hourly averages, but there were also small increases in median $PM_{2.5}$ concentrations at 06:00 and 20:00 ET. Together, both studies are important in distinguishing $PM_{2.5}$ increases from smoke in this region.

3.4 Determining regional impacts of smoke $PM_{2.5}$

Using the ≥ 20 μg m^{-3} threshold for designating smoke, monitors in the inland region were impacted by smoke approximately twice as often as monitors in the coastal region during the 2022-2023 burning season (Figure 2.6). Specifically, 13% of inland monitor days were deemed smoke-impacted compared to 8% of days for coastal monitors. However, when the coastal region was impacted by smoke, the median observed daily $PM_{2.5}$ concentration was 11.8 μg m^{-3} compared to 9.1 μg m^{-3} for the inland region. On smoke-free days, concentrations were similar between regions, with a median $PM_{2.5}$ concentration of 4.5 μg m^{-3} for the coastal monitors and 4.4 μg m^{-3} for the inland monitors. While there were fewer instances of smoke-impact at the coastal monitors, the smoke-impacted periods were characterized by slightly higher median $PM_{2.5}$ concentrations.

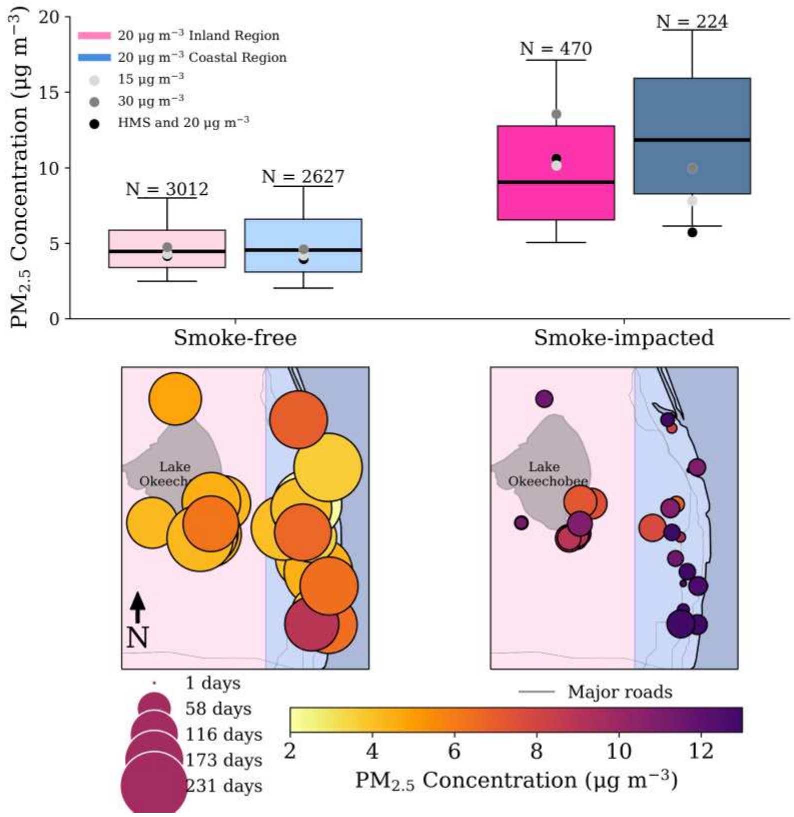

Figure 2.6. Top Row: Boxplots of daily average $PM_{2.5}$ for smoke-free days and smoke-impacted days using the ≥ 20 μg m^{-3} designation method. The distributions are separated by monitors near the coast (blues) and monitors in the inland region (pinks). Outliers have been excluded, and the bold line represents the median for each category. The edges of the boxes represent the 1st and 3rd quartiles. The whiskers are 10th and 90th percentiles. Bottom Row: Maps of median $PM_{2.5}$ concentrations at each monitor on smoke-free (left) and smoke-impacted days (right). Markers are sized by the corresponding number of days at a site that as designated as smoke-impacted or smoke-free. Map regions are shaded by the inland versus coastal designation. Note: the color bar has a lower limit of 2 μg m^{-3}. Other smoke designation methods are shown in Figures A1.13-1.15.

Extreme smoke events ($PM_{2.5}$ > 40 μg m^{-3}) during the 2022-2023 agricultural burning season also show distinct temporal and spatial patterns (Figure A1.17). Inland monitors had more frequent periods of $PM_{2.5}$ > 40 μg m^{-3} during early morning and evening hours compared to the coastal region. This suggests that smoke may persist overnight, potentially due to nighttime smoldering or atmospheric conditions that limit dispersion and ventilation. These spatial differences further support the hypothesis that smoke exposure differs regionally, with inland areas experiencing more extreme smoke exposure compared to the coastal region.

The NOAA HYSPLIT model was used to further explore the regional differences of smoke transported from agricultural burning (Figure 2.7). We calculated 12-hour forward trajectories initiated from HMS fire hotspots, which includes detections from the GOES-R/ABI Fire Detection product, the JPSS/VIIRS products, and the EOS MODIS product. The maximum number of HMS hotspots (1.1 hotspots per km^2) was detected south-southwest of Lake Okeechobee, coinciding with the region of maximum HYSPLIT trajectory points south of the lake (19.4 points per km^2). Due to the limitations with HMS in this region, this analysis may provide an estimate of the minimum difference in smoke exposure between regions. When considering all trajectories on days where HMS hotspots were detected, 26% of the total trajectories moved westward ($\leq$ -81.36°W), 21% moved eastward ($\geq$ -80.36°W), and the majority of trajectories (49%) stayed within the bounds ($-81.2^{\circ} \leq x \leq -80.36^{\circ}$W) in the agricultural region (Figure A1.18). If we only consider trajectories that transport away from the agricultural region, 59% of trajectories moved westward ($\leq$ -81.36°W) and 41% moved eastward ($\geq$ -80.36°W). These findings are consistent with Figure 2.6, as there were fewer smoke-impacted days during the campaign for the coastal monitors (224 total days) than the inland monitors (470 total days).

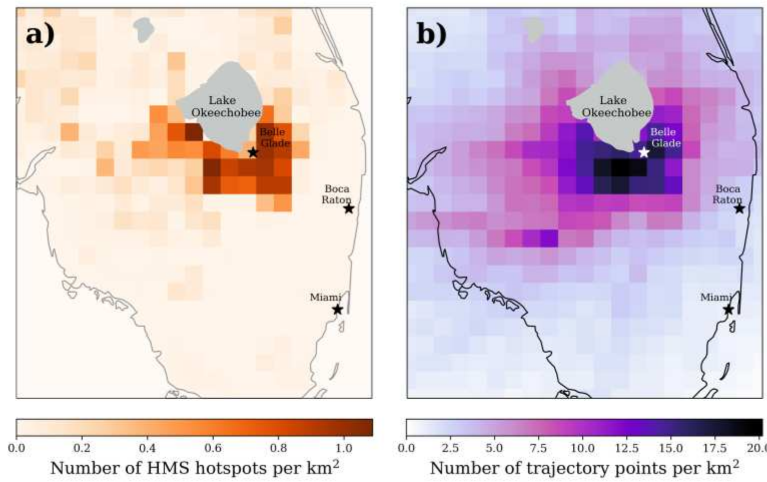

Figure 2.7. a) Sum of gridded HMS fire hotspots per gridded area for the October to May 2022-23, b) Sum of 10-min interpolated 12-hour forward trajectories per gridded area initiated from each HMS fire hotspot from the NOAA HYSPLIT model.

2.4 CONCLUSIONS

Air quality in rural regions is often under-monitored. To fill monitor gaps in the rural Everglades Agricultural Area (EAA) in Florida, citizen scientists hosted 29 PurpleAir sensors. To quantify smoke from sugarcane burning on $PM_{2.5}$ concentrations from October 2022 to May 2023, we incorporated data from study-specific and public PurpleAir, as well as regulatory monitors. Due to the limitations of satellite observations in the study region and the agricultural fires being short-lived and small, several smoke designation methods were used to quantify the uncertainties in smoke $PM_{2.5}$ estimates. These methods include using three thresholds of $PM_{2.5}$ (15 µg m^{-3}; 20 µg m^{-3}; 30 µg m^{-3}) and a method that uses a combination of HMS observations and the 20 µg m^{-3} threshold. Median 24-hour $PM_{2.5}$ concentrations increased by 2.3 - 6.9 µg m^{-3} on smoke-impacted days compared to unimpacted days, with 4 - 28% of days between October 2022 and May 2023 exhibiting smoke influence.

Smoke was observed to occur throughout all hours of the day near the burning region, although most of the agricultural-fire smoke occurred during the daytime. Due to atmospheric conditions and the potential for overnight smoldering, there were cases of smoke during the evening and early morning hours. A distinct, consistent diurnal cycle in median smoke $PM_{2.5}$ for inland or coastal monitors was not identified; however, there were extreme smoke events (e.g., 98th percentile; hours > 40 µg m^{-3}) overnight.

During this study, the inland region, near the EAA, experienced more smoke-impacted days than the coastal region. The median $PM_{2.5}$ on smoke-impacted days in the coastal region was 11.8 µg m^{-3} compared to 9.1 µg m^{-3} for the inland region. This result suggests that smoke transport to the coast is infrequent but results in higher $PM_{2.5}$ concentrations when it occurs. The HYSPLIT model was used to calculate the trajectories of air parcels initiated from identified HMS hotspots to understand the predominant transport pathways of smoke from agricultural fires in this region. The majority of trajectories moved westward, away from the east coast, consistent with less frequent smoke impacts in the coastal region. The greater frequency of smoke impact in low-income, rural, inland regions emphasizes the critical need to expand air quality monitoring to these underserved areas (US Census Bureau, 2023).

Overall, satellite products were not well suited for identifying smoke and fires in this region due to: 1) the consistent presence of clouds, 2) overnight smoke, and 3) the occurrence of many small, short-lived fires, which satellites are not able to accurately quantify. Products that rely on HMS to identify smoke (e.g., O'Dell et al., 2019) to diagnose the presence of smoke will likely underestimate smoke at the surface in southern Florida, particularly from local fires. Without consistent satellite observations, resources to detect the presence of smoke are limited. Alternative approaches, such as using surface-based measurements, can be used to identify the presence of smoke. In this study, multiple methods were used to designate smoke-impact that leveraged the surface measurements. Given the strengths and weaknesses of our methods, the estimations in this manuscript provide a lower and upper bound of smoke exposure during the study.

Isolating the impacts of sugarcane agricultural fires from other fire types presents inherent challenges. While this analysis focused on the primary sugarcane burning season (October–May), other fires also occurred during this period, including prescribed (silvicultural) burns for ecological purposes, agricultural fires for pasture and range management, and wildfires. These overlapping fire activities may have contributed to overestimating the smoke $PM_{2.5}$ attributed to sugarcane burning.

The use of low-cost PurpleAir sensors may introduce uncertainty to $PM_{2.5}$ measurements. PurpleAir sensors have been shown to measure a low bias at low concentrations and high bias at high concentrations (Sayahi et al., 2019; Tryner et al., 2020). Most measurements in this study were at low concentrations due to the infrequency of smoke-impacted days, likely leading to an underestimation of $PM_{2.5}$. To address this, we applied the Barkjohn et al. (2021) correction factor. Despite inherent biases, PurpleAir sensors provide valuable data in regions with limited monitoring resources.

This study contributes to the growing understanding of smoke impacts from agricultural sugarcane burning in Florida. While the results highlight differences in smoke exposure between inland and coastal areas, they also show the need for improved monitoring strategies to capture fine-scale and short-lived smoke events. Satellite-based approaches for smoke identification face challenges in this region due to frequent cloud cover, the small size of fires, and the presence of overnight smoke. Nighttime smoke exposure is particularly concerning, as residents in nearby agricultural areas, many of whom are low-income and lack air conditioning, may unknowingly leave their windows open to cool their homes. This behavior can exacerbate health risks from smoke exposure. It is essential to implement measures to reduce smoke exposure. We recommend strategies such as encouraging residents to keep windows closed at night and use air conditioning, air purifiers, or box fans with filters to improve indoor air quality. Future research should further explore the health impacts of sugarcane agricultural fire smoke exposure, a critical yet understudied area in this region, and accurate smoke exposure estimates are fundamental for determining health impacts.

2.5 Data Availability Statement

The PurpleAir data from the field deployment can be downloaded from Sablan et al., (2025). The PurpleAir data from public monitors can be accessed through the PurpleAir API, and the details can be found here: https://community.purpleair.com/t/making-api-calls-with-the-purpleair-api/180. The EPA regulatory $PM_{2.5}$ data is publicly available and can be downloaded from https://aqs.epa.gov/aqsweb/airdata/download_files.html. The MODIS MCD64A1 burned area product is from Giglio et al., (2021). The NOAA/NEDIS Hazard Mapping System Smoke Product is available at "Hazard Mapping System Smoke Product," (2022) and the Fire Product is available at "Hazard Mapping System Fire Product," (2022). Administrative Open Burn Authorizations from the Florida Fire Service can be requested at (Florida Department of Agriculture and Consumer Services, 2025). The MODIS/Aqua Aerosol Cloud Water Vapor Ozone Monthly L3 Global 1Deg CMG (MYD08_M3) and the MODIS/Terra Aerosol Cloud Water Vapor Ozone Monthly L3 Global 1Deg CMG (MOD08_M3) data is from Patnick (2015). MERRA-2 Hourly 0.625 x 0.5 degree V5.12.4 (M2T1NXFLX) data is from Global Modeling and Assimilation Office (GMAO) (2015). Automated Surface Observation Station data can be downloaded at: https://www.ncei.noaa.gov/products/land-based-station/automated-surface-weather-observing-systems. Meteorological data for the HYbrid Single-Particle Lagrangian

Integrated Trajectory (HYSPLIT) model was from the NOAA High-Resolution Rapid Refresh (HRRR) model (Dowell et al., 2022). The HYSPLIT model can be run at: https://www.ready.noaa.gov/HYSPLIT.php. The interpolated monthly gridded output for the HYSPLIT model can be found at: https://doi.org/10.5061/dryad.70rxwdc9k.

CHAPTER 3

HEALTH IMPACTS OF WILDFIRE SMOKE EXPOSURE IN NEW MEXICO DURING 2022 AND SENSITIVITY TO EXPOSURE ESTIMATE AND REFERENT PERIOD [3]

3.1 INTRODUCTION

Wildfires are increasing in duration, frequency, and intensity due to climate change (Abatzoglou et al., 2021; Westerling, 2016), leading to more widespread and increased wildfire smoke exposure across the United States (Burke et al., 2023; Childs et al., 2022; Volckens, 2024). The EPA National Emissions Inventory consistently shows wildfires to be the largest source of primary $PM_{2.5}$ in the US (US EPA, 2017, 2020), and exposure to smoke $PM_{2.5}$ has been shown in previous studies to be associated with a suite of negative health outcomes. These outcomes include increased risk of cardiorespiratory morbidity (e.g., emergency department visits, hospitalizations, medication use, etc.) (Delfino et al., 2009; Gan et al., 2017; Hahn et al., 2021; Liu et al., 2015; Reid et al., 2016), particularly asthma-related morbidity (Gan et al., 2020; Johnston et al., 2002; Rappold et al., 2011), adverse pregnancy outcomes (e.g., low-birth weight) (Abdo et al., 2019; Holstius et al., 2012), and increased risk of mortality (Magzamen et al., 2021; O'Dell et al., 2021). With the increasing trend of wildfires expected to persist (Ford et al., 2018), we will likely see increasing rates of related morbidity and mortality in the future.

New Mexico suffered several large wildfires in 2022, including the largest in state history, the Calf Canyon/Hermit's Peak Fire. The Hermit's Peak fire started on April 6, 2022, and the Calf Canyon fire started on April 19, 2022. The two fires merged and were 100% contained

[3] Adapted from a manuscript under review: Sablan, O., Ford, B., Hawkinson, C., Hu, L., Langer, C. E., Maichak, C., et al. (under review). Health impacts of wildfire smoke exposure in New Mexico during 2022 and sensitivity to exposure estimate and referent period. *GeoHealth*.

by August 21, 2022, after burning a total of 1,382 km^2 (Tunby et al., 2023). In total, New Mexico experienced 748 wildfires total in 2022, burning about 3,700 km^2 (National Interagency Fire Center, 2025). The Black Fire was the second largest and burned 1,316 km^2 in southwestern New Mexico from May - June 2022 (Hulburd, 2022). Smaller wildfires also occurred in 2022, including the Cooks Peak Fire (InciWeb, 2024), the Cerro Pelado Fire (InciWeb, 2022a), and the Bear Trap Fire (InciWeb, 2022b).

Quantifying wildfire smoke exposure remains a major challenge, especially in regions like New Mexico, where regulatory monitoring is sparse. While Environmental Protection Agency (EPA) monitors provide highly accurate and precise $PM_{2.5}$ measurements, their limited coverage has led to growing interest in using low-cost sensors. For example, PurpleAir low-cost sensors have a large network that can be leveraged in the US; however, they are less accurate than regulatory monitors. Modeling wildfire smoke can provide data at high spatiotemporal resolution but may not always provide estimates that are representative of ground-based monitoring. Accurately estimating smoke exposure is critical for epidemiological studies to produce meaningful results. In three studies conducted in Colorado, odds ratios (ORs), which express the likelihood of experiencing health impacts due to smoke exposure, associated with a 10 $\mu g\ m^{-3}$ increase in wildfire smoke $PM_{2.5}$ ranged from 0.9 to 2.2, with varying confidence intervals (Alman et al., 2016; Magzamen et al., 2021; Stowell et al., 2019). This means that there were protective effects under some smoke-impacted conditions (OR = 0.9), likely associated with behavior changes when residents were highly aware of the presence of local smoke. These studies used different smoke exposure estimates, which contributes to variations in results. Gan et al. (2017) also found that different smoke estimation methods resulted in varying associations with health outcomes. Through this study, we aim to evaluate how the choice of exposure estimate affects epidemiological results in a region with limited in situ monitoring.

The case-crossover study design has been widely used to evaluate the health effects of smoke exposure (Gan et al., 2017, 2020; Hahn et al., 2021; Magzamen et al., 2021); however, the sensitivity of the selection of the referent period has not been explored. The case-crossover design is valuable because it controls for individual-level confounders (e.g., age, sex, race). Selection of an appropriate referent period, or the time period which the exposure event is compared to, is a critical component of the case-crossover framework (Janes et al., 2005b, 2005a). In this analysis, we used a time-stratified technique, which has been shown to address some challenges associated with referent periods (Janes et al., 2005a). The potential for different referent period choices to influence case-crossover studies of short-term pollution impacts is not well understood. This is especially relevant in New Mexico during the Calf Canyon/Hermit's Peak fire, when some regions experienced nearly continuous smoke exposure for an extended period. Investigating the impact of different referent periods in a case-crossover study provides insight to the sensitivity of the results.

We investigated the dependencies of inputs on ORs associated with wildfire smoke exposure in New Mexico during summer 2022. We tested several smoke estimates, including in situ measurement-based estimates and chemical transport model output. Additionally, we used two different referent periods to determine the impact on our results. By evaluating exposure estimates and referent period selection, we identify key uncertainties with assessing the impact of smoke on human health, specifically in a region with limited in situ $PM_{2.5}$ monitoring during an intense wildfire season.

3.2 METHODS

3.2.1 Study area

The study area includes all regions in the state of New Mexico that have a ZIP code reported in the US Census Bureau 2010 5-Digit ZIP Code Tabulation Area (ZCTA) (US Census Bureau, 2010). We did not use the 2020 ZCTA data; however, there were minimal changes from 2010, and our results would not be impacted. Due to a majority of New Mexico being rural, there are several areas where there are no ZCTAs. In 2022, New Mexico had 11 active EPA regulatory $PM_{2.5}$ monitors, which are primarily located in more populated urban centers (e.g., Albuquerque, Santa Fe, Las Cruces). There were seven Interagency Monitoring of PROtected Visual Environments (IMPROVE) monitors in the area during 2022. IMPROVE monitor data are available through the EPA Air Quality System, but the primary purpose of the network is to monitor visibility trends in US National Parks and Wilderness Areas (Hand et al., 2024; Malm et al., 1994). IMPROVE monitors report measurements every three days, whereas monitors used for the National Ambient Air Quality Standards (NAAQS) typically have hourly or daily observations. Additionally, New Mexico had 91 low-cost PurpleAir $PM_{2.5}$ sensors at the time of the study (Figure 3.1).

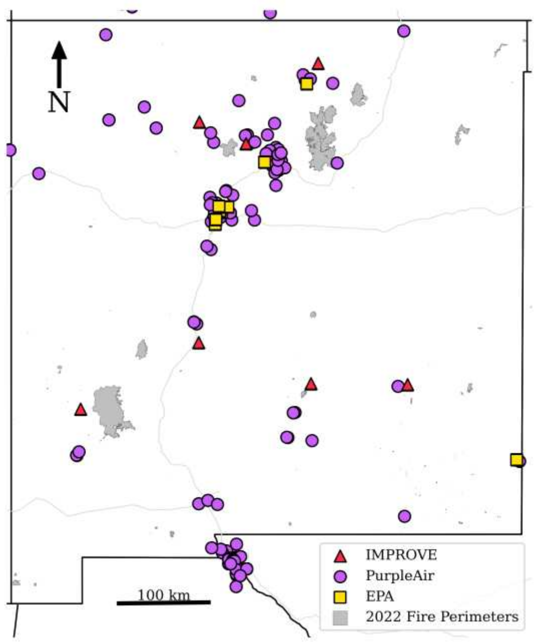

Figure 3.1. Map of study region and ground-based $PM_{2.5}$ sensors including the Environmental Protection Agency regulatory monitors (yellow squares), the Interagency Monitoring of PROtected Visual Environments (IMPROVE) monitors (red triangles), and the PurpleAir sensors (purple circles). The fire perimeters from the National Interagency Fire Center (2025) during April 1 - September 30, 2022, are shaded gray.

3.2.1.1 Study population

New Mexico (NM) has a population of ~2.1 million people throughout 315,194 km^2 of area (US Census Bureau, 2023). It is the 5th largest state by land mass but sparsely populated. The majority of the population identifies as Hispanic/Latino (50%) or American Indian and Alaska Native (11%). Nearly 18% of the NM population lives below the poverty line, where poverty is computed by the U.S. Census Bureau using income and family size in conjunction with defined Poverty Thresholds (US Census Bureau, 2023). Around 20% of the total population of NM is age 65 or older (US Census Bureau, 2023). The counties in northeastern NM, which were more impacted by the Calf Canyon/Hermit's Peak wildfire in 2022, have a higher population of people 65 or older in age. About 41% of Harding County (northeast of Las Vegas, NM), is 65 or older (US Census Bureau, 2023).

3.2.2 Smoke exposure estimates

We used four smoke $PM_{2.5}$ estimates for our 2022 analysis: 1) $PM_{2.5}$ from the EPA regulatory-grade monitors, 2) $PM_{2.5}$ from both the EPA regulatory-grade monitors and low-cost PurpleAir observations, 3) modeled 24-hour average wildfire smoke $PM_{2.5}$ from the Community Multiscale Air Quality Modeling System (CMAQ), and 4) CMAQ daily 1-hour maximum wildfire smoke $PM_{2.5}$. Conducting our analysis with four different exposure estimates for 2022 allowed us to assess the usefulness of each product in a case-crossover study in NM.

3.2.2.1 Regulatory-only smoke product

We used the 24-hour smoke product from O'Dell et al., (2019) as our "Regulatory-only" estimates. These estimates are produced by spatially interpolating in situ $PM_{2.5}$ measurements from the EPA Air Quality System (AQS). This includes EPA regulatory monitors (yellow squares in Figure 3.1) and IMPROVE monitors (red triangles in Figure 3.1). To spatially interpolate, we used ordinary kriging, a geostatistical method recently applied in air quality research, to estimate $PM_{2.5}$ concentrations between monitoring sites across a gridded surface (Gan et al., 2017; Isaaks & Srivastava, 1989; Janssen et al., 2008). $PM_{2.5}$ estimates are calculated for total (all-source) $PM_{2.5}$ and smoke $PM_{2.5}$, where $PM_{2.5}$ attributable to smoke is determined by the presence of HMS smoke plumes from the National Oceanic and Atmospheric Science Hazard Mapping System (NOAA HMS) ("Hazard Mapping System Smoke Product," 2022). HMS does not distinguish fire type (i.e., prescribed fire, wildfire, agriculture fire); therefore, the smoke may not be exclusively from wildfires. We studied the wildfire season to decrease the likelihood of smoke from other types of fires. The product includes 24-hour average $PM_{2.5}$ on a 15 x 15 km grid for the contiguous US. Seasonal background concentrations for four climatological seasons (December-February, March-May, June-August, September-November) were determined by calculating the median $PM_{2.5}$ at each grid cell on days without NOAA HMS smoke plumes and were removed from the $PM_{2.5}$ smoke estimates.

We used the NASA Socioeconomic Data and Applications Center (SEDAC) world population (GPWv4) to calculate population-weighted ZIP code-level daily averages (Center for International Earth Science Information Network, 2023). We determined the fractional overlap of each grid with a ZCTA. Thus, a concentration is the sum of all gridded concentrations (*Pop_i*) multiplied by the population (*Pop_i*, regridded) (Center for International Earth Science Information Network, 2023) and the fractional overlap (*f_i*) of the grid (*i*) and the ZIP code, divided by the total population in the ZIP code, as shown in Equation 1.

$$PM_{2.5,ZIP\ Code} = \frac{\sum_{i=1}^{n} f_i * Pop_i * PM_i}{\sum_{i=1}^{n} f_i * Pop_i} \qquad \text{(eq. 1)}$$

3.2.2.2 Regulatory + PA smoke product

Because the majority of the NAAQS regulatory monitors are located in more populated areas, we incorporated low-cost sensors (PurpleAir) to the O'Dell et al. (2019) (Regulatory-only) product, allowing for greater in situ coverage of the largely rural state. We refer to this product as "Regulatory + PA." PurpleAir sensors are low-cost (~$300 USD) and commercially available. The sensors contain two Plantowers (channels A and B), which use light-scattering techniques to estimate $PM_{2.5}$ mass at 680 ± 10 nm every 2-minutes. PurpleAirs also have a BOSCH BME280 to measure pressure, temperature, and humidity. They have been tested in various settings (Barkjohn et al., 2021; Jaffe et al., 2023; Malings et al., 2020; Ouimette et al., 2022; Tryner et al., 2020) and have been shown to perform best for particles of size 0.3 - 1 µm (Kuula et al., 2020; Molina Rueda et al., 2023).

We took 10-minute averages of PurpleAir channels A and B for our data quality procedures. Data were removed from the analysis when: 1) channels A and B had an absolute difference of more than 10 μg m^{-3} or a relative difference of more than 10%, 2) the measurement was outside of the range of 0-1000 μg m^{-3}, 3) there was no corresponding humidity measurement, which was needed for the subsequent correction factor, 4) the A and B channels' correlation coefficient over the entire time period of available data was less than 0.75 (O'Dell et al., 2022). After completing our quality control procedures, we applied the Barkjohn et al. (2022) correction factor. This correction factor was developed by the US EPA for extreme wildfire smoke $PM_{2.5}$. It reduces bias in PurpleAir estimates by scaling based on the measured concentrations and relative humidity.

We spatially interpolated the PurpleAir and regulatory-monitor $PM_{2.5}$ measurements using ordinary kriging (described in Section 2.1.1) to a 0.1° x 0.1° grid of NM. We optimized the kriging parameters (i.e., sill, range, nugget) by leave-one-out cross-validation (LOOCV) to maximize the correlation and minimize the error between the interpolated value and the measurement over the full year. When using the same variogram parameters as O'Dell et al. (2019) in our analyses, we had similar results to the optimized parameters (Figure A2.1), with the largest difference in ORs of 0.20. We used the optimized parameters in the following case-crossover results. To determine the presence of smoke we used the presence of HMS smoke plumes overlapping the grid cell, with the addition of a 25 km buffer around each plume to account for dilute smoke not identified by HMS.

We removed the seasonal background $PM_{2.5}$ concentration from our smoke estimates, similarly to O'Dell et al. (2019). Because smoke was present for most of spring and summer months in 2022, we used only two seasons (smoke season: April - August; non-smoke season: January-March, September - December), in contrast to the four climatological seasons used in O'Dell et al. (2019). The 24-hour average smoke $PM_{2.5}$ concentration for each grid cell was determined by subtracting the background concentration from the total $PM_{2.5}$ concentration on days with an HMS smoke plume over the grid. Negative values were set to zero.

3.2.2.3 CMAQ 24-hour average and 1-hour maximum $PM_{2.5}$

Maji et al. (2024) used the Community Multiscale Air Quality Modeling System (CMAQ, version 5.4) to model $PM_{2.5}$ from six selected wildfires in NM during April 6, 2024 - August 22, 2024. These fires represented approximately 90% of the burned area during this period. While the majority of smoke was likely produced by larger fires, smoke from small fires was not included in this model, which could lead to an underestimation of smoke $PM_{2.5}$. Additionally, Maji et al. (2024) does not take into account the potential impacts of smoke from any other source not included in the emissions (e.g., prescribed fire smoke, smoke transported from other regions). We used estimates of 24-hour mean smoke $PM_{2.5}$ concentrations and the 1-hour daily maximum smoke $PM_{2.5}$ concentrations from this model, which were bias-corrected for the season using routine monitoring network data.

3.2.2.4 Comparison of total $PM_{2.5}$ estimates to in situ measurements

We compared total gridded $PM_{2.5}$ to all ground-based monitors (PurpleAir and EPA AQS sites) during April 6 - August 22, 2022, for the four products (Figure A2.2). Each product was gridded at 15 x 15 km, and the monitor observations were compared to the overlapping grid cell. The Regulatory-only product ($R^2 = 0.13$) and Regulatory + PA product ($R^2 = 0.51$) correlate more to all ground-based monitoring sites than the CMAQ 24-hour average ($R^2 = 0.09$) and CMAQ 1-hour maximum ($R^2 = 0.04$). The Regulatory + PA product mean absolute difference (1.49 $\mu g\ m^{-3}$) is lower than the other products (Regulatory only: 2.86 $\mu g\ m^{-3}$; CMAQ 24-hour average: 2.72 $\mu g\ m^{-3}$; CMAQ 1-hour maximum: 9.66 $\mu g\ m^{-3}$). The mean bias for the Regulatory + PA product (< 0.01%) is also lower than the other products (Regulatory-only: 0.17%; CMAQ

24-hour average: 12%; CMAQ 1-hour maximum mean bias: 1.48%). Lower values for the Regulatory + PA product are expected, since this product incorporates PurpleAir in situ measurements, where the other estimates do not. We could not directly compare our smoke $PM_{2.5}$ estimates that were used in this paper to in situ measurements because we lack the ability to determine whether observed $PM_{2.5}$ originated from smoke or other sources.

There is a relatively low R^2 for the Regulatory-only product compared to the Regulatory + PA product because we used all ground-based monitors (PurpleAir and EPA AQS sites) for this evaluation, and the Regulatory-only product does not use PurpleAir sensors to make estimates. The poor correlation between the Regulatory-only product and the PurpleAir sensors emphasizes that the low-cost sensors are monitoring more spatial variability than what is observed by the EPA AQS monitors. This suggests that the regulatory-monitor density may be too low to capture local wildfire smoke exposure. Additionally, we optimized the kriging parameters in the Regulatory + PA product for the spatial interpolation using the full year of observations, and the Regulatory-only product uses several years to develop the kriging parameters. If we had used kriging parameters derived for each day, the correlations for both products would be higher; however, daily optimization increases computational demands and reduces repeatability, which limits its applicability for long-term or large-scale epidemiological studies. We instead chose fixed kriging parameters for the whole season consistency with prior work and to make the product more reproducible.

3.2.3 Measures of health outcomes

We retrieved 2022 ZIP code-level daily counts of emergency department (ED) visits, through the New Mexico Department of Health databases. Non-federal facilities (i.e., Indian Health Services and Veterans Affairs facilities) are not included in this dataset, thus undercounting those populations. We investigated a suite of ED primary diagnoses, including visits for asthma morbidity (J45), pneumonia (J12-J18), acute bronchitis (J20-J22), chronic obstructive pulmonary disease (COPD; J44), heart failure (I50), cardiac arrest (I46), heart arrhythmia (I47-I49), ischemic heart disease (I20-I22, I24-I25), myocardial infarction (I21-I22), and cerebrovascular disease (I60-I163, I65-I69, G45, I23). We also investigated "all respiratory" and "all cardiovascular" related ED visits, which include a broader range of billing codes. The ICD-10 codes defining each diagnosis are provided in the supplemental material (Table B 1.1).

For this analysis, we used health data from patients who reported a billing address with a valid NM ZIP code. This excludes patients who are not NM residents and individuals who are unhoused (2% of total visits). There were also several records with erroneously reported ZIP codes (e.g., "XXXXX", less than 5 digits, etc.) that were removed (1% of total visits).

3.2.3.1 Health data quality procedures

We removed duplicates from the ED data, when single individuals were recorded as having visited a facility two or more times on a given date using the patient identification number (< 1% of total visits). All diagnosis codes from duplicate records were included in the singular record that was used for analysis when multiple records existed with different codes. Because patient identification numbers are facility-specific, it was not possible to remove duplicate records if a patient was transferred to another facility. Although transferring is not very common with ED visits, this could result in potential overcounting of incident outcomes.

Patients may have visited the ED multiple times during the duration of our study. Due to the nature of our analysis, ED visits must be a rare event and not a frequent occurrence. We used the patient identification number to remove all facility visits following the first recorded visit during the study period (1% of total visits). Since identification numbers are facility-specific, we cannot remove multiple visits for patients who visited several different facilities in NM, again resulting in potential overcounting of incident outcomes.

3.2.4 Merging health records and smoke exposure estimates

We used the US Census Bureau 2010 5-Digit ZIP Code Tabulation Area (ZCTA) shape files to produce population-weighted smoke exposure estimates (US Census Bureau, 2010). In NM, there are several ZIP codes that correspond to Postal Office (PO) boxes, which do not contain geographic/spatial coordinates. ZIP codes relating to PO boxes were not included in the 2010 ZCTA files, and were excluded from the subsequent analysis

3.2.5 Time-stratified case-crossover study design

To evaluate the associations between health outcomes and $PM_{2.5}$ from smoke, we used a time-stratified case-crossover study design (Gan et al., 2017, 2020; Hahn et al., 2021; Janes et al., 2005a, 2005b; Magzamen et al., 2021). In this method, the reported case is used as its own control, which adjusts for individual-level confounders (e.g., age, sex, race). To account for exposures causing delayed health effects, we used a distributed lag-model for days 0-5. Using this model allowed us to assess the effects of exposure to smoke $PM_{2.5}$ across each lagged day. We constrained the models with a natural spline with three degrees of freedom (Gasparrini et al., 2017).

We matched 24-hour (and 1-hour maximum) smoke $PM_{2.5}$ data to each corresponding case. We compared the smoke $PM_{2.5}$ for each case to the same day of the week for all weeks during the two different referent periods: April 1 - September 30, 2022, and April 6 - August 22, 2022. The shorter referent period was selected because the CMAQ smoke data was only produced during the Calf Canyon/Hermit's Peak fire (April 6 - August 22, 2022) (Maji et al., 2024). By conducting this sensitivity analysis, we acknowledge the ZIP codes may have had constant smoke exposure in the shortened referent period, potentially affecting result accuracy. We used conditional logistic regression to estimate associations between cardiorespiratory ED visits and a 10 μg m^{-3} increase in $PM_{2.5}$.

The daily population-weighted heat index was used as a time-varying confounder and lagged over days 0-5 with the daily smoke $PM_{2.5}$. The heat index was calculated using 4 x 4 km daily PRISM data (https://prism.oregonstate.edu/), which was averaged to ZIP-code level and population-weighted using NASA Socioeconomic Data and Applications Center (SEDAC) gridded world population (GPWv4) (Center for International Earth Science Information Network, 2023). We compared several $PM_{2.5}$ smoke products by conducting our analysis for each dataset, using the ED data for 2022. We calculated ORs with 95% confidence intervals (CIs).

3.3 Results

3.3.1 Wildfire smoke $PM_{2.5}$ seasonal overview

The $PM_{2.5}$ ground-based monitors in New Mexico measured varying concentrations during 1 April – 30 September 2022. Daily (24-hour) $PM_{2.5}$ concentrations ranged from 0 – 198 μg m^{-3} across all monitors (i.e., EPA regulatory monitors, IMPROVE monitors, PurpleAir sensors), with a standard deviation of 44.8 μg m^{-3}. About 14% of days during the wildfire smoke season had at least one monitor in the state with an AQI classified as "Unhealthy for sensitive groups" (24- hour $PM_{2.5}$ concentration ≥ 35.5 μg m^{-3} and ≤ 55.4 μg m^{-3}) and 9% of the days had an AQI classified as "Unhealthy" (24- hour $PM_{2.5}$ concentration ≥ 55.5 μg m^{-3} and ≤ 125.4 μg m^{-3}) (US EPA, 2024a) The maximum concentration of 198 μg m^{-3} was observed by a PurpleAir sensor on 24 June 2022 near the Calf Canyon/ Hermit's Peak fire.

In 2022, the population-weighted, state-wide $PM_{2.5}$ average for the Regulatory + PA smoke product was higher than the Regulatory-only product during 1 April - 30 September (1.3 versus 0.9 µg m^{-3}) as well as in the shorter period, during Calf Canyon/Hermit's Peak (1.6 versus 1.1 µg m^{-3}). The addition of PurpleAir sensors to the Regulatory-only estimate provided more measurements of $PM_{2.5}$ in northeastern New Mexico (NM), where Calf Canyon/Hermit's Peak occurred. There were more PurpleAir sensors in regions with higher percentages of days with HMS smoke plumes in the column during the wildfire (April 6 - August 22, 2022) than regulatory monitors (Figure A2.5); therefore, by only using the Regulatory-only measurements, smoke is missed. The CMAQ 24-hour average smoke $PM_{2.5}$ is on average lower than the Regulatory-only and Regulatory + PA product. The long-term average of the CMAQ 1-hour maximum is a more similar value to the Regulatory-only and Regulatory + PA products.

Table 3.1. State-wide average of New Mexico wildfire smoke and total $PM_{2.5}$ average concentrations (µg m^{-3}) for the four population-weighted smoke estimates during summer 2022. Standard deviation between ZIP codes is reported in parentheses.

Exposure Estimate	Dates in 2022	Smoke $PM_{2.5}$ Concentration (µg m^{-3})	Total $PM_{2.5}$ Concentration (µg m^{-3})
Regulatory-only product	1 April – 30 September	0.9 (2.4)	6.0 (3.9)
Regulatory-only product	6 April - 22 August	1.1 (2.7)	6.6 (4.2)

Regulatory + PA product	1 April - 30 September	1.3 (2.8)	6.0 (3.9)
Regulatory + PA product	6 April - 22 August	1.6 (3.1)	6.3 (4.2)
CMAQ 24-hour average	6 April - 22 August	0.3 (0.6)	5.7 (3.2)
CMAQ daily 1-hr maximum	6 April - 22 August	0.8 (2.1)	12.3 (9.7)

To investigate spatial variability in the smoke products, we compared estimates by ZIP code during summer 2022 (Figure 3.2). During the Calf Canyon/Hermit's Peak fire (April 6 – August 22, 2022), the ZIP code with the highest average smoke $PM_{2.5}$ concentration in the Regulatory-only product was 2.4 µg m^{-3} This occurred in Jal, NM (ZIP code: 88252) and was driven by a single nearby regulatory monitor in Hobbes, NM. All other regulatory monitors in NM were to the west of the Calf Canyon/Hermit's Peak wildfire and likely upwind. Although eastern NM experienced higher smoke $PM_{2.5}$ concentrations than western NM, this product does not show a clear increase in smoke $PM_{2.5}$ near the Calf Canyon/Hermit's Peak wildfire, likely due to the lack of monitors in close proximity to the fire. In comparison, the ZIP code with the highest average smoke $PM_{2.5}$ concentration for the Regulatory + PA product occurred near the wildfire. Cuevro, NM (ZIP code: 88417), located slightly southeast of the fire, had the highest average $PM_{2.5}$ of 4.6 µg m^{-3}. The PurpleAir sensors located east of the regulatory monitors, closer to the fire, provided additional estimates that contributed to higher smoke $PM_{2.5}$ concentrations in ZIP codes near the fire. The addition of PurpleAir sensors to the regulatory monitors was crucial for capturing smoke $PM_{2.5}$ near the wildfire, highlighting the importance of low-cost monitors in regions where regulatory networks are sparse.

For both CMAQ products (24-hour average and 1-hour maximum), the highest average smoke $PM_{2.5}$ concentration occurred at the wildfire location (ZIP code: 87731). Since Calf Canyon/Hermit's Peak was the largest wildfire included in the model, this result is expected. For the 24-hour average product, the highest average smoke $PM_{2.5}$ concentration was 2.6 $\mu g\ m^{-3}$, and the highest concentration for the 1-hour maximum product was 9.2 $\mu g\ m^{-3}$. The highest CMAQ 24-hour average smoke $PM_{2.5}$ during the wildfire gave closer estimates to the Regulatory-only and Regulatory + PA products. However, the CMAQ 1-hour maximum had a wider spread of smoke impacts than the CMAQ 24-hour product, with more ZIP codes with higher concentrations. The measurement-based products showed a more similar pattern, with many smoke-impacted ZIP codes near the wildfire. We conducted our subsequent epidemiological analysis with both the CMAQ 24-hour average and the CMAQ 1-hour maximum.

Estimates of total $PM_{2.5}$ have diverse spatial patterns across the products. The Calf Canyon/Hermit's Peak fire is most distinguishable in total $PM_{2.5}$ from the Regulatory + PA smoke product, with the highest ZIP code smoke $PM_{2.5}$ estimate occurring near the fire (ZIP code: 88421: Garita, NM). For both CMAQ total $PM_{2.5}$ estimates, there were also increased concentrations in southeast NM compared to central and northern NM. Because the model uses anthropogenic emissions from the EPA National Emissions Inventory (NEI), this increase in southeastern NM likely occurred due to oil and natural gas production in this region.

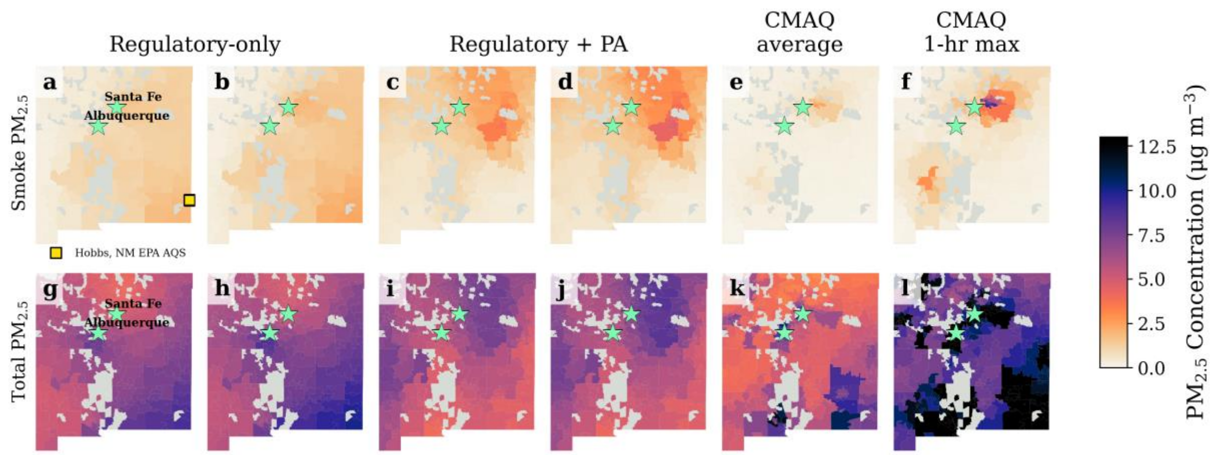

Figure 3.2. Comparison of ZIP code average population-weighted smoke $PM_{2.5}$ (top row) and total $PM_{2.5}$ (bottom row) for 2022. The Regulatory-only is shown for the entire wildfire season April 1 - September 30 (a & g) and for the duration of the Calf Canyon/Hermit's Peak wildfire (April 6 - August 22; b & h). The Regulatory + PA product is also shown for the entire wildfire season (c & i) and the shortened period (d & j). The CMAQ 24-hour average (e & k) and 1-hr maximum (f & l) products are limited to April 6 - August 22. One regulatory monitor is shown with a yellow square in subplot a). Gray areas are not affiliated with ZIP codes. Two major cities are identified with cyan stars.

3.3.2 Descriptive overview of cardiorespiratory emergency department visits

Cardiorespiratory-related emergency department (ED) visits for all patients in NM with valid ZIP codes during April 1 - September 30, 2022, and the corresponding age-related, gender-related, and race-related strata are reported in Table 3.2. Data for the shortened referent period (April 6 - August 22, 2022) can be found in the Supplement (Table B 1.2). During April 1 - September 30, 2022, there were a total of 73,766 visits to the ED for the health outcomes of interest. However, because broader categories (e.g., all-respiratory) encompass specific conditions (e.g., asthma), this total includes duplicate counts of visits classified under multiple health outcome categories. About 40% of the ED visits were due to all respiratory-related outcomes (n = 29,489), compared to 20% for cardiovascular-related outcomes (n = 15,478). Pneumonia accounted for the highest number of visits among individual health outcomes, representing 7% of the total.

NM has a higher proportion of people who identify as Hispanic/Latino and American Indian and Alaska Native compared to other US states, as shown in the demographic summary (Table 2). The largest percentage of people who visited the ED during this period were Hispanic (46%). The next largest was white (42%). There were over 12% more Hispanic patients who visited the ED for a respiratory-related health outcome (49.4%) than Hispanic patients who visited for a cardiovascular-related health outcome (36.7%); however, there were > 17% more white patients with cardiovascular-related health outcomes (51.6%) than respiratory-related (33.9%). Our study did not include data from the Indian Health Services (IHS) or Veterans Affairs (VA) facilities; therefore, our race-related strata may not be completely representative of the entire NM population. About 6% of the NM population are veterans and 11% identify as American Indian/Alaskan Native (US Census Bureau, 2023), but the precise number of these populations who used IHS or VA facilities in 2022 is unknown.

Table 2. Summary of cardiorespiratory-related Emergency Department (ED) visits in New Mexico between April 1 - September 30, 2022. American Indian/Alaskan Native is abbreviated as AIAN, and Asian/Native Hawaiian/Pacific Islander is abbreviated as AANHPI. Corresponding ICD-10 codes are provided in Table S1 and a summary for ED visits from April 6 - August 22, 2022, in Table S2.

		Age Category			Sex		Race/Ethnicity					
Health Outcomes	Cases (n)	<15 (%)	15 to 65 (%)	65 (%)	Male (%)	Female (%)	AIAN (%)	AANHPI (%)	Black (%)	Hispanic (%)	White (%)	Unknown (%)
All respiratory	29,489	30.7	49.7	19.6	46.7	53.3	9.0	0.7	2.7	49.4	33.9	4.3
Asthma	3,373	32.2	59.7	8.1	45.4	54.6	8.1	0.8	4.7	54.3	27.9	4.2
COPD	1,887	0.2	38.0	61.8	44.7	55.3	1.5	0.5	2.4	30.0	62	3.7
Pneumonia	5,102	15.1	42.9	42.1	50.2	49.8	6.4	0.5	2.4	42	45.4	3.3
Acute bronchitis	4,082	44.9	42.6	12.6	47.7	52.3	7.9	0.5	2.3	55.3	30.3	3.7
All Cardiovascular	15,478	0.3	43.5	56.2	53.9	46.1	3.7	0.8	2.6	36.7	51.6	4.4
Cardiac Arrest	487	4.1	46.2	48.9	61.2	38.8	5.1	0.8	4.3	38.6	39	12.1
Arrhythmia	3,121	0.2	38.5	61.3	52.6	47.4	2.8	0.8	1.4	26	63.5	5.4
Heart Failure	856	-	41	59	56.1	43.9	3.4	0.7	1.5	37.1	53.4	3.9
Ischemic Heart Disease	3,587	-	46.1	53.9	63.5	36.5	2.9	0.9	2.0	39.8	50.8	3.6
Myocardial Infarction	3,173	-	46.2	53.8	64.3	35.6	2.7	1.0	2.1	40.0	50.4	3.8
Cerebrovascular Disease	3,131	0.3	34.9	64.8	51.1	48.9	5.2	0.9	2.2	37.0	50.9	3.7
TOTAL	73,766	9,097	21,540	14,850	22,349	23,137	4,678	537	1,923	32,225	31,308	3,095

3.3.3 Comparison of smoke estimates in epidemiological results

Odds ratios (ORs) from distributed-lag models for a 10 μg m^{-3} increase in smoke $PM_{2.5}$ exposure are shown in Figure 3.3 for the four smoke estimates: Regulatory-only, Regulatory + PA, CMAQ 24-hour average, and CMAQ 1-hour maximum. To facilitate this comparison, we used the referent period April 6 - August 22, 2022 because the CMAQ $PM_{2.5}$ was only produced during this time. By using this shortened referent period, we acknowledge that some ZIP codes may have had constant smoke exposure, potentially affecting result accuracy. A more detailed comparison of referent period selection is provided in Section 3.3.4.

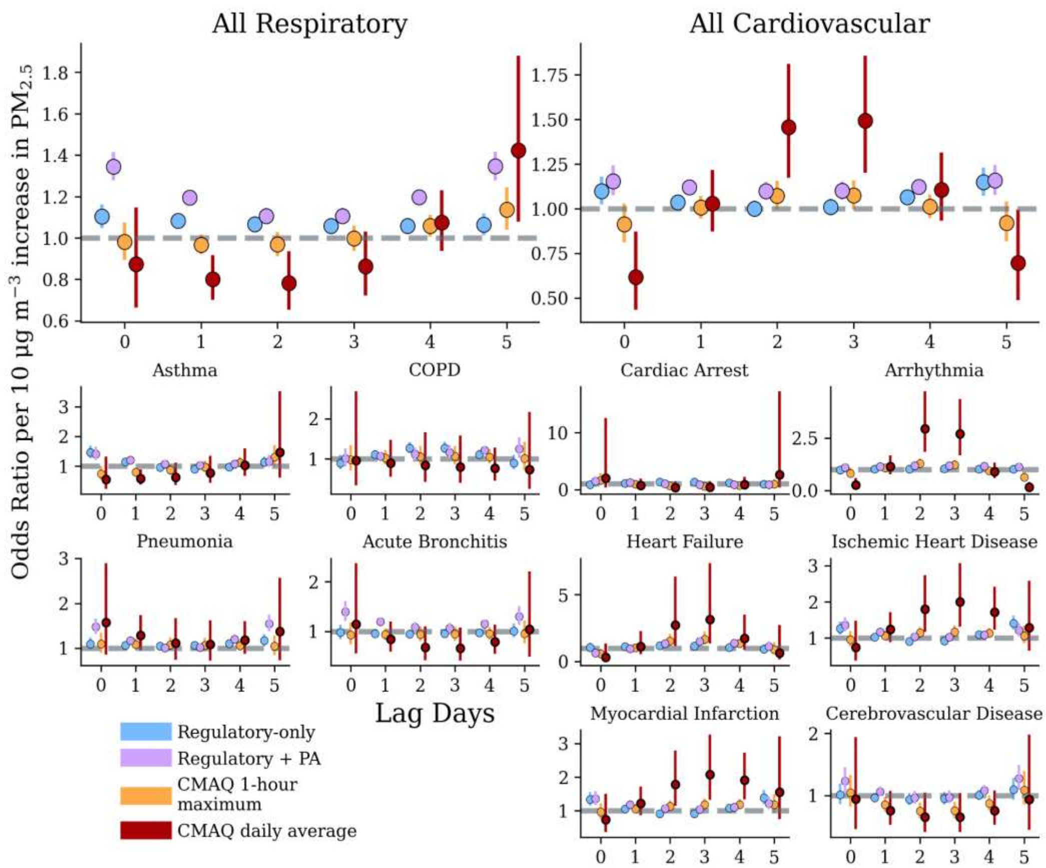

Figure 3.3. Distributed-lag effects of a 10 μg m^{-3} increase in wildfire smoke $PM_{2.5}$ on likelihood of cardiorespiratory emergency department visits during April 6 - August 22, 2022 for the smoke products: Regulatory-only (blue), Regulatory + PA (purple) and the CMAQ 1-hour maximum (orange) and CMAQ 24-hour average (red).

Smoke misclassification can lead to inconsistent results. With EPA monitors in only five out of 33 counties in NM, smoke misclassification can be considerable even when leveraging permanent ground-based monitors. Smoke $PM_{2.5}$ exposure had a negative association for all respiratory-related ED visits using the CMAQ 24-hour average product (Lag 1 OR = 0.80, 95% CI = 0.70, 0.92; Lag 2 OR = 0.78, 95% CI = 0.65, 0.94); however, all other products show increased odds or results that were not significant. Wildfire smoke exposure should not cause a decrease in ED visits for all-respiratory health outcomes as shown with the CMAQ data. The "false protective" effects (OR < 1) from using the CMAQ 24-hour average is likely due to smoke misclassification. For example, if there were high concentrations of smoke $PM_{2.5}$ in a region corresponding to an increase in all respiratory-related ED visits, but the CMAQ model results showed low concentrations in that region, there would be a false protective effect.

The ORs for the CMAQ 24-hour average smoke $PM_{2.5}$ estimates are much higher in magnitude, with larger confidence intervals (CIs) than the other products. The largest OR for the CMAQ 24-hour average is 3.16 (Heart Failure: Lag 3 OR = 3.16, 95% CI = 1.36, 7.36), compared to the largest OR for the Regulatory + PA product of 1.55 (Pneumonia: Lag 5 OR = 1.55, 95% CI = 1.38, 1.74). The largest CIs for the CMAQ 24-hour average (Cardiac Arrest: Lag 5 OR = 2.58, 95% CI = 0.39, 17.18) is over 15 times larger than the largest interval for the Regulatory + PA product (Cardiac Arrest: Lag 0 OR = 1.50, 95% CI = 0.97, 2.31). Our epidemiological results change considerably across smoke exposure products.

Modeling smoke in this region is particularly challenging for prognostic models like CMAQ due to complex terrain and the dynamic nature of the local Calf Canyon/Hermit's Peak fire. These factors can increase the potential for exposure misclassification. Additionally, because the CMAQ estimates included only six fires in NM during 2022, they may underestimate smoke exposure. Smaller fires in NM occurred during this time period that were not included in the model, and there may have been transported smoke from other states, leading to an underestimation of smoke $PM_{2.5}$ concentrations. All smoke estimates used in this study rely on the regulatory monitoring network, which may not provide sufficient spatial coverage to create quantitative smoke $PM_{2.5}$ estimates in NM, particularly in rural and fire-impacted regions. Expanding low-cost sensor networks, such as PurpleAir, could improve exposure estimates in areas with limited monitoring. Given these limitations, the use of smoke $PM_{2.5}$ estimates in epidemiological studies should be carefully evaluated on a case-by-case basis.

3.3.4 Epidemiological results when implementing different referent periods

We compared results of the distributed-lag models for the Regulatory-only and Regulatory + PA smoke products for two referent periods: April 1 - September 30, 2022, and April 6 – August 22, 2022 (Figure 3.4). Results are shown for all-respiratory and all-cardiovascular ED visits, with referent period comparisons for all individual ICD-10 codes available in the Supplement (Figures A2.6 and 2.7). The addition of PurpleAir observations to the EPA AQS monitors provided more $PM_{2.5}$ measurements in regions with higher percentages of days with smoke in the atmospheric column (Figure A2.5), leading to an increase in smoke $PM_{2.5}$ concentrations. While we acknowledge these differences, our focus in this section is to evaluate the impact of referent period selection.

The results across referent periods for all respiratory-related ED visits with the Regulatory-only product are more consistent compared to all-cardiovascular as well as the all-respiratory related results for the Regulatory + PA product. There were significant associations on Lags 0-2 and 4 for the April 1 - September 30 referent period with the Regulatory-only product (Lag 0 OR = 1.05, 95% CI: 1.01, 1.10; Lag 1 OR = 1.04, 95% CI: 1.02, 1.06; Lag 2 OR

= 1.03, 95% CI: 1.00, 1.06; Lag 4 OR = 1.02, 95% CI: 1.00, 1.05) and for the April 6 - August 22 referent period (Lag 0 OR = 1.10, 95% CI: 1.05, 1.16; Lag 1 OR = 1.08, 95% CI: 1.06, 1.11; Lag 2 OR = 1.07, 95% CI: 1.03, 1.10; Lag 4 OR = 1.06, 95% CI: 1.03, 1.08). In comparison, all lagged days for the Regulatory-only product had significant associations with all-respiratory related ED visits for the shorter referent period during the wildfire. There were several lagged days for the Regulatory-only product and the longer referent period without significant results. There were no significant associations for the Regulatory-only product and all-cardiovascular related ED visits for the longer referent period. The shorter referent period for this product had significant associations for all lagged days 0-1 and 4-5 (Lag 0 OR = 1.10, 95% CI: 1.02, 1.18; Lag 1 OR = 1.04, 95% CI: 1.00, 1.07; Lag 4 OR = 1.06, 95% CI: 1.03, 1.10; Lag 5 OR = 1.15, 95% CI: 1.07, 1.23). With Calf Canyon/Hermit's Peak burning for the duration of the April 6 - August 22 referent period, there likely were not enough days with lower smoke $PM_{2.5}$ concentrations to provide a meaningful comparison for exposure. While the shorter referent period showed more significant associations, we have greater confidence in the longer referent period due to including a smoke-free period at the end of the smoke season.

Similar to the Regulatory-only smoke estimate, there were significant associations with all respiratory-related ED visits and a 10 $\mu g\ m^{-3}$ increase in smoke $PM_{2.5}$ for both referent periods using the Regulatory + PA estimates. The magnitude of the ORs for the shorter referent period (Lag 0 OR = 1.34; Lag 1 OR = 1.20; Lag 2 OR = 1.11; Lag 3 OR = 1.11; Lag 4 OR = 1.20; Lag 5 OR = 1.35) were higher than odds for the longer referent period (Lag 0 OR = 1.09; Lag 1 OR = 1.05; Lag 2 OR = 1.03; Lag 3 OR = 1.02; Lag 4 OR = 1.03; Lag 5 OR = 1.05). There were no significant results for all-cardiovascular related ED visits and the longer referent period; however all lagged days for the shorter referent period had significant associations. These findings emphasize the importance of selecting a suitable referent period.

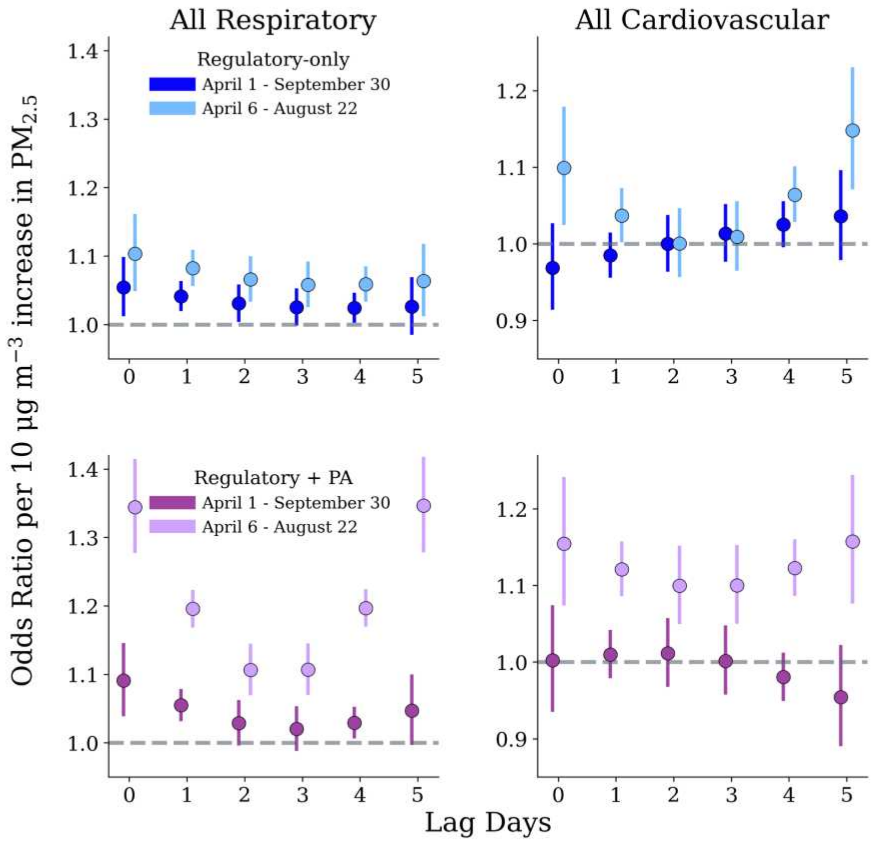

Figure 3.4. Distributed-lag effects of a 10 μg m^{-3} increase in wildfire smoke $PM_{2.5}$ on likelihood of all respiratory (left) and cardiovascular (right) related emergency department visits during April 1 - September 30, 2022 and April 6 - August 22, 2022 for two smoke products: Regulatory-only (top; blue) top) and Regulatory + PA (bottom; purple).

3.3.5 Association with smoke exposure by health outcome

In the following section, we present quantitative findings on significant association with a 10 μg m^{-3} increase in smoke $PM_{2.5}$ and ED visits. We have shown that the selection of the referent period and the smoke estimation method can influence these associations; therefore, the following discussion should provide insight into overall patterns during the 2022 NM wildfire season but should not be interpreted as precise and absolute results. We compare the Regulatory-only product and the Regulatory + PA for the referent period April 1 - September 30, 2022, as we have more confidence in these estimates and referent period (Figure 3.5).

Asthma morbidity is often associated with exposure to wildfire smoke (Gan et al., 2020; Johnston et al., 2002; Rappold et al., 2011; Reid et al., 2016); however, we did not observe this in our results. With the Regulatory + PA product, we observed protective effects for asthma on lag days 4-5 (Lag 4 OR = 0.91, 95% CI: 0.84, 0.98; Lag 5 OR = 0.83, 95% CI: 0.70, 0.97). There were no significant associations with the Regulatory-only product. These results may be due to variations in smoke exposure estimates or misclassification of exposure, as we have demonstrated how different smoke estimates can influence results. There were also no significant associations observed for COPD, cardiac arrest, and heart arrhythmia for either product.

Other contextual factors may also explain the lack of positive associations between smoke exposure and asthma. Asthma is more prevalent in children than older adults (Global Asthma Network, 2022), and the most smoke-impacted regions in NM had a large population of people 65 or older (US Census Bureau, 2023). This demographic difference may explain why our study did not find significant positive associations with asthma, as observed in previous studies. Additionally, there were evacuation orders in northeastern NM during the wildfire season (Baca & Schear, 2022), and health agencies strongly communicated about smoke risks. The communication with the public may have prompted behavior changes (e.g., sheltering indoors, using air filtration, etc.), which could have reduced exposure and asthma morbidity. These protective actions, combined with population characteristics, may have decreased the associations between wildfire smoke exposure and asthma-related ED visits.

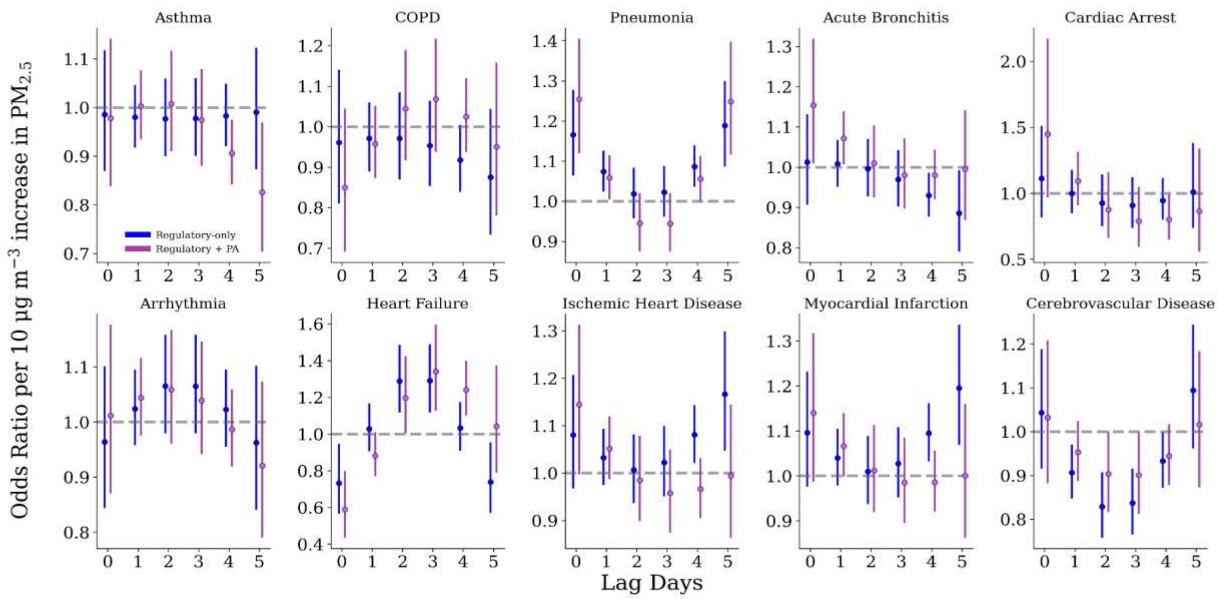

Figure 3.5. Distributed-lag effects of a 10 μg m^{-3} increase in wildfire smoke $PM_{2.5}$ on likelihood of cardiorespiratory emergency department visits during April 1 - September 30, 2022 for the smoke products: Regulatory-only (blue) and Regulatory + PA (purple).

We observed significant increased risk in ED visits for pneumonia during Lags 0-1 for both the Regulatory-only smoke product (Lag 0 OR = 1.17, 95% CI: 1.06, 1.28; Lag 1 OR = 1.07, 95% CI: 1.02, 1.13) and the Regulatory + PA smoke product (Lag 0 OR = 1.25, 95% CI: 1.12, 1.41; Lag 1 OR = 1.06, 95% CI: 1.00, 1.11). Pneumonia is caused by a suite of infectious respiratory pathogens with the highest prevalence in winter. The positive associations observed in this analysis with exposure to wildfire smoke may be a result of exposure misclassification. There were significant associations with acute bronchitis for the Regulatory + PA product (Lag 0 OR = 1.15, 95% CI: 1.01, 1.32; Lag 1 OR = 1.07, 95% CI: 1.01, 1.14), with the most inconsistent results between the Regulatory + PA and the Regulatory-only product ORs on Lag 0 (difference: 0.14). These findings suggest a potential association between wildfire smoke exposure and respiratory infections, though differences between smoke exposure estimates highlight the need for careful consideration of exposure misclassification in epidemiological studies.

Our distributed-lag model showed increased odds of heart failure on lag days 2 and 3 for the Regulatory-only smoke product (Lag 2 OR = 1.29, 95% CI: 1.12, 1.49; Lag 3 OR = 1.29, 95% CI = 1.12, 1.49) and Regulatory + PA (Lag 2 OR = 1.20, 95% CI: 1.01, 1.42; Lag 3 OR = 1.34, 95% CI = 1.13, 1.60). Older populations are often more susceptible to experiencing heart failure, and there was a large percentage of people 65 or older near the wildfire. Although heart failure has a strong significant association with smoke exposure in this analysis, when considering all cardiovascular-related health outcomes (Figure 3.4), there is not a significant association. Previous studies have shown that exposure to wildfire smoke corresponds more consistently to respiratory-related health effects than cardiovascular-related (Liu et al., 2015; Reid et al., 2016). The increased odds for heart failure in this study may be influenced by the high proportion of residents aged 65 and older in the smoke-impacted region or potential misclassification of smoke exposure.

Overall, the Regulatory-only and the Regulatory + PA product provide similar results for our distributed-lag model for all health outcomes. Although the Regulatory + PA product includes more observations than the Regulatory-only, the shared methodological framework for the two products and overlapping measurements from regulatory sites contributes to their comparable outcomes. The largest difference in ORs for these products occurred with cardiac arrest (Regulatory-only: Lag 0 OR = 1.11, 95% CI: 0.82, 1.51; Regulatory + PA: Lag 0 OR = 1.45, 95% CI: 0.97, 2.17). For some health outcomes, the choice of smoke product impacted the significance and overall conclusions. For example, there are significant protective effects with the Regulatory-only smoke estimates and cerebrovascular disease (Lag 1 OR = 0.91, 95% CI: 0.85, 0.97; Lag 2 OR = 0.83, 95% CI: 0.76, 0.91; Lag 3 OR = 0.84, 95% CI: 0.76, 0.92; Lag 4 OR = 0.93, 95% CI: 0.87, 0.99). This relationship was only present with the Regulatory + PA product on Lag 3 (OR = 0.90, 95% CI: 0.81, 0.99), with all other days having no significant associations. This again demonstrates the importance of selecting a smoke exposure estimate in epidemiological studies.

3.4 Conclusions

We investigated how different smoke exposure inputs to an epidemiological study impacted the assessment of health outcomes associated with wildfire smoke exposure in New Mexico (NM) during 2022. The Calf Canyon/Hermit's Peak Fire occurred in northeastern NM from April - August 2022. We used NM Emergency Department (ED) visits by ZIP code and a 10 $\mu g\ m^{-3}$ increase in smoke $PM_{2.5}$ to calculate the distributed-lag effects. We compared four exposure estimates in our analysis: 1) $PM_{2.5}$ from the EPA AQS monitors, 2) $PM_{2.5}$ from both the EPA AQS monitors and low-cost PurpleAir observations, 3) modeled 24-hour average wildfire smoke $PM_{2.5}$ from the Community Multiscale Air Quality Modeling System (CMAQ), and 4) CMAQ daily 1-hour maximum wildfire smoke $PM_{2.5}$. Modeling smoke $PM_{2.5}$ for a dynamic fire in an environment with varying topography brings many challenges, and we determined the chemical transport model estimates (CMAQ) were not as useful for estimating exposure-response relationships for acute events.

Low-cost monitors were essential for creating useful smoke estimates, particularly in rural areas where regulatory monitors are sparse. In NM, most regulatory monitors are located in populated areas like Albuquerque, Santa Fe and Las Cruces, making them less effective for capturing wildfire smoke exposure in rural regions. We found the regulatory monitor density may be too low to capture wildfire smoke exposure in this region due to the poor correlation between the regulatory monitor product and the PurpleAir sensor observations. Adding low-cost sensors improved spatial coverage for our smoke exposure estimates, but large areas of the state likely impacted by smoke still lacked monitors. Therefore, gaps in monitors remained in our smoke estimates that used EPA AQS monitors and PurpleAir sensors, potentially leading to exposure misclassification. For ground-based smoke estimates to be accurate, the monitoring network must be dense enough to capture spatial gradients in smoke exposure. This challenge is particularly evident with large, dynamic fires like Calf Canyon/Hermit's Peak, where smoke conditions changed rapidly across the landscape.

Selection of the referent period in our study impacted the results. We compared all-cardiovascular and all-respiratory related ED visits for two referent periods: April 6 - August 22, 2022 (during Calf Canyon/Hermit's Peak) and April 1 - September 30, 2022 (the entire wildfire season). Because the CMAQ output was only available for the shortened referent period, we conducted this sensitivity analysis to investigate exposure and adverse health outcome differences. We found our results were inconsistent using different referent periods because the shorter referent period had a lack of days without smoke exposure in some ZIP codes.

We used the smoke estimates from the EPA AQS monitors and PurpleAir sensors to explore associations between smoke exposure and individual health outcomes, acknowledging their dependence on referent period and smoke exposure selection. We did not find a significant association with asthma, which has been found in other studies. Heart failure was the most significant association compared to the other health outcomes. These findings may be due to the large population of people 65 or older in the ZIP codes most impacted, or it may be due to exposure errors remaining, even in the product with both EPA AQS and PurpleAir $PM_{2.5}$ measurements.

There were many factors in 2022 that may have impacted our results. First, the COVID-19 virus may have resulted in residents not visiting the ED for smoke-related health impacts despite experiencing facing symptoms. In addition, many of the most smoke-impacted areas were rural, where residents often live farther from care facilities, potentially deterring ED visits due to longer travel times. Mandatory fire evacuations in many communities may have reduced the number of affected residents or led them to seek healthcare in other regions. There may have also been behavioral changes (e.g., staying indoors, wearing masks outdoors, changing home filters, etc.), due to the strong communication from health agencies as well as the persistent visibility of smoke in the air, which may have led to a decrease in ED visits. In addition to wildfire smoke, NM is impacted by prescribed and agricultural fire smoke, as well as transported smoke from fires in other regions. In 2017, the largest source of landscape-fire smoke $PM_{2.5}$ emissions was wildfires. Emissions from prescribed and agricultural fires are much smaller than those from wildfires (US EPA, 2017), but still contribute to the $PM_{2.5}$ concentrations. Smoke was transported to NM in 2022 from other regions, such as California, Arizona, and Mexico. These sources of smoke may have contributed to the smoke $PM_{2.5}$ exposure estimates from the ground-based measurements, while the chemical transport model output did not include these sources.

The exposure inputs to epidemiological studies are critical. Our analysis demonstrates that using different smoke exposure estimates can lead to varying health outcome associations, showing the importance of selecting appropriate exposure estimates based on study objectives and environmental factors. To overall improve smoke estimates, air quality monitoring networks must be expanded, especially in rural regions. As wildfires continue to grow in intensity and frequency due to climate change, accurately evaluating smoke exposure impacts on health will be critical for informing public health responses and healthcare planning.

3.5 Data Availability Statement

Population-weighted smoke $PM_{2.5}$ estimates for the four products ($PM_{2.5}$ from the EPA AQS monitors; $PM_{2.5}$ from both the EPA AQS monitors and low-cost PurpleAir observations; modeled 24-hour average wildfire smoke $PM_{2.5}$ from the Community Multiscale Air Quality Modeling System (CMAQ); CMAQ daily 1-hour maximum wildfire smoke $PM_{2.5}$) by ZIP code and population-weighted heat index by ZIP code can be accessed here: https://doi.org/10.5061/dryad.gb5mkkx2f. The code written to conduct this analysis can be found here: https://github.com/oliviasablan/New_Mexico_Wildfire. The emergency department data in this manuscript include protected health information (e.g., patient identification number, patient ZIP code, etc.) covered by the Health Information Portability and Accountability Act. Therefore, these data are not available due to data use agreements with the New Mexico Department of Health. Parties interested in reproducing or extending this work will need to set up their own data use agreements with the New Mexico Department of Health to receive this data.

CHAPTER 4

INVESTIGATING SMOKE-RELATED EMERGENCY DEPARTMENT VISITS AND SYNDROMIC SURVEILLANCE REPORTS IN NEW MEXICO 2019-2022[4]

4.1 INTRODUCTION

One limiting factor in determining health impacts of wildfire smoke is the unavailability and delay of health data. ED visits and hospitalizations are valuable datasets for retrospective analyses, but these data are typically released often a year following a wildfire smoke event. Previous studies using these datasets have linked $PM_{2.5}$ from wildfire smoke to increased risk of cardiorespiratory-related Emergency Department (ED) visits (Alman et al., 2016; Gan et al., 2020; Hahn et al., 2021; Rappold et al., 2011) and hospitalizations (Gan et al., 2017; Magzamen et al., 2021; Stowell et al., 2019), adverse pregnancy outcomes (e.g., low birth weight) (Abdo et al., 2019; Holstius et al., 2012), and cognitive decline (Zhang et al., 2023). Syndromic Surveillance (SS) is a real-time reporting system of chief complaints alongside or instead of discharge diagnoses of Emergency Department (ED) visits; however, there are fewer epidemiological studies that use SS reports (e.g., Doubleday et al., 2023; Miko et al., 2023; Smith et al., 2023; Swedo et al., 2023) compared to hospitalizations and ED visits. SS was developed to allow for faster detection of health events (e.g., disease outbreaks, natural disasters, opioid crises, etc.) by reporting symptoms either instead of or alongside confirmed diagnoses. Because these data are reported in real-time, SS can provide public health officials and healthcare providers with timely information to assess

[4] Adapted from a manuscript in preparation: Sablan, O., Ford, B., Hawkinson, C., Hu, L., Langer, C. E., Maichak, C., et al. (in prep) Investigating smoke-related emergency department visits and syndromic surveillance reports in New Mexico 2019-2022.

emerging health trends and make informed decisions but has been used less frequently in epidemiological studies of wildfire smoke exposure.

New Mexico (NM) is impacted annually by wildfires and often experiences transported smoke from more western states, but health impacts of smoke exposure are understudied in this region. In 2021, smoke was transported to NM from wildfires outside of the state (e.g., Arizona Telegraph Fire, California wildfires, etc.). In 2022, the state's largest wildfire, Calf Canyon/Hermit's Peak, burned a total of 1,382 km^2 (Tunby et al., 2023). The Black Fire in 2022 also burned 1,316 km^2 in southwestern NM in 2022 (Hulburd, 2022). Prior work suggests that transported and local smoke may have different health effects (Magzamen et al., 2021), but there is a lack of understanding of how different smoke events (i.e., long-range transport versus local wildfires) impacts health in rural populations, such as in NM. Many studies have focused on densely populated regions, like California (e.g., Delfino et al., 2009; Heft-Neal et al., 2023; Holstius et al., 2012; Jerrett et al., 2005; Wen et al., 2023), due to the greater data availability and larger sample sizes (i.e., population). In contrast, New Mexico is the 5th largest state by land mass, but ranks 36th in population, which results in a sparsely populated state with many rural and frontier areas.

Previous studies based in NM have evaluated impacts of specific smoke events or single regions within the state (e.g., Carrico & Karacaoglu, 2023; Maji et al., 2024; Resnick et al., 2015), providing valuable insight into localized effects and helping to build the foundation for wildfire smoke epidemiology in NM. Our study builds on this work by investigating state-wide health impacts across multiple years. This is especially important in a state like NM, which includes a large rural population with frequent exposure to both local and transported smoke.

We seek to understand the potential benefit of SS reports in assessing wildfire smoke exposure impacts in comparison to ED visits. SS reports have not been evaluated in NM to determine use for wildfire events. Here, we use 2019-2022 ED visits and SS reports along with our smoke exposure estimate which leverages regulatory monitors and satellite observations to calculate odds ratios in an epidemiological study. In Section 3.1, we compare seasonal, state-wide smoke $PM_{2.5}$ averages for each year of our study. We summarize the ED visits and SS reports in Section 3.2. We then compare results for three health outcomes in Section 3.3: respiratory-related, cardiovascular-related, and asthma. In Section 3.3, we also investigate the use of the air-quality related health outcomes for SS reports in determining smoke exposure impacts. Our goal is to determine if SS is useful for identifying health impacts associated with wildfire smoke exposure to allow for better planning and resource allocation during a wildfire smoke event in NM.

4.2 METHODS

4.2.1 Study area

This study focused on New Mexico regions with ZIP codes defined in the 2010 U.S. Census Bureau 5-Digit ZIP Code Tabulation Areas (ZCTAs) (US Census Bureau, 2010). Although more recent ZCTA data are available, the 2010 boundaries were used due to minimal changes in ZIP code coverage across the state, particularly in rural areas, and are not expected to impact results. Because New Mexico is largely rural, several sparsely populated regions lack defined ZCTAs and were therefore excluded. PM2.5 monitoring across the state was limited to 18 active EPA Air Quality System (AQS) monitors, which were concentrated in urban areas such as Albuquerque, Santa Fe, and Las Cruces (Figure 4.1).

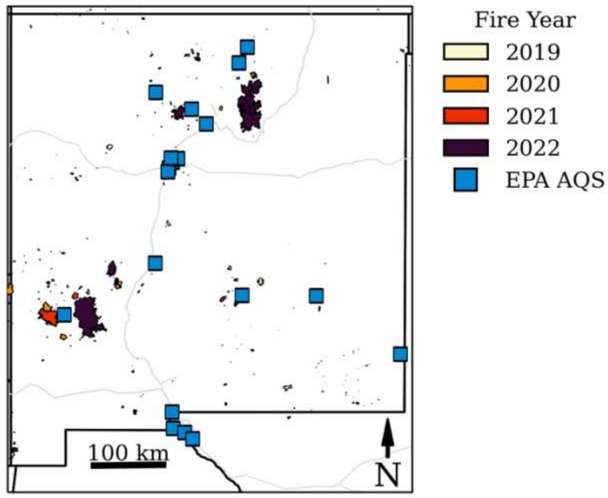

Figure 4.1. Map of study region and ground-based $PM_{2.5}$ sensors from the Environmental Protection Agency Air Quality System (EPA AQS) (blue squares). The fire perimeters from the National Interagency Fire Center (2025) during 2019-2022 are shaded by year of the fire. Major highways are provided in gray.

4.2.1.1 Study population

New Mexico (NM) has a population of ~2.1 million people across 315,194 km^2, so it is largely rural (US Census Bureau, 2023). Compared to other states, New Mexico has a large population of people that identify as Hispanic/Latino (49%), with a relatively lower percentage of people who identify as white (37%) (US Census Bureau, 2023). NM also has a large percentage of American Indian and Alaska Native (11%) compared to the entire US (1%). There are socioeconomic challenges in NM, with nearly 18% of the NM population living below the poverty line, as computed by the U.S. Census Bureau using income and family size in conjunction with defined Poverty Thresholds (US Census Bureau, 2023). This has implications for our study because populations in rural and underserved areas may face barriers to healthcare access and limited monitoring coverage.

4.2.2 Smoke exposure estimate

For our exposure estimate, we used daily smoke $PM_{2.5}$ concentrations derived using the method from O'Dell et al. (2019, referred to as the "O'Dell method product"), which provides total (all-source) $PM_{2.5}$ and smoke attributable $PM_{2.5}$. This product is created by spatially interpolating in situ $PM_{2.5}$ measurements from the US Environmental Protection Agency Air Quality System (EPA AQS; Figure 4.1), using ordinary kriging, a method for spatial interpolation (Gan et al., 2017; Isaaks & Srivastava, 1989; Janssen et al., 2008). Kriging assigns weights to observations based on their distance and spatial correlation. These values are used to estimate concentrations at every grid cell across the study region to result in a continuous, gridded surface. $PM_{2.5}$ is attributed to smoke using the presence of HMS smoke plumes from the National Oceanic and Atmospheric Science Hazard Mapping System (NOAA HMS) over the grid cell ("Hazard Mapping System Smoke Product," 2022). Fire type (i.e., prescribed fire, wildfire, agriculture fire) is not distinguished in the HMS; therefore, $PM_{2.5}$ estimates may not be exclusively from wildfire smoke. We focused on the April–September period to align with the typical wildfire season and reduce the likelihood of including smoke from prescribed or agricultural burns. However, during this period, transported smoke from wildfires upwind may still impact the estimates. The O'Dell method product has a gridded spatial resolution of 15 x 15 km. Seasonal background concentrations were removed from each grid cell by computing the median $PM_{2.5}$ concentration on days without an identified HMS plume for four climatological seasons (December-February, March-May, June-August, September-November).

Population-weighted ZIP code-level daily smoke $PM_{2.5}$ estimates were calculated using the NASA Socioeconomic Data and Applications Center (SEDAC) Gridded Population of the World, Version 4 (GPWv4) (Center for International Earth Science Information Network, 2023).

We computed the fractional overlaps between each 15 km grid cell and ZIP Code Tabulation Areas (ZCTAs). Therefore, a concentration is the sum of all gridded concentrations (*Pop_i*) multiplied by the population (*Pop_i*, regridded) (Center for International Earth Science Information Network, 2023) and the fractional overlap (*f_i*) of the grid (*i*) and the ZIP code, divided by the total population in the ZIP code, as shown in Equation 2.

$$PM_{2.5,ZIP\ Code} = \frac{\Sigma_{i=1}^{n} f_i * Pop_i * PM_i}{\Sigma_{i=1}^{n} f_i * Pop_i} \qquad \text{(eq. 2)}$$

The accuracy of this exposure estimate in NM is limited by the state's sparse monitoring network. Chapter 3 showed that smoke estimates require a sufficiently dense network to capture spatial gradients. Because we investigated several years, we used the O'Dell et al. (2019) product, while understanding the limitations.

4.2.3 Measures of health outcomes

We retrieved ZIP code-level daily counts of Emergency Department (ED) visits and SS reports, through the New Mexico Department of Health databases. The National Syndromic Surveillance Program (NSSP) is a voluntary healthcare facility reporting system that was initiated to provide near real-time reports of ED visits. This system was developed to support rapid detection of outbreaks and other public health emergencies by using chief complaints, either alongside or instead of discharge diagnoses. Because ED visits inform SS, these data sources should be similar; however, since reporting ED visits is mandatory and SSP is voluntary, the datasets are not identical. In addition, we cannot distinguish between primary and secondary diagnoses within SS, so all records with diagnoses codes of interest were included in our analysis, whereas only primary diagnoses were included from ED visits. Non-federal facilities (i.e., Indian Health Services and Veterans Affairs facilities) are not included in this dataset, thus undercounting populations served by these agencies.

We investigated a suite of ED primary diagnoses from 2019-2022, including visits for asthma (J45), pneumonia (J12-J18), acute bronchitis (J20-J22), chronic obstructive pulmonary disease (COPD; J44), heart failure (I50), cardiac arrest (I46), heart arrhythmia (I47-49), ischemic heart disease (I20-I22, I24-I25), myocardial infarction (I21-I22), and cerebrovascular disease (I60-I163, I65-I69, G45, I23). We also investigated “all respiratory” (J00-J98) and “all cardiovascular” (I00-I78) related ED visits, which include a broader range of billing codes. The ICD-10 codes defining each diagnosis are provided in the Appendix (Table A3.1).

We used four SS queries in our analysis: Broad Acute Respiratory DD v1, Air Quality-Related Respiratory Illness v1, Asthma, and Cardiovascular (Text A3.1). The Broad Acute Respiratory query identifies visits based on discharge diagnosis with a range of acute respiratory illnesses, including ICD-10 codes associated with general respiratory illness (e.g., cough, pneumonia). It is important to note that the broad respiratory query may include coronavirus, and our study period ends in 2022; however, we conducted an analysis for each year to investigate potential changes COVID-19 may have caused. The Air Quality-Related Respiratory query identifies ED visits based on discharge diagnosis and/or chief complaints for respiratory illnesses that are associated with poor air quality (e.g., shortness of breath and wheezing, acute bronchitis, acute respiratory distress syndrome, etc.). Although coronavirus is not explicitly included in the air quality-related respiratory illness query, coronavirus-related visits could be included based on the chief complaints. The NM-developed asthma query includes asthma morbidity and associated symptoms (e.g., wheezing, shortness of breath) and excludes coronavirus-related visits. The cardiovascular query follows the same ICD-10 codes as the ED “all cardiovascular” diagnosis. SS data was available for 2019-2022. Further information on the data queries is available in the Appendix.

For this analysis, we used health data from patients who reported a billing address with a valid NM ZIP code. This excludes patients who are not NM residents and individuals who are unhoused (2% of total visits). There were also several records with erroneously reported ZIP codes (e.g., “XXXXX”, less than 5 digits, etc.). For ED data, 1.15% of all data had an erroneous ZIP code or were representative of unhoused individuals and 0.01% in the SS data.

4.2.3.1 Health data quality control procedures

The SS data contained duplicated entries of reports within each query. To remove these duplicates, we followed the methods agreed upon by the National Environmental Health Public Tracking Syndromic Surveillance Content Workgroup and removed a visit if there was more than one entry with the same healthcare facility name, visit identification number, and medical record number. Duplicates accounted for 0.44% of all SS data, including all four queries. Additionally, we removed duplicates from the ED data, when single individuals were recorded as having visited a facility two or more times on a given date using the patient identification number (< 1% of total visits), and used the first visit. All diagnosis codes from duplicate records were included in the singular record that was used for analysis when multiple records existed with different codes. Because patient identification numbers are facility-specific, it was not possible to remove duplicate records if a patient was transferred to another facility. Although transferring is not very common with ED visits, this could result in potential overcounting of incident outcomes.

In addition, patients may have visited the ED multiple times during the duration of our study, potentially impacting both health datasets. Due to the nature of our analysis, ED visits must be a rare event and not a frequent occurrence. We used the patient identification number to remove all visits following the first recorded visit in our study period (2019-2022). Since identification numbers are specific to facilities, we cannot remove multiple visits for patients who visited several different facilities in New Mexico, again resulting in potential overcounting of incident outcomes. Data removed due to multiple visits accounted for 1% of all SS reports and <1% of ED total visits.

Because SS is not mandated, facilities occasionally have periods where they stopped reporting to this system. This can be due to technical issues, decreased staff, increased patient volume, facility closure, etc. For our case crossover analysis, we cannot consider the offline periods for SS in our referent period, as this could introduce a "false negative" by wrongly indicating there were no patients during this time, when instead the reporting system was offline. We determined 24 of the facilities in New Mexico remained completely online for the duration of the study period, and 12 facilities had periods where they stopped reporting. The regional hospital that serves the area most impacted by Calf Canyon/Hermit's Peak wildfire in 2022 went offline during the time of the fire. To find offline periods, we compared the daily total ED visits and the total SS reports, where all diagnoses were considered, including those not used in this study (Figure A3.1). We defined an offline period in SS to be when the number of daily ED visits were two times that of the daily SS reports. This accounted for 9.0% of SS data, after excluding facilities that were continuously online during the study period. Periods where SS facilities went offline were removed from all analysis.

4.2.4 Merging health records and smoke exposure estimates

We used the US Census Bureau 2010 5-Digit ZIP Code Tabulation Area (ZCTA) shape files to produce population-weighted smoke exposure estimates (US Census Bureau, 2010). In New Mexico, there are several ZIP codes that correspond to Postal Office (PO) boxes, which do not contain geographic/spatial coordinates. ZIP codes relating to PO boxes were not included in the 2010 ZCTA files and were excluded from the subsequent analysis. Overall, 1.8% of the SS data did not have a ZIP code included in the 2010 ZCTA file and 2.1% of the ED visit data.

4.2.5 Time-stratified case-crossover study design

To evaluate the associations between health outcomes and $PM_{2.5}$ from smoke, we used a time-stratified case crossover study design (Gan et al., 2017, 2020; Hahn et al., 2021; Janes et al., 2005b, 2005a; Magzamen et al., 2021). In this method, the reported case is used as its own control, which adjusts for individual-level confounders (e.g., age, sex, race). To account for past exposure causing delayed health effects, we used a distributed lag-model for days 0-5. We used a distributed-lag to assess the effects of exposure to smoke $PM_{2.5}$ across each lag day. Using this model allowed us to assess the effects of exposure to smoke $PM_{2.5}$ across each lagged day. We constrained the models with a natural spline with three degrees of freedom(Gasparrini et al., 2017).

We compared the smoke $PM_{2.5}$ for each case to the same day of the week for all weeks during the referent periods: April 1 - September 30 for 2019 - 2022. We matched 24-hour smoke $PM_{2.5}$ data to each corresponding case. Referent periods for SS facilities that went offline were removed. We used conditional logistic regression to estimate associations between cardiorespiratory ED visits and SS reports and a 10 $\mu g\ m^{-3}$ increase in $PM_{2.5}$.

The daily population-weighted heat index was used as a time-varying confounder and lagged over days 0 - 5 with the daily smoke $PM_{2.5}$. The heat index was calculated using 4 x 4 km daily PRISM data (https://prism.oregonstate.edu/), which was averaged to ZIP-code level and population-weighted using NASA Socioeconomic Data and Applications Center (SEDAC) gridded world population (GPWv4) (Center for International Earth Science Information Network, 2023). We calculated ORs with 95% confidence intervals (CIs).

4.2.6 Impacts of COVID-19 on our datasets and results

COVID-19 cases were reported in the US beginning in January 2020 (CDC, 2024), causing irregular patterns in the cardiorespiratory-related ED visits and SS reports from 2020-2021 (Figures A3.1). Because COVID-19 can cause symptoms that may also be associated with smoke exposure (e.g., shortness of breath, cough, congestion, fatigue, sore throat, etc.), ED visits and SS reports in this study may have included patients with coronavirus, especially before testing was widely available. Additionally, COVID-19 caused changes in health-seeking behaviors (Czeisler, 2020; Murray, 2021; Smith et al., 2023). For example, in one hospital in NM there were large decreases in total number of all-cause ED visits in March 2020, followed by steadily increasing ED visits until December 2020, where there is a brief decrease again associated with a spike in COVID-19 cases (Figure A3.1, a). Similar patterns were also observed at a hospital close to Calf Canyon/Hermit's Peak fire region (Figure A3.1, b). COVID-19 led to exceptional changes to total ED visits in NM.

Smoke $PM_{2.5}$ concentrations and COVID-19 rates both varied simultaneously across the study period in NM. We observed state-wide weekly average smoke $PM_{2.5}$ concentrations from our product to have interannual variability from 2020-2022 (Figure A3.2), with wildfire seasons generally occurring from April-September, though peak concentrations varied by month. COVID-19 rates were typically highest in October - December and January- February of 2020 and 2021, somewhat offset from the wildfire season. However, in 2022, increased COVID-19 rates coincided with increased smoke $PM_{2.5}$, resulting in overlapping exposure periods. These shifting temporal patterns highlight the complexity of studying smoke exposure during a pandemic.

To understand interannual variability and the potential impact of COVID-19 pandemic on our study, we examined all-respiratory-related ED visits and SS reports for each year individually from 2019 to 2022 (Figure A3.3). Both health datasets showed significantly decreased odds of respiratory-related visits/reports associated with wildfire smoke exposure during 2020 and 2021, which were the years most affected by COVID-19. It is important to note, the SS reports may have included COVID-19 cases, as the data did not distinguish between primary and secondary diagnoses, and SS reports chief complaints and/or billing codes. During these years, individuals experiencing smoke-related symptoms may have avoided the ED due to concerns about exposure to the virus or limited hospital capacity for care (Czeisler, 2020; Murray, 2021; Smith et al., 2023). These findings highlight how pandemic-related healthcare-seeking behavior may have influenced observed associations during 2020–2021, limiting our ability to draw strong conclusions about smoke exposure impacts in any individual year; instead, our results reflect aggregated results across 2019-2022.

4.3 RESULTS

4.3.1 Seasonal average wildfire smoke $PM_{2.5}$

We found interannual variability in the O'Dell et al. (2019) smoke product ("O'Dell method product") between wildfire seasons in NM. The state-wide population-weighted ZIP code smoke PM2.5 ranged from an seasonal average (April - September) of 0.2 µg m^{-3} to 1.7 µg m^{-3} across 2019-2022 (Table 4.1; Figure 4.2). Total $PM_{2.5}$ from this product also had variability year-to-year following the same pattern qualitatively as the $PM_{2.5}$ attributed to smoke. Following wildfire smoke, the second major source of primary $PM_{2.5}$ in NM was unpaved road dust in 2017 (US EPA, 2017), likely contributing to some changes in total $PM_{2.5}$ between years.

Table 4.1. Wildfire smoke ZIP code population-weighted $PM_{2.5}$ averages (μg m^{-3}) during summer (April - September) for 2019-2022. The 5th and 95th percentiles are reported in parentheses.

Year	Smoke	Total
2019	0.2 (0.1, 0.5)	4.8 (3.0, 7.2)
2020	1.1 (0.6, 1.6)	6.3 (5.1, 7.4)
2021	1.7 (1.4, 2.3)	7.3 (6.0, 9.2)
2022	0.9 (0.3, 1.6)	6.0 (4.4, 8.1)
All years	1.0 (0.8, 1.3)	6.1 (4.7, 7.6)

In 2022, Calf Canyon/Hermit's Peak burned for the majority of the wildfire season (April - August); however, there is not a clear regional increase in our smoke $PM_{2.5}$ product in the region most affected by the fire (Figure 4.2). Despite being the largest wildfire in state history, the impact is not distinguishable in the smoke $PM_{2.5}$ estimates, largely due to the lack of regulatory monitors in northeastern New Mexico near the burn area (Figure 4.1Only two EPA AQS monitors were located in the main direction of smoke outflow toward the southeast, contributing to the increased smoke $PM_{2.5}$ values observed in southern New Mexico in 2022. Other years (2020-2021) had higher seasonal average smoke $PM_{2.5}$ than 2022, despite less active wildfire seasons in NM. This shows the limitations of the smoke exposure estimates in NM, as they rely on interpolation of sparse monitor coverage, with large regions where smoke can be misclassified.

NM was impacted by transported smoke largely from Arizona and California during this study, leading to widespread, spatially homogeneous increases in $PM_{2.5}$ (Figure 4.2). The most significant years for smoke $PM_{2.5}$ for this product are 2020 and 2021 with seasonal averages of 1.1 and 1.7 µg m^{-3}, respectively. Both of these seasons were impacted by transported smoke. The summer of 2021 was more impacted by transported smoke than 2020, due to several large wildfires in other nearby states. In July 2021, the Telegraph Fire burned over 180,000 acres in south-central Arizona (Arizona Game and Fish Department, 2024). During April - September 2021, there were also several large wildfires in southern California, including the Palisades Fire, Chaparral Fire, and the Southern Fire (Cal Fire, 2025). There were large wildfires near NM in 2020. The Bush Fire occurred in south-central Arizona, and southern California was impacted by the Apple Fire and Ranch 2 Fire.

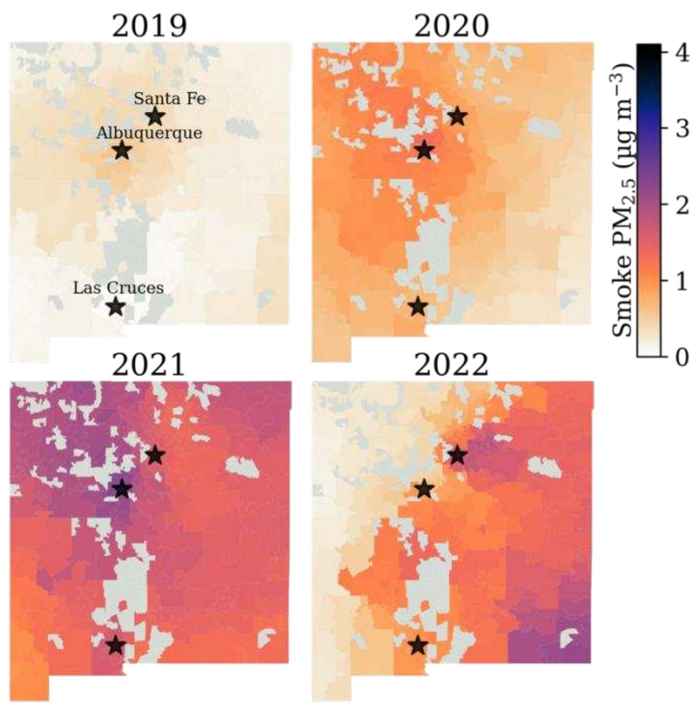

Figure 4.2. ZIP code average smoke $PM_{2.5}$ in New Mexico from 2019 - 2022 for April - September. Gray regions do not have a ZCTA code. Averages for 2016-2018 can be found in the Supporting Information (Figure A3.4).

4.3.2 Cardiorespiratory Emergency Department visits and Syndromic Surveillance reports

During the study period, there were a total of 253,772 visits to the ED for the health outcomes of interest. However, because broader categories (e.g., all-respiratory) encompass specific conditions (e.g., asthma), this total includes duplicate counts of visits classified under multiple health outcome categories. There were over 10% more Hispanic patients who visited the ED for a respiratory-related health outcome (48%) than Hispanic patients who visited for a cardiovascular-related health outcome (35%); however, there were over 15% more white patients with cardiovascular-related health outcomes (52%) than respiratory-related (35%). A summary of the cardiorespiratory-related ED visits for all patients in NM with valid ZIP codes during the 2016-2022 wildfire smoke season (April-September) with age, gender, and race-related strata can be found in Table 4.2.

Table 4.2. Summary of cardiorespiratory-related Emergency Department (ED) visits in New Mexico between April-September for 2019-2022. American Indian/Alaskan Native is abbreviated as AIAN, and Asian/Native Hawaiian/Pacific Islander is abbreviated as AANHPI. Corresponding ICD-10 codes are provided in the Supporting Information (Table A3.1).

		Age Category			Sex		Race/Ethnicity					
Health Outcomes	**Cases (n)**	**<15 (%)**	**15 to 65 (%)**	**65 (%)**	**Male (%)**	**Female (%)**	**AIAN (%)**	**AANHPI (%)**	**Black (%)**	**Hispanic (%)**	**White (%)**	**Unknown (%)**
All Respiratory	94,729	24.9	55	20.1	46.3	53.7	9.0	0.7	3.0	47.8	35.2	4.2
Asthma	10,899	25.5	66	8.5	43.8	56.2	9.1	0.8	4.9	50.9	30.2	4
COPD	7,094	0.3	39.7	60	46.5	53.5	1.5	0.4	2.7	29.3	62.3	3.7
Pneumonia	17,094	11.5	47.2	41.3	50.8	49.2	7.8	0.7	2.5	41.3	44.1	3.5
Acute bronchitis	11,745	37.8	49.5	12.6	47.1	52.9	8.6	0.4	2.7	52.3	32.0	3.9
All Cardiovascular	58,138	0.4	43.5	56.2	53	47	4.4	0.7	2.6	36.0	52.4	3.9
Cardiac Arrest	2,122	4.7	49.7	48.1	61.4	38.6	8.3	0.7	3.0	37.0	42.1	8.9
Arrhythmia	11,551	0.5	38.4	61	51.7	48.3	2.9	0.6	1.7	27.1	63.6	4
Heart Failure	3,224	0.1	39.8	60.1	52.6	47.4	4.6	0.8	2.1	36.2	53.4	3
Ischemic Heart Disease	13,703	-	45.2	54.8	61.5	38.4	4.2	0.6	1.9	37.4	52.2	3.7
Myocardial Infarction	11,779	-	44.6	55.4	62	38	4.0	0.6	1.9	37.7	52.0	3.8
Cerebrovascular Disease	11,694	0.2	35.2	64.6	49.7	50.3	5.3	0.8	2.0	36.4	51.9	3.5
TOTAL	**253,772**	**33,244**	**123,587**	**96,941**	**127,394**	**126,378**	**16,894**	**1,761**	**6,871**	**105,989**	**112,159**	**10,098**

A summary of the SS reports from our select queries during the 2019-2022 wildfire smoke season (April-September) and the corresponding age-related and gender-related strata can be found in Table 4.3. We did not include race-related strata for SS reports, as they are less accurate than ED reports. There were a total of 605,984 SS reports during our study period, exceeding the total number of ED visits. SS queries are broader and include a larger number of reports than ED visits per health outcome. For example, the broad respiratory query for SS includes coronavirus-related reports, which are not included in the all respiratory-related ED visits. SS reports do not distinguish between primary and secondary diagnoses, leading to a larger count in each category compared to ED, where we only rely on primary diagnoses. Additionally, there is overlap of health outcomes in some categories (e.g., asthma in broad respiratory and air quality respiratory queries).

Table 4.3. Summary of cardiorespiratory-related Syndromic Surveillance reports in New Mexico between April - September for 2019-2022. Corresponding Syndromic queries are provided in the Supporting Information.

		Age Category			Sex	
Health Outcomes	**Reports (n)**	**<15 (%)**	**15 to 65 (%)**	**>65 (%)**	**Male (%)**	**Female (%)**
Broad Respiratory	224,017	25.3	54.4	20.3	45.8	54.2
Asthma	10,233	22.2	66.9	10.9	42.5	57.5
Air Quality Respiratory	148,589	9.7	57.8	32.5	45.4	54.6
Cardiovascular	223,145	0.8	48.1	51.2	50.4	49.6
TOTAL	**605,984**	**75,126**	**321,789**	**209,069**	**286,781**	**319,151**

4.3.3 Assessing differences in ED visits and SS reports

Due to the limited network of regulatory monitors in New Mexico, the O'Dell method smoke product is under-constrained in this region. For example, in 2018 the 416 and the Burro

Fire produced smoke in southwestern Colorado (InciWeb, 2019), and there was a lack of regulatory monitors in NM near the fire. Because of this, the interpolation of ground-based monitors led to an increase in smoke $PM_{2.5}$ in northwestern NM, where there likely was not as much smoke as estimated (Figure A3.5). Although 2018 was not included in our results, this example shows clear deficiencies in the exposure estimate, an issue that impacts all years of the smoke product.

COVID-19, in addition to smoke misclassification, further complicates interpretation of health outcomes. The impacts of COVID-19 (described in Section 4.2.6) caused changes in the cardiorespiratory-related ED visits/SS reports, limiting our ability to draw strong conclusions about smoke exposure impacts during our study period. Therefore, the following results do not aim to quantify the health impacts of smoke exposure. Instead, we use odds ratios to compare patterns in SS and ED data. These results are intended to assess the consistency and agreement between the two health datasets during the wildfire smoke seasons (Figure 4.3), rather than to draw definitive conclusions about the magnitude of smoke-related health effects.

We combined the 2019–2022 wildfire seasons to compare three health outcome categories: all respiratory, asthma-specific, and all cardiovascular (Figure 4.3). SS outcomes were identified mostly through query-based definitions, while ED visits were classified using ICD-10 diagnosis codes. We also assessed the air-quality-related respiratory query from SS, although there is not a clear comparison to ED visits.

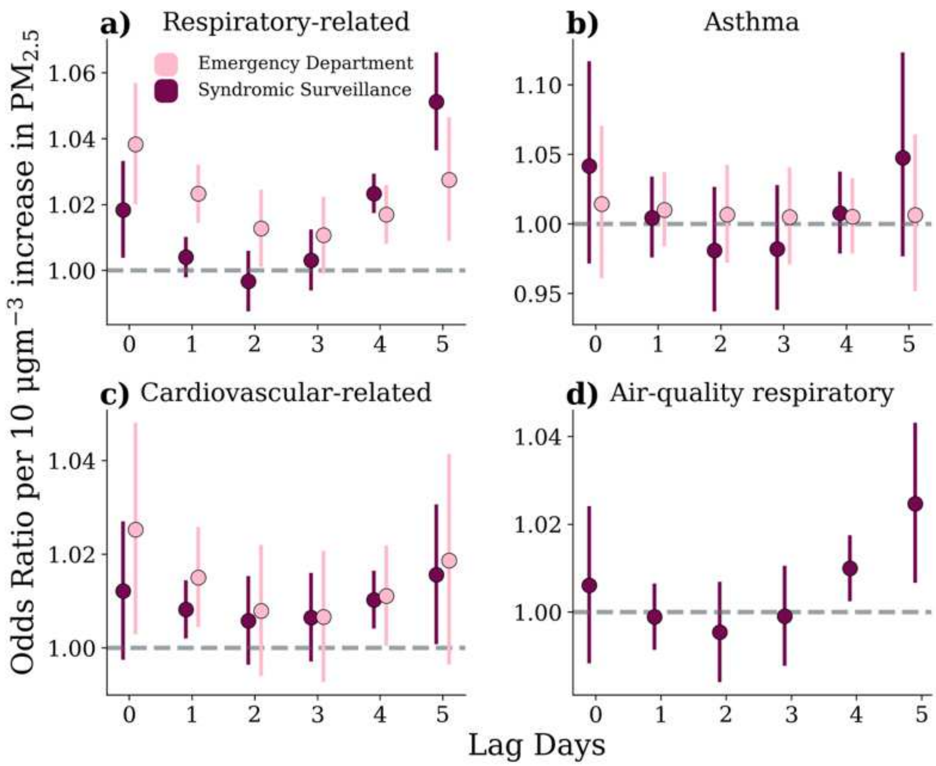

Figure 4.3. Distributed lag effects of a 10 μg m^{-3} increase in wildfire smoke $PM_{2.5}$ on likelihood of Emergency Department visits (light pink) and Syndromic Surveillance reports (dark red) during April - September 2019 - 2022 for all respiratory-related, asthma, and all cardiovascular-related, and air quality-related respiratory.

Associations between smoke $PM_{2.5}$ exposure and health outcomes were somewhat similar across the ED and SS datasets but had meaningful differences in magnitudes and significance. For example, there were more lag days with significantly increased odds of all respiratory-related ED visits with wildfire smoke exposure than SS reports. On Lag 1 and Lag 2, there are significantly increased odds for all-respiratory ED visits, but insignificant results for SS reports, leading to contradictory conclusions. On Lag 5, there is a notable difference in the magnitude of odds ratios, with ED suggesting a 3% increase in odds and SS suggesting a 5% increase. However, there were some similarities, with both health datasets showing decreased odds from Lag 0 to Lag 3 and then increased odds for Lag 4 to Lag 5. Results were overall inconsistent between all-respiratory related ED versus SS reports.

Although asthma morbidity is consistently associated with exposure to wildfire smoke (Gan et al., 2020; Johnston et al., 2002; Rappold et al., 2011; Reid et al., 2016), our results did not show significant associations with asthma-related ED/SS visits. Odds ratios varied in magnitude between health datasets, with Lag 5 showing a 0.6% increase in odds for ED visits and 5% for SS reports. However, all point estimates included the null value, which is inconsistent with the literature. These conflicting findings reflect the effects of exposure misclassification in the smoke $PM_{2.5}$ estimates used in this study. Additionally, COVID-19 impacted the health datasets, likely contributing to our results being inconsistent with previous research.

Associations between wildfire smoke exposure and all-cardiovascular outcomes showed the greatest similarity between the two health datasets, though key differences remain. Because the SS system does not include a predefined “all-cardiovascular” query, we identified cardiovascular-related SS reports using the same ICD-10 codes as the ED data. This consistent case definition likely contributed to the similar odds ratios observed across all lag days. The total number of cardiovascular-related ED visits (58,138) was lower than the number of cardiovascular-related SS reports (223,145), contributing to wider confidence intervals for the ED estimates. Because SS reports symptoms rather than final billing codes, the dataset is broader. Despite similarities, there is a difference in statistical significance on Lag 1 between health datasets, leading to contradictory conclusions of the associations of wildfire smoke exposure. Overall, while cardiovascular outcomes appeared most comparable between datasets, differences in significance highlight the need for further investigation to draw conclusions.

The air-quality-related respiratory query from SS showed significant associations with a 10 $\mu g\ m^{-3}$ increase in smoke $PM_{2.5}$ (Figure 4.3 d). There were significantly increased odds for

Lag 4-5 (Lag 4 OR = 1.01, 95% CI: 1.00, 1.02; Lag 5 OR = 1.02, 95% CI: 1.00, 1.04). These results are similar in magnitude, but lower than the ORs observed for all-respiratory related SS reports, because the air quality respiratory category includes a more select range of symptoms. These results suggest the query could be capturing health outcomes associated with poor air quality specifically, though additional testing is needed.

4.4 Conclusions and Limitations

We compared Syndromic Surveillance (SS) reports to Emergency Department (ED) visits in an epidemiological study of wildfire smoke exposure in New Mexico (NM) from 2019 - 2022. SS is a voluntary reporting system of Emergency Department (ED) visits, which provides chief complaints and/or discharge diagnoses. The purpose of SS is to provide real-time counts of symptoms to healthcare and public health officials for quick detection of health events (e.g., disease outbreak, bioterrorism, influenza outbreaks, etc.). SS is less frequently used in epidemiological studies of wildfire smoke exposure; therefore, comparing the two datasets to determine the usefulness of SS reports is of value.

Overall, our results from our epidemiological study showed the odds ratios had meaningful differences in significance and magnitude for ED versus SS across several health outcomes. The Odd Ratios (ORs) for all respiratory-related ED/SS reports had the most inconsistencies between health datasets compared to asthma and all-cardiovascular. There were no significant associations with wildfire smoke exposure and asthma ED/SS reports, which is contradictory from the literature suggesting issues with smoke misclassification in our analysis. The SS air quality related respiratory query showed similar results to the all-respiratory related query and should be researched further to determine use in studying the impact of acute exposure to wildfire smoke on health.

There were several limitations with the health data in this study. The COVID-19 virus impacted the health datasets from 2020-2021. We observed changes in cardiorespiratory-related ED visits/SS reports, making it difficult to isolate the effects of smoke exposure during these years. Additionally, there were no SS reports available from the main regional hospital near the Calf Canyon/Hermit's Peak Fire, the largest wildfire in New Mexico's history, during the fire period. These limitations show the challenges in using a voluntary system of health-data reporting to assess the impacts of wildfire smoke exposure.

Our results are also impacted by smoke-exposure misclassification. Our smoke exposure estimate was based on spatially interpolated in situ measurements from the US Environmental Protection Agency Air Quality System (EPA AQS), a network of regulatory monitors that is sparse in NM. Calf Canyon/Hermit's Peak was the largest fire in NM state history; however, our exposure estimates for wildfire smoke $PM_{2.5}$ does not have a clear increase near the fire region during 2022 due to the lack of monitors nearby. Additionally, we rely on the NOAA Hazard Mapping System (HMS) smoke plumes to distinguish wildfire smoke $PM_{2.5}$ from other sources of $PM_{2.5}$. This dataset does not specify between different fire types. Although we focus on the wildfire season (April - September), there may be impacts from prescribed and agricultural fires. NM was also impacted by transported smoke during the study from California and Arizona. To make quantitative conclusions about the impact on ED visits, we need a more accurate smoke estimate.

The SS reporting system may be a useful tool for New Mexico to better assess the health impacts of wildfire smoke and allocate resources during smoke events but requires further testing. Because this system gives real-time reports, it allows for immediate action to ensure all patients get adequate care, especially during health emergencies, like an intense, local wildfire.

As wildfire smoke events become more frequent, making quick decisions about resource distribution, especially in rural and under-resourced areas, will become increasingly more important. Our research adds to the growing work of using SS in a wildfire smoke epidemiological study, but future work is needed to support these findings.

4.5 Data Availability Statement

Population-weighted smoke $PM_{2.5}$ estimates for the smoke product can be accessed here: https://doi.org/10.25675/10217/230602 (2006-2018), http://doi.org/10.25675/10217/233962, (2019-2020), https://doi.org/10.25675/10217/235551 (2021), and https://doi.org/10.5061/dryad.gb5mkkx2f. The code written to conduct this analysis can be found here: https://github.com/oliviasablan/New_Mexico_Wildfire. The emergency department and syndromic surveillance data in this manuscript include protected health information (e.g., patient identification number, patient ZIP code, etc.) covered by the Health Information Portability and Accountability Act. Therefore, these data are not available due to data use agreements with the New Mexico Department of Health. Parties interested in reproducing or extending this work will need to set up their own data use agreements with the New Mexico Department of Health to receive this data.

CHAPTER 5

SUMMARY, CONCLUSIONS, AND FUTURE WORK

5.1 SUMMARY AND CONCLUSIONS

This dissertation aimed to quantify smoke from agricultural fires and wildfires and investigate health impacts. We present findings on smoke exposure from two case studies in the rural U.S.: southern Florida and New Mexico. Chapter 2 determines the $PM_{2.5}$ contribution to smoke from sugarcane burning in southern Florida via low-cost sensor deployment and satellite observations. Chapter 3 tests different wildfire smoke exposure estimates in an epidemiological study in New Mexico. Chapter 4 investigates the use of syndromic surveillance data in NM, a voluntary real-time reporting system of Emergency Department visits.

In Chapter 2, we investigated smoke $PM_{2.5}$ from sugarcane-agricultural burning in southern Florida from October 2022 - May 2023 with in situ measurements from regulatory monitors, public and study-specific PurpleAir sensors, using multiple smoke designation methods. Because agricultural fires are short-lived, can occur overnight, and there is frequent cloud cover, satellite observations were limited in detecting smoke. To designate smoke-impacted days, we used three surface-based $PM_{2.5}$ thresholds (15, 20, and 30 $\mu g\ m^{-3}$) and a hybrid method with NOAA Hazard Mapping System smoke plumes and a threshold of 20 $\mu g\ m^{-3}$ data. Median $PM_{2.5}$ increased on smoke-impacted days by 2.3- 6.9 $\mu g\ m^{-3}$. Smoke occurred throughout the day but was most common during the day, with occasional extreme overnight events. Inland areas near the Everglades Agricultural Area (EAA) had more frequent smoke days than east coast, though east-coast smoke events were more intense when they did occur. We used

HYSPLIT trajectories to determine that most smoke was transported westward, away from the east coast.

In Chapter 3, we investigated using four different smoke exposure estimation methods in an epidemiological study of wildfire smoke in NM during 2022. This included in situ and satellite-based estimates and modeled output from CMAQ. The magnitude and significance of odds ratios varied across the four smoke-exposure products during the state's largest wildfire in history. We found the CMAQ model estimates to be less suitable for this type of study as only the largest fires were simulated. The exposure estimate with the low-cost sensors likely provided more precise exposure estimates, highlighting the importance of the increased spatial coverage afforded by low-cost sensors in rural regions. We also tested two referent periods in our study and found a longer referent period to be beneficial due to the continuous smoke exposure in some regions throughout the shorter referent period.

In Chapter 4, we conducted an epidemiological study in NM to compare two health datasets from 2019-2022: Emergency Department (ED) visits and Syndromic Surveillance (SS) reports. SS is a voluntary, real-time reporting system of ED visits. Because SS is not mandatorily reported, like ED visits, there are some differences between the datasets that we explored. Additionally, the study included periods impacted by the COVID-19 pandemic. The pandemic changed health-seeking behaviors; however, our goal was to compare results for the two health datasets, rather than make conclusions about health outcomes. We found SS reports generally give similar results in our epidemiological results as ED visits. The results for cardiovascular-related ED visits/SS reports were more similar between health datasets than asthma and respiratory-related visits. This has important implications for the use of SS in resource allocation for a rural state like NM.

In this work, we demonstrated how landscape fire smoke contributes to $PM_{2.5}$ concentrations, but sparse monitoring impacts our ability to quantify the contribution and the associated health effects in rural regions. Across the chapters, we observe that both small-scale agricultural fires in Florida and large wildfires in New Mexico are under-monitored. The regulatory monitoring network better measures urban air quality, as monitors are placed in more populated areas. In New Mexico, we found wildfire smoke exposure was associated with cardiorespiratory ED visits, similar to previous studies. However, these results changed with data inputs, including the smoke product used. Overall, to best understand the impacts of landscape fire smoke, we must have more in situ monitors. Without accurate smoke estimates, the true health impacts remain uncertain, limiting how public health officials can anticipate, respond to, and prepare for smoke events.

Previous research found that minoritized and low-income groups are disproportionately impacted by air pollution (Chakraborty et al., 2022; Jbaily et al., 2022; Mohai et al., 2009). This dissertation adds to that work by demonstrating that air quality monitoring is inequitable, with sparse monitoring especially in rural regions and areas with higher proportions of marginalized populations. These communities also face inequities in healthcare access (Blendon et al., 2002; Cromer et al., 2019; Kreps, 2006). Rural and low-income areas often have fewer hospitals, under-staffed facilities, and longer travel distances for care, creating additional barriers during smoke events.

Addressing these disparities will require action from both air quality monitoring and public health agencies. Future efforts should prioritize expanding air quality monitors in underserved regions and conducting accurate epidemiological studies so hospitals and health agencies have the best information for planning and resource allocation. Regulatory monitors would be ideal to deploy in these regions, as low-cost sensors offer estimates that are often less accurate or precise but allow for greater coverage. In high-burden areas, policies should support clean air shelters, provide air filtration systems to households in need, and improve public education on smoke risks and protective behaviors. Closing these gaps in monitoring and healthcare access is essential to reduce smoke exposure and health impacts on vulnerable populations (Holm et al., 2021; Rappold et al., 2017; Vargo et al., 2023).

5.2 FUTURE WORK

Sections 5.2.1 – 5.2.3 explore several potential avenues for directly building upon the work presented in this dissertation. Broader changes in research are discussed in Section 5.3.4

5.2.1 Agricultural fires in Florida

The goal of Chapter 2 was to quantify smoke exposure from sugarcane-agricultural fires; however, there was uncertainty in our estimations of smoke $PM_{2.5}$. Although low-cost sensors provided essential data, it would be beneficial to deploy more instruments to better diagnose smoke presence and better quantify $PM_{2.5}$. For example, an Aerosol Chemical Speciation Monitor (ACSM) or the Aerosol Mass Spectrometer (AMS) should be deployed to gain information about the speciation of the $PM_{2.5}$. We should also use carbon monoxide measurements from a Picarro, Organic Aerosol from an AMS, and the Florida Fire Service Burn

Authorizations to determine plume age and dilution. These instruments would be placed in the EAA, where the majority of burning occurs. This deployment would allow researchers to better determine pollutant concentrations from smoke, to distinguish between fresh/local and aged/transported smoke, and to characterize the chemical composition and toxicity of the particles, which are key factors that influence how harmful the smoke is to human health. Overall, deploying more instruments to the field would allow us to estimate smoke $PM_{2.5}$ more accurately in southern Florida.

To further investigate smoke in southern Florida, it would be valuable to use the exposure estimates from Chapter 2 in an epidemiological study to determine the associated health outcomes. The epidemiological analysis could follow the methods in Chapters 3 and 4 by taking Emergency Department visits or hospitalizations in southern Florida and connecting them to smoke exposure. The health effects of exposure to agricultural fires is less studied than wildfires (e.g., Boopathy et al., 2002; Nowell et al., 2022; Stem et al., 2024). Nowell et al. (2022) conducted a health impact assessment for agricultural-smoke exposure in Florida; however, the Concentration-Response Function (CRF) used was not developed for agricultural fire-smoke specifically. It would be beneficial to conduct agricultural-smoke specific research to add to the growing body of literature.

Other regions of the US practice sugarcane burning and should also be studied. Louisiana is the second largest producer of sugar in the US, after Florida (USDA, 2025). Previous research has investigated sugarcane burning in Louisiana (e.g., Beary et al., 2002; Boopathy et al., 2002; Hiscox et al., 2015; McCarty, 2011); however, exploring agricultural fire smoke $PM_{2.5}$

concentrations with a ground-based sensor network across Louisiana has not been done. There are several regulatory monitors in southern Louisiana, but sugarcane is also burned in the central part of the state, where only one monitor in Alexandria, LA is located. It would be valuable to study Louisiana sugarcane-burning and compare to Florida because they may have different burn management practices (e.g., time of day, acreage burned, timing and length of burning season). The geography of Louisiana is different, with only one side of the state being coastal compared to Florida. Investigating agricultural-fire smoke in Louisiana would improve our knowledge of sugarcane burning in the US.

Previous studies have shown that PurpleAir sensors give precise, but less accurate estimates of $PM_{2.5}$ but are typically corrected using various correction factors to improve observation accuracy. These correction factors vary by source and environmental conditions; therefore, creating a correction factor specific to agricultural fire smoke to southern Florida would be valuable. Mathieu-Campbell et al., (2024) recently created a southeastern US specific correction factor to better account for the humidity; however, this study only included two PurpleAir sensors in Florida, both not in the sugarcane burning region. There are several smoke-specific correction factors for PurpleAir; however, we tested these in Chapter 2 and found them to be insufficient. If PurpleAir were going to be used in the future to quantify southern Florida agricultural burning again, a sensor should be placed in Belle Glade co-located with the regulatory monitor. In Chapter 2, we noted that the PurpleAir sensors were likely underestimating smoke $PM_{2.5}$ when comparing to the regulatory monitors and creating a correction factor for this region would decrease this disagreement. PurpleAir are useful, low-cost sensors; however, in order to provide more accurate estimates of $PM_{2.5}$ concentrations, more co-located studies with regulatory monitors are necessary to develop region-specific correction factors.

5.2.2 Wildfires in New Mexico

$PM_{2.5}$ monitors should be deployed to under-monitored regions of NM. Because wildfires often occur in rural areas, where regulatory monitoring of $PM_{2.5}$ is sparse, accurately quantifying smoke $PM_{2.5}$ in NM is challenging. The Calf Canyon/Hermits Peak wildfire occurred near Las Vegas, NM, where there are currently no regulatory monitors. Introducing low-cost monitors, such as PurpleAir, could help support the regulatory monitoring network. To make more accurate smoke exposure estimates in New Mexico, we should fill in monitoring gaps.

Additionally, our studies focused on outdoor air quality, but researchers should study indoor air quality in New Mexico as people spend much time inside. The US EPA suggests sheltering indoors during landscape fire smoke events to mitigate exposure risks (US EPA, 2021). To evaluate the effectiveness of this recommendation, especially in rural areas like New Mexico, it is crucial to better quantify indoor air quality during smoke events. Several studies have used the PurpleAir network to study the relationship between indoor and outdoor $PM_{2.5}$ in other regions of the western US, mainly California (e.g., Gupta et al., 2018; Krebs et al., 2021; Liang et al., 2021; O'Dell et al., 2022; Wallace et al., 2022); however, in New Mexico, there are only nine indoor PurpleAir sensors with publicly available data during the study period. Additionally, NM has a high percentage (18%) of people living below the poverty line (U.S. Census Bureau, 2024); therefore, homes may lack AC units or filtration systems to protect residents against smoke exposure. With a limited network of indoor sensors, it would be difficult to determine relationships between indoor and outdoor $PM_{2.5}$. Therefore, it would be useful to deploy in-home sensors to study the ratio of indoor to outdoor $PM_{2.5}$ during smoke-impacted periods across a range of home types. The findings of this research would allow public health officials to make recommendations that are more targeted towards the communities most impacted and determine the effectiveness of sheltering indoors to reduce smoke exposure.

We compared two health datasets in Chapter 4; however, a large percentage of New Mexicans identify as American Indian, and Indian Health Services data (IHS; https://www.ihs.gov/) was not included in our studies. There are 23 federally recognized American Indian tribes in New Mexico and 19 pueblos (sovereign nations). A total of 11% of New Mexicans identify as American Indian and Alaska Native (11%) compared to the entire US (1%) (US Census Bureau, 2023). Low income and minoritized groups, such as American Indian, are often more susceptible to health impacts from air pollution due to a variety of factors (O'Neill et al., 2012; Sacks et al., 2011). For example, American Indians can be more susceptible to having underlying health conditions (Espey et al., 2014; O'Connell et al., 2017) and may face barriers when it comes to seeking healthcare (e.g., proximity to care facilities, ability to travel, lack of transportation) (Cromer et al., 2019). These challenges can contribute to greater vulnerability to smoke exposure. With such a large population of American Indians in NM, many seek care through IHS. Our work in Chapters 3 and 4 used Emergency Department visits and Syndromic Surveillance reports, which are federal health dataset, but including non-federal health data, like IHS, would allow us to best evaluate health impacts for all New Mexico residents. Results for our study may yield different results because of American Indian populations may be more susceptible to facing health outcomes from wildfire smoke exposure.

5.2.3 Summary of proposed immediate future work directly tied to dissertation

There are many avenues to expand on the work in this dissertation. To better quantify smoke $PM_{2.5}$ from agricultural fires in Florida, the research community should deploy a suite of instruments in a field campaign. Because smoke from sugarcane fires is generally understudied in the US, these fires should be studied in other regions, like Louisiana. Future studies should develop region-specific correction factors, especially in places with high humidity, like Florida. In NM, the scientific community should build upon our work, by deploying PurpleAir sensors, both indoors and outdoors to make better smoke exposure estimates. Indoor air quality is important to quantify to determine if public health recommendations are effective. Additionally, epidemiological analyses of wildfire smoke exposure should be conducted with data from IHS, as there is a large American Indian population in some regions of the US, like NM.

5.3.4 Broad changes in research

To better quantify wildfire smoke, there must be a more equitable $PM_{2.5}$ monitoring network that is designed to capture smoke. Kelp et al., (2022) calculated an optimal placement of $PM_{2.5}$ monitors to capture wildfire smoke and found more the eastern coast to have a large number of EPA monitors, but there are more high-priority monitoring location in the western US. There are more monitors on the eastern coast because the network was designed primarily for regulatory purposes, enforcing air quality standards and reducing emissions from urban areas, rather than for detecting smoke from wildfires in rural or remote areas. In addition to better capturing smoke from landscape fires, monitors should be placed with more equitable coverage for rural, low-income, and minoritized groups. Air pollution disproportionately impacts these groups, and we must work to provide accurate ground-based measurements for all. Additionally, there should be a focus on organizing emergency deployment of monitors during smoke events. The New Mexico Environmental Department (NMED) currently deploys a portable $PM_{2.5}$ monitoring network that can be moved to capture air pollution. The EPA Wildfire Smoke Air Monitoring Response Technology (WSMART) program loans monitors to state, local or Tribal agencies; however, not all these agencies have the resources to be able to manage monitors, especially during smoke events. Portable and adaptive monitoring for emergencies should be adapted nationally. Overall, $PM_{2.5}$ monitoring in the US needs to better capture landscape fire smoke with more equity.

Reliable and timely health data are essential for accurately assessing the health impacts of smoke exposure. ED visits and hospitalizations are important datasets for retrospective analyses because these data are released after a substantial delay. In contrast, the Syndromic Surveillance (SS) system reports symptoms in real-time for public health and healthcare professionals to quickly monitor health events; however, the system in voluntary. During times of high traffic in the ED, the hospital's SS system occasionally stops reporting. SS could be a valuable tool for detecting impacts from a landscape fire smoke exposure and would have added value if all hospitals across the US opted in and stayed consistently online.

There must be more consideration in selecting smoke exposure estimates for the region of study in an epidemiological analysis. Smoke exposure estimates are often chosen for their accessibility or because they have been applied in previous studies; however, one product is unlikely to accurately capture smoke across all regions. Even with leveraging all methods to estimate smoke (i.e., satellite observations, ground-based measurements, chemical transported models) there are limitations. Regulatory monitors are typically concentrated in urban areas, leaving rural regions, where many wildfires occur, underrepresented. Satellite observations of smoke are unavailable overnight and cannot be used to determine the presence of smoke with dense cloud cover. Chemical transport models may perform poorly in areas with complex terrain, often are limited by emissions inventories which can be underestimates and do not include transported smoke from other regions. Given these limitations, researchers must critically evaluate the suitability of smoke exposure estimates for their specific study region.

Overall, there must be more research on the health impacts of smoke exposure in more diverse regions with diverse populations. The western US is annually impacted by wildfires, and many studies have found associated health outcomes in these states. However, smoke does not have boundaries, and there have been recent wildfire smoke events impacting other regions of the US. For example, in 2023, Canadian wildfire smoke impacted the eastern coast of the US (Maldarelli et al., 2024; Yu et al., 2024; Zhang et al., 2025). With a warming climate, there will be more events impacting regions other than the western US (Burke et al., 2021; Ford et al., 2018; O'Dell et al., 2021). In these regions, avoidance and mitigation behaviors during wildfire smoke events may differ by region. For example, housing stock may differ extensively by region, with many homes lacking centralized heating, ventilation, and air conditioning (HVAC) due to moderate temperatures when homes were initially built. Following, during summer months when heat and wildfire smoke may co-occur, households may struggle managing multiple environmental risk factors, particularly if there are susceptible populations in the home. There may also be different vulnerabilities faced by certain populations. For example, older populations (65+) may have trouble evacuating during smoke events and may also be predisposed to experience certain health outcomes (e.g., heart failure, heart arrhythmia, pneumonia). We must continue to study and bring attention to the impacts of wildfire smoke exposure to improve our understanding of health risks and support better planning and response during future smoke events in a warming climate.

REFERENCES

Abatzoglou, J. T., Battisti, D. S., Williams, A. P., Hansen, W. D., Harvey, B. J., & Kolden, C. A. (2021). Projected increases in western US forest fire despite growing fuel constraints. *Communications Earth & Environment*, *2*(1), 1–8. https://doi.org/10.1038/s43247-021-00299-0

Abdo, M., Ward, I., O'Dell, K., Ford, B., Pierce, J. R., Fischer, E. V., & Crooks, J. L. (2019). Impact of Wildfire Smoke on Adverse Pregnancy Outcomes in Colorado, 2007–2015. *International Journal of Environmental Research and Public Health*, *16*(19), 3720. https://doi.org/10.3390/ijerph16193720

Alman, B. L., Pfister, G., Hao, H., Stowell, J., Hu, X., Liu, Y., & Strickland, M. J. (2016). The association of wildfire smoke with respiratory and cardiovascular emergency department visits in Colorado in 2012: a case crossover study. *Environmental Health*, *15*(1), 64. https://doi.org/10.1186/s12940-016-0146-8

Al-Saadi, J. A., Soja, A. J., Pierce, R. B., Szykman, J. J., Wiedinmyer, C., Emmons, L. K., et al. (2008). Intercomparison of near-real-time biomass burning emissions estimates constrained by satellite fire data. *Journal of Applied Remote Sensing*, *2*(1), 021504. https://doi.org/10.1117/1.2948785

Arizona Game and Fish Department. (2024). Telegraph and Mescal Fires | Arizona Wildlife Conservation Strategy. Retrieved May 23, 2025, from https://awcs.azgfd.com/conservation-opportunity-areas/terrestrial/telegraph-and-mescal-fires

Barkjohn, K. K., Gantt, B., & Clements, A. L. (2021). Development and application of a United States-wide correction for $PM_{2.5}$ data collected with the PurpleAir sensor. *Atmospheric Measurement Techniques*, *14*(6), 4617–4637. https://doi.org/10.5194/amt-14-4617-2021

Baucum, L. E., & Rice, R. W. (2009). An Overview of Florida Sugarcane. *University of Florida IFAS Extension*. Retrieved from https://ufdc.ufl.edu/IR00003414/00001

Beary, T. P., Boopathy, R., & Templet, P. (2002). Accelerated decomposition of sugarcane crop residue using a fungal–bacterial consortium. *International Biodeterioration & Biodegradation*, *50*(1), 41–46. https://doi.org/10.1016/S0964-8305(02)00056-2

Blendon, R. J., Schoen, C., DesRoches, C. M., Osborn, R., & al, et. (2002). Inequities in health care: A five-country survey. *Health Affairs*, *21*(3), 182–91. https://doi.org/10.1377/hlthaff.21.3.182

Boopathy, R., Asrabadi, B. R., & Ferguson, T. G. (2002). Sugar Cane (Saccharum officinarum L) Burning and Asthma in Southeast Louisiana, USA. *Bulletin of Environmental Contamination & Toxicology*, *68*(2), 173–179. https://doi.org/10.1007/s00128-001-0235-3

Bordonal, R. de O., Carvalho, J. L. N., Lal, R., de Figueiredo, E. B., de Oliveira, B. G., & La Scala, N. (2018). Sustainability of sugarcane production in Brazil. A review. *Agronomy for Sustainable Development*, *38*(2), 13. https://doi.org/10.1007/s13593-018-0490-x

Brey, S. J., & Fischer, E. V. (2016). Smoke in the City: How Often and Where Does Smoke Impact Summertime Ozone in the United States? *Environmental Science & Technology*, *50*(3), 1288–1294. https://doi.org/10.1021/acs.est.5b05218

Brey, S. J., Ruminski, M., Atwood, S. A., & Fischer, E. V. (2018). Connecting smoke plumes to sources using Hazard Mapping System (HMS) smoke and fire location data over North America. *Atmospheric Chemistry and Physics*, *18*(3), 1745–1761. https://doi.org/10.5194/acp-18-1745-2018

Buchholz, R. R., Park, M., Worden, H. M., Tang, W., Edwards, D. P., Gaubert, B., et al. (2022). New seasonal pattern of pollution emerges from changing North American wildfires. *Nature Communications*, *13*(1), 2043. https://doi.org/10.1038/s41467-022-29623-8

Burke, M., Driscoll, A., Heft-Neal, S., Xue, J., Burney, J., & Wara, M. (2021). The changing risk and burden of wildfire in the United States. *Proceedings of the National Academy of Sciences*, *118*(2), e2011048118. https://doi.org/10.1073/pnas.2011048118

Burke, M., Childs, M. L., de la Cuesta, B., Qiu, M., Li, J., Gould, C. F., et al. (2023). The contribution of wildfire to PM2.5 trends in the USA. *Nature*, *622*(7984), 761–766. https://doi.org/10.1038/s41586-023-06522-6

Cal Fire. (2025). 2021 Fire Season Incident Archive. Retrieved May 23, 2025, from https://www.fire.ca.gov/incidents/2021

Carrico, C. M., & Karacaoglu, J. (2023). Impacts of a Prescribed Fire on Air Quality in Central New Mexico. *Atmosphere*, *14*(2), 316. https://doi.org/10.3390/atmos14020316

CDC. (2024, July 8). CDC Museum COVID-19 Timeline. Retrieved July 22, 2025, from https://www.cdc.gov/museum/timeline/covid19.html

CDC. (2025, June 5). Respiratory Virus Hospitalization Surveillance Network (RESP-NET). Retrieved July 23, 2025, from https://www.cdc.gov/resp-net/dashboard/index.html

Center for International Earth Science Information Network. (2023). Gridded Population of the World, Version 4.11 (GPWv4): Population Count. *NASA Socioeconomic Data and Applications Center (SEDAC)*, *Revision 11*. https://doi.org/10.7927/H4JW8BX5

Chakraborty, J., Collins, T. W., Grineski, S. E., & Aun, J. J. (2022). Air pollution exposure disparities in US public housing developments. *Scientific Reports*, *12*(1), 9887. https://doi.org/10.1038/s41598-022-13942-3

Chang, D., & Song, Y. (2009). Comparison of L3JRC and MODIS global burned area products from 2000 to 2007. *Journal of Geophysical Research: Atmospheres*, *114*(D16). https://doi.org/10.1029/2008JD011361

Childs, M. L., Li, J., Wen, J., Heft-Neal, S., Driscoll, A., Wang, S., et al. (2022). Daily Local-Level Estimates of Ambient Wildfire Smoke PM2.5 for the Contiguous US. *Environmental Science & Technology*, *56*(19), 13607–13621. https://doi.org/10.1021/acs.est.2c02934

Corwin, K. A., Corr, C. A., Burkhardt, J., & Fischer, E. V. (2022). Smoke-Driven Changes in Photosynthetically Active Radiation During the U.S. Agricultural Growing Season. *Journal of Geophysical Research: Atmospheres*, *127*(23), e2022JD037446. https://doi.org/10.1029/2022JD037446

Cromer, K. J., Wofford, L., & Wyant, D. K. (2019). Barriers to Healthcare Access Facing American Indian and Alaska Natives in Rural America. *Journal of Community Health Nursing*, *36*(4), 165–187. https://doi.org/10.1080/07370016.2019.1665320

Czeisler, M. É. (2020). Delay or Avoidance of Medical Care Because of COVID-19–Related Concerns — United States, June 2020. *MMWR. Morbidity and Mortality Weekly Report*, *69*. https://doi.org/10.15585/mmwr.mm6936a4

Delfino, R. J., Brummel, S., Wu, J., Stern, H., Ostro, B., Lipsett, M., et al. (2009). The relationship of respiratory and cardiovascular hospital admissions to the southern California wildfires of 2003. *Occupational and Environmental Medicine*, *66*(3), 189–197. https://doi.org/10.1136/oem.2008.041376

Dennison, P. E., Brewer, S. C., Arnold, J. D., & Moritz, M. A. (2014). Large wildfire trends in the western United States, 1984–2011. *Geophysical Research Letters*, *41*(8), 2928–2933. https://doi.org/10.1002/2014GL059576

Doubleday, A., Sheppard, L., Austin, E., & Busch Isaksen, T. (2023). Wildfire smoke exposure and emergency department visits in Washington State. *Environmental Research, Health: ERH*, *1*(2), 025006. https://doi.org/10.1088/2752-5309/acd3a1

Dowell, D. C., Alexander, C. R., James, E. P., Weygandt, S. S., Benjamin, S. G., Manikin, G. S., et al. (2022). The High-Resolution Rapid Refresh (HRRR): An Hourly Updating Convection-Allowing Forecast Model. Part I: Motivation and System Description. *Weather and Forecasting*, *37*(8), 1371–1395. https://doi.org/10.1175/WAF-D-21-0151.1

Espey, D. K., Jim, M. A., Cobb, N., Bartholomew, M., Becker, T., Haverkamp, D., & Plescia, M. (2014). Leading Causes of Death and All-Cause Mortality in American Indians and Alaska Natives. *American Journal of Public Health*, *104*(S3), S303–S311. https://doi.org/10.2105/AJPH.2013.301798

Florida Department of Agriculture and Consumer Services. (2024). Burn Authorizations. Retrieved May 20, 2024, from https://www.fdacs.gov/Forest-Wildfire/Wildland-Fire/Burn-Authorizations?fbclid=IwAR2ZOgFhhuGIPOLRPadQzq-iiU3AiRXnlaCFJb5AeCyQHpIeGw2hyDosuFs

Florida Department of Agriculture and Consumer Services. (2025). Web-Based Open Burn Authorization Request (WebOBA). Retrieved January 21, 2025, from https://www.fdacs.gov/Forest-Wildfire/Wildland-Fire/Resources/Fire-Tools-and-Downloads/Web-Based-Open-Burn-Authorization-Request-WebOBA

Ford, B., Val Martin, M., Zelasky, S. E., Fischer, E. V., Anenberg, S. C., Heald, C. L., & Pierce, J. R. (2018). Future Fire Impacts on Smoke Concentrations, Visibility, and Health in the Contiguous United States. *GeoHealth*, *2*(8), 229–247. https://doi.org/10.1029/2018GH000144

Gan, R. W., Ford, B., Lassman, W., Pfister, G., Vaidyanathan, A., Fischer, E., et al. (2017). Comparison of wildfire smoke estimation methods and associations with cardiopulmonary-related hospital admissions. *GeoHealth*, *1*(3), 122–136. https://doi.org/10.1002/2017GH000073

Gan, R. W., Liu, J., Ford, B., O'Dell, K., Vaidyanathan, A., Wilson, A., et al. (2020). The association between wildfire smoke exposure and asthma-specific medical care utilization in Oregon during the 2013 wildfire season. *Journal of Exposure Science & Environmental Epidemiology*, *30*(4), 618–628. https://doi.org/10.1038/s41370-020-0210-x

Gasparrini, A., Scheipl, F., Armstrong, B., & Kenward, M. G. (2017). A Penalized Framework for Distributed Lag Non-Linear Models. *Biometrics*, *73*(3), 938–948. https://doi.org/10.1111/biom.12645

Giglio, L., Justice, C., Boschetti, L., & Roy, D. (2021). MODIS/Terra+Aqua Burned Area Monthly L3 Global 500m SIN Grid V061 [Data set]. NASA EOSDIS Land Processes DAAC. https://doi.org/10.5067/MODIS/MCD64A1.061

Global Modeling and Assimilation Office (GMAO). (2015). MERRA-2 tavg1_2d_flx_Nx: 2d,1-Hourly,Time-Averaged,Single-Level,Assimilation,Surface Flux Diagnostics V5.12.4 [Data set]. Greenbelt, MD, USA: Goddard Earth Sciences Data and Information Services Center (GES DISC). https://doi.org/10.5067/7MCPBJ41Y0K6

Gupta, P., Doraiswamy, P., Levy, R., Pikelnaya, O., Maibach, J., Feenstra, B., et al. (2018). Impact of California Fires on Local and Regional Air Quality: The Role of a Low-Cost Sensor Network and Satellite Observations. *GeoHealth*, *2*(6), 172–181. https://doi.org/10.1029/2018GH000136

Hahn, M. B., Kuiper, G., O'Dell, K., Fischer, E. V., & Magzamen, S. (2021, April 21). Wildfire Smoke Is Associated With an Increased Risk of Cardiorespiratory Emergency Department Visits in Alaska - Hahn - 2021 - GeoHealth - Wiley Online Library. Retrieved September 27, 2023, from https://agupubs.onlinelibrary.wiley.com/doi/10.1029/2020GH000349

Hand, J. L., Prenni, A. J., Raffuse, S. M., Hyslop, N. P., Malm, W. C., & Schichtel, B. A. (2024). Spatial and Seasonal Variability of Remote and Urban Speciated Fine Particulate Matter in the United States. *Journal of Geophysical Research: Atmospheres*, *129*(23), e2024JD042579. https://doi.org/10.1029/2024JD042579

Hazard Mapping System Fire Product. (2022). [Data set]. National Oceanic and Atmospheric Administration. Retrieved from https://satepsanone.nesdis.noaa.gov/pub/FIRE/web/HMS/Fire_Points/Text/2022/

Hazard Mapping System Smoke Product. (2022). [Data set]. National Oceanic and Atmospheric Administration. Retrieved from https://satepsanone.nesdis.noaa.gov/pub/FIRE/web/HMS/Smoke_Polygons/Shapefile/2022/

Heft-Neal, S., Gould, C. F., Childs, M. L., Kiang, M. V., Nadeau, K. C., Duggan, M., et al. (2023). Emergency department visits respond nonlinearly to wildfire smoke. *Proceedings of the National Academy of Sciences*, *120*(39), e2302409120. https://doi.org/10.1073/pnas.2302409120

Hiscox, A. L., Flecher, S., Wang, J. J., & Viator, H. P. (2015). A comparative analysis of potential impact area of common sugar cane burning methods. *Atmospheric Environment*, *106*, 154–164. https://doi.org/10.1016/j.atmosenv.2015.02.005

Holm, S. M., Miller, M. D., & Balmes, J. R. (2021). Health effects of wildfire smoke in children and public health tools: a narrative review. *Journal of Exposure Science & Environmental Epidemiology*, *31*(1), 1–20. https://doi.org/10.1038/s41370-020-00267-4

Holstius, D. M., Reid, C. E., Jesdale, B. M., & Morello, -Frosch Rachel. (2012). Birth Weight following Pregnancy during the 2003 Southern California Wildfires. *Environmental Health Perspectives*, *120*(9), 1340–1345. https://doi.org/10.1289/ehp.1104515

Huang, R., Zhang, X., Chan, D., Kondragunta, S., Russell, A. G., & Odman, M. T. (2018). Burned Area Comparisons Between Prescribed Burning Permits in Southeastern United States and Two Satellite-Derived Products. *Journal of Geophysical Research: Atmospheres*, *123*(9), 4746–4757. https://doi.org/10.1029/2017JD028217

Hulburd, A. (2022, June 22). Suppression repair continues despite rains on the Black Fire. Retrieved March 12, 2025, from https://nmfireinfo.com/2022/06/22/suppression-repair-continues-despite-rains-on-the-black-fire/

InciWeb. (2019). 416 Fire Information. Retrieved May 28, 2025, from https://web.archive.org/web/20200109030045/https://inciweb.nwcg.gov/incident/5822/

InciWeb. (2022a, June 15). | InciWeb. Retrieved March 12, 2025, from http://inciweb.wildfire.gov/incident-information/nmsnf-cerro-pelado

InciWeb. (2022b, October 12). Incident Information. Retrieved March 12, 2025, from http://inciweb.wildfire.gov/incident-information/nmcif-bear-trap-fire

InciWeb. (2023, May 26). Incident Information. Retrieved November 29, 2024, from http://inciweb.wildfire.gov/incident-information/flbcp-sandy-fire

InciWeb. (2024, July 29). Incident Information. Retrieved March 12, 2025, from http://inciweb.wildfire.gov/incident-information/nmn4s-cooks-peak

Isaaks, E. H., & Srivastava, R. M. (1989). *Applied Geostatistics*. New York: Oxford University Press.

Jaffe, D. A., Miller, C., Thompson, K., Finley, B., Nelson, M., Ouimette, J., & Andrews, E. (2023). An evaluation of the U.S. EPA's correction equation for PurpleAir sensor data in smoke, dust, and wintertime urban pollution events. *Atmospheric Measurement Techniques*, *16*(5), 1311–1322. https://doi.org/10.5194/amt-16-1311-2023

Janes, H., Sheppard, L., & Lumley, T. (2005a). Case–Crossover Analyses of Air Pollution Exposure Data: Referent Selection Strategies and Their Implications for Bias. *Epidemiology*, *16*(6), 717. https://doi.org/10.1097/01.ede.0000181315.18836.9d

Janes, H., Sheppard, L., & Lumley, T. (2005b). Overlap bias in the case-crossover design, with application to air pollution exposures. *Statistics in Medicine*, *24*(2), 285–300. https://doi.org/10.1002/sim.1889

Janssen, S., Dumont, G., Fierens, F., & Mensink, C. (2008). Spatial interpolation of air pollution measurements using CORINE land cover data. *Atmospheric Environment*, *42*(20), 4884–4903. https://doi.org/10.1016/j.atmosenv.2008.02.043

Jbaily, A., Zhou, X., Liu, J., Lee, T.-H., Kamareddine, L., Verguet, S., & Dominici, F. (2022). Air pollution exposure disparities across US population and income groups. *Nature*, *601*(7892), 228–233. https://doi.org/10.1038/s41586-021-04190-y

Jerrett, M., Burnett, R. T., Ma, R., Pope, C. A., Krewski, D., Newbold, K. B., et al. (2005). Spatial analysis of air pollution and mortality in Los Angeles. *Epidemiology (Cambridge, Mass.)*, *16*(6), 727–736. https://doi.org/10.1097/01.ede.0000181630.15826.7d

Johnston, F. H., Kavanagh, A. M., Bowman, D. M. J. S., & Scott, R. K. (2002). Exposure to bushfire smoke and asthma: an ecological study. *Medical Journal of Australia*, *176*(11), 535–538. https://doi.org/10.5694/j.1326-5377.2002.tb04551.x

June, N. A., Hodshire, A. L., Wiggins, E. B., Winstead, E. L., Robinson, C. E., Thornhill, K. L., et al. (2022). Aerosol size distribution changes in FIREX-AQ biomass burning plumes: the impact of plume concentration on coagulation and OA condensation/evaporation. *Atmospheric Chemistry and Physics*, *22*(19), 12803–12825. https://doi.org/10.5194/acp-22-12803-2022

Kelly, K. E., Whitaker, J., Petty, A., Widmer, C., Dybwad, A., Sleeth, D., et al. (2017). Ambient and laboratory evaluation of a low-cost particulate matter sensor. *Environmental Pollution*, *221*, 491–500. https://doi.org/10.1016/j.envpol.2016.12.039

Kelp, M. M., Lin, S., Kutz, J. N., & Mickley, L. J. (2022). A new approach for determining optimal placement of PM2.5 air quality sensors: case study for the contiguous United States. *Environmental Research Letters*, *17*(3), 034034. https://doi.org/10.1088/1748-9326/ac548f

Krebs, B., Burney, J., Zivin, J. G., & Neidell, M. (2021). Using Crowd-Sourced Data to Assess the Temporal and Spatial Relationship between Indoor and Outdoor Particulate Matter. *Environmental Science & Technology*, *55*(9), 6107–6115. https://doi.org/10.1021/acs.est.0c08469

Kreps, G. L. (2006). Communication and Racial Inequities in Health Care. *American Behavioral Scientist*, *49*(6), 760–774.

Kuula, J., Mäkelä, T., Aurela, M., Teinilä, K., Varjonen, S., González, Ó., & Timonen, H. (2020). Laboratory evaluation of particle-size selectivity of optical low-cost particulate matter sensors. *Atmospheric Measurement Techniques*, *13*(5), 2413–2423. https://doi.org/10.5194/amt-13-2413-2020

Liang, Y., Sengupta, D., Campmier, M. J., Lunderberg, D. M., Apte, J. S., & Goldstein, A. H. (2021). Wildfire smoke impacts on indoor air quality assessed using crowdsourced data in California. *Proceedings of the National Academy of Sciences of the United States of America*, *118*(36), e2106478118. https://doi.org/10.1073/pnas.2106478118

Liu, J. C., Pereira, G., Uhl, S. A., Bravo, M. A., & Bell, M. L. (2015). A systematic review of the physical health impacts from non-occupational exposure to wildfire smoke. *Environmental Research*, *136*, 120–132. https://doi.org/10.1016/j.envres.2014.10.015

Liu, J. C., Mickley, L. J., Sulprizio, M. P., Dominici, F., Yue, X., Ebisu, K., et al. (2016). Particulate air pollution from wildfires in the Western US under climate change. *Climatic Change*, *138*(3), 655–666. https://doi.org/10.1007/s10584-016-1762-6

Magzamen, S., Gan, R. W., Liu, J., O'Dell, K., Ford, B., Berg, K., et al. (2021). Differential Cardiopulmonary Health Impacts of Local and Long-Range Transport of Wildfire Smoke. *GeoHealth*, *5*(3), e2020GH000330. https://doi.org/10.1029/2020GH000330

Maji, K. J., Ford, B., Li, Z., Hu, Y., Hu, L., Langer, C. E., et al. (2024). Impact of the 2022 New Mexico, US wildfires on air quality and health. *Science of The Total Environment*, *946*, 174197. https://doi.org/10.1016/j.scitotenv.2024.174197

Maldarelli, M. E., Song, H., Brown, C. H., Situt, M., Reilly, C., Mahurkar, A. A., et al. (2024). Polluted Air from Canadian Wildfires and Cardiopulmonary Disease in the Eastern US. *JAMA Network Open*, *7*(12), e2450759. https://doi.org/10.1001/jamanetworkopen.2024.50759

Malings, C., Tanzer, R., Hauryliuk, A., Saha, P. K., Robinson, A. L., Presto, A. A., & Subramanian, R. (2020). Fine particle mass monitoring with low-cost sensors: Corrections and long-term performance evaluation. *Aerosol Science and Technology*, *54*(2), 160–174. https://doi.org/10.1080/02786826.2019.1623863

Malm, W. C., Sisler, J. F., Huffman, D., Eldred, R. A., & Cahill, T. A. (1994). Spatial and seasonal trends in particle concentration and optical extinction in the United States. *Journal of Geophysical Research: Atmospheres*, *99*(D1), 1347–1370. https://doi.org/10.1029/93JD02916

McCarty, J. L. (2011). Remote Sensing-Based Estimates of Annual and Seasonal Emissions from Crop Residue Burning in the Contiguous United States. *Journal of the Air & Waste Management Association*, *61*(1), 22–34. https://doi.org/10.3155/1047-3289.61.1.22

Miko, S., Poniatowski, A. R., Troeschel, A. N., Felton, D. J., Banerji, S., Bolduc, M. L. F., et al. (2023). Community health impacts after a jet fuel leak contaminated a drinking water system: Oahu, Hawaii, November 2021. *Journal of Water and Health*, *21*(7), 956–971. https://doi.org/10.2166/wh.2023.109

Mohai, P., Pellow, D., & Roberts, J. (2009). Environmental Justice. *Annual Review of Environment and Resources*, *34*. https://doi.org/10.1146/annurev-environ-082508-094348

Mohler, R., & Goodin, D. (2012). Identifying a suitable combination of classification technique and bandwidth(s) for burned area mapping in tallgrass prairie with MODIS imagery. *Int. J. Applied Earth Observation and Geoinformation*, *14*, 103–111. https://doi.org/10.1016/j.jag.2011.08.008

Molina Rueda, E., Carter, E., L'Orange, C., Quinn, C., & Volckens, J. (2023). Size-Resolved Field Performance of Low-Cost Sensors for Particulate Matter Air Pollution. *Environmental Science & Technology Letters*, *10*(3), 247–253. https://doi.org/10.1021/acs.estlett.3c00030

Murray, T. (2021). Stay-at-Home Orders, Mobility Patterns, and Spread of COVID-19. *American Journal of Public Health*, *111*(6), 1149–1156. https://doi.org/10.2105/AJPH.2021.306209

National Centers for Environmental Information. (n.d.-a). Storm Events Database. Retrieved November 29, 2024, from https://www.ncdc.noaa.gov/stormevents/eventdetails.jsp?id=1086664

National Centers for Environmental Information. (n.d.-b). Storm Events Database. Retrieved November 29, 2024, from https://www.ncdc.noaa.gov/stormevents/eventdetails.jsp?id=1094484

National Interagency Fire Center. (2025, April 8). WFIGS Interagency Fire Perimeters. Retrieved April 8, 2025, from https://www.arcgis.com/sharing/rest/content/items/70ff5accb0ce45c68554d8fdd90aac10/info/metadata/metadata.xml?format=default&output=html

Nowell, H., Wirks, C., Val, M. M., van, D. A., Martin, R. V., Uejio, C. K., & Holmes, C. D. (2022). Impacts of Sugarcane Fires on Air Quality and Public Health in South Florida. *Environmental Health Perspectives*, *130*(8), 087004. https://doi.org/10.1289/EHP9957

Nowell, H. K., Holmes, C. D., Robertson, K., Teske, C., & Hiers, J. K. (2018). A New Picture of Fire Extent, Variability, and Drought Interaction in Prescribed Fire Landscapes: Insights From Florida Government Records. *Geophysical Research Letters*, *45*(15), 7874–7884. https://doi.org/10.1029/2018GL078679

O'Connell, J., Rockell, J., Ouellet, J. C., & LeBeau, M. (2017). Disparities in Potentially Preventable Hospitalizations Between American Indian and Alaska Native and Non-Hispanic White Medicare Enrollees. *Medical Care*, *55*(6), 569. https://doi.org/10.1097/MLR.0000000000000698

O'Dell, K., Ford, B., Fischer, E. V., & Pierce, J. R. (2019). Contribution of Wildland-Fire Smoke to US PM2.5 and Its Influence on Recent Trends. *Environmental Science & Technology*, *53*(4), 1797–1804. https://doi.org/10.1021/acs.est.8b05430

O'Dell, K., Bilsback, K., Ford, B., Martenies, S. E., Magzamen, S., Fischer, E. V., & Pierce, J. R. (2021). Estimated Mortality and Morbidity Attributable to Smoke Plumes in the United States: Not Just a Western US Problem. *GeoHealth*, *5*(9), e2021GH000457. https://doi.org/10.1029/2021GH000457

O'Dell, K., Ford, B., Burkhardt, J., Magzamen, S., Anenberg, S. C., Bayham, J., et al. (2022). Outside in: the relationship between indoor and outdoor particulate air quality during wildfire smoke events in western US cities. *Environmental Research: Health*, *1*(1), 015003. https://doi.org/10.1088/2752-5309/ac7d69

O'Neill, M. S., Breton, C. V., Devlin, R. B., & Utell, M. J. (2012). Air pollution and health: emerging information on susceptible populations. *Air Quality, Atmosphere, & Health*, *5*(2), 189–201. https://doi.org/10.1007/s11869-011-0150-7

Ouimette, J. R., Malm, W. C., Schichtel, B. A., Sheridan, P. J., Andrews, E., Ogren, J. A., & Arnott, W. P. (2022). Evaluating the PurpleAir monitor as an aerosol light scattering instrument. *Atmospheric Measurement Techniques*, *15*(3), 655–676. https://doi.org/10.5194/amt-15-655-2022

Pennington, A. F., Vaidyanathan, A., Ahmed, F. S., Manangan, A., Mirabelli, M. C., Sircar, K. D., et al. (2023). Large-scale agricultural burning and cardiorespiratory emergency department visits in the U.S. state of Kansas. *Journal of Exposure Science & Environmental Epidemiology*. https://doi.org/10.1038/s41370-023-00531-3

Pinakana, S. D., Robles, E., Mendez, E., & Raysoni, A. U. (2023). Assessment of Air Pollution Levels during Sugarcane Stubble Burning Event in La Feria, South Texas, USA. *Pollutants*, *3*(2), 197–219. https://doi.org/10.3390/pollutants3020015

Platnick, S. (2015). MODIS Atmosphere L3 Monthly Product [Data set]. Goddard Space Flight Center: NASA MODIS Adaptive Processing System. http://dx.doi.org/10.5067/MODIS/MYD08_M3.061

Rappold, A. G., Stone, S. L., Cascio, W. E., Neas, L. M., Kilaru, V. J., Carraway, M. S., et al. (2011). Peat Bog Wildfire Smoke Exposure in Rural North Carolina Is Associated with

Cardiopulmonary Emergency Department Visits Assessed through Syndromic Surveillance. *Environmental Health Perspectives*, *119*(10), 1415–1420. https://doi.org/10.1289/ehp.1003206

Rappold, A. G., Reyes, J., Pouliot, G., Cascio, W. E., & Diaz-Sanchez, D. (2017). Community Vulnerability to Health Impacts of Wildland Fire Smoke Exposure. *Environmental Science & Technology*, *51*(12), 6674–6682. https://doi.org/10.1021/acs.est.6b06200

Reid, C. E., Brauer, M., Johnston, F. H., Jerrett, M., Balmes, J. R., & Elliott, C. T. (2016). Critical Review of Health Impacts of Wildfire Smoke Exposure. *Environmental Health Perspectives*, *124*(9), 1334–1343. https://doi.org/10.1289/ehp.1409277

Resnick, A., Woods, B., Krapfl, H., & Toth, B. (2015). Health Outcomes Associated With Smoke Exposure in Albuquerque, New Mexico, During the 2011 Wallow Fire. *Journal of Public Health Management and Practice*, *21*, S55. https://doi.org/10.1097/PHH.0000000000000160

Rolph, G. D., Draxler, R. R., Stein, A. F., Taylor, A., Ruminski, M. G., Kondragunta, S., et al. (2009). Description and Verification of the NOAA Smoke Forecasting System: The 2007 Fire Season. *Weather and Forecasting*, *24*(2), 361–378. https://doi.org/10.1175/2008WAF2222165.1

Ruminski, M., Kondragunta, S., Draxler, R., & Zeng, J. (2023). Recent changes to the Hazard Mapping System.

Sablan, O., Ford, B., Gargulinski, E., Hammer, M. S., Henery, G., Kondragunta, S., et al. (2024). Quantifying Prescribed-Fire Smoke Exposure Using Low-Cost Sensors and Satellites:

Springtime Burning in Eastern Kansas. *GeoHealth*, *8*(4), e2023GH000982. https://doi.org/10.1029/2023GH000982

Sablan, O., Ford, B., Fischer, E., & Pierce, J. (2025). Southern Florida PurpleAir PM2.5 data from October 2022 - May 2023 [Data set]. Dryad. https://doi.org/10.5061/dryad.rn8pk0pnk

Sacks, J. D., Stanek, L. W., Luben, T. J., Johns, D. O., Buckley, B. J., Brown, J. S., & Ross, M. (2011). Particulate matter-induced health effects: who is susceptible? *Environmental Health Perspectives*, *119*(4), 446–454. https://doi.org/10.1289/ehp.1002255

Sayahi, T., Butterfield, A., & Kelly, K. E. (2019). Long-term field evaluation of the Plantower PMS low-cost particulate matter sensors. *Environmental Pollution*, *245*, 932–940. https://doi.org/10.1016/j.envpol.2018.11.065

Scholtz, R., Prentice, J., Tang, Y., & Twidwell, D. (2020). Improving on MODIS MCD64A1 Burned Area Estimates in Grassland Systems: A Case Study in Kansas Flint Hills Tall Grass Prairie. *Remote Sensing*, *12*(13), 2168. https://doi.org/10.3390/rs12132168

Smith, A. R., DeVies, J., Carey, K., Sheppard, M., Radhakrishnan, L., Njai, R., et al. (2023). COVID-19 pandemic–associated changes in overall emergency department visits by age group, race, and ethnicity — United States, January 2019–April 2022. *The American Journal of Emergency Medicine*, *69*, 121–126. https://doi.org/10.1016/j.ajem.2023.04.005

Soja, A. J., Al-Saadi, J. A., Giglio, L., Randall, D., Kittaka, C., Pouliot, G. A., et al. (2009). Assessing satellite-based fire data for use in the National Emissions Inventory. *Journal of Applied Remote Sensing*, *3*(1), 031504. https://doi.org/10.1117/1.3148859

Stein, A. F., Draxler, R. R., Rolph, G. D., Stunder, B. J. B., Cohen, M. D., & Ngan, F. (2015). NOAA's HYSPLIT Atmospheric Transport and Dispersion Modeling System. *Bulletin of the American Meteorological Society*, *96*(12), 2059–2077. https://doi.org/10.1175/BAMS-D-14-00110.1

Stem, A. D., Gibb, M., Roncal-Jimenez, C. A., Johnson, R. J., & Brown, J. M. (2024). Health burden of sugarcane burning on agricultural workers and nearby communities. *Inhalation Toxicology*, *36*(5), 327–342. https://doi.org/10.1080/08958378.2024.2316875

Stowell, J. D., Geng, G., Saikawa, E., Chang, H. H., Fu, J., Yang, C.-E., et al. (2019). Associations of wildfire smoke PM2.5 exposure with cardiorespiratory events in Colorado 2011–2014. *Environment International*, *133*, 105151. https://doi.org/10.1016/j.envint.2019.105151

Sugar Field Burning. (2024). Retrieved October 23, 2024, from https://www.sierraclub.org/florida/sugar-field-burning

Swedo, E. A., Alic, A., Law, R. K., Sumner, S. A., Chen, M. S., Zwald, M. L., et al. (2023). Development of a Machine Learning Model to Estimate US Firearm Homicides in Near Real Time. *JAMA Network Open*, *6*(3), e233413. https://doi.org/10.1001/jamanetworkopen.2023.3413

Travis, K. R., Crawford, James. H., Soja, A. J., Gargulinski, E. M., Moore, R. H., Wiggins, E. B., et al. (2023). Emission Factors for Crop Residue and Prescribed Fires in the Eastern US During FIREX-AQ. *Journal of Geophysical Research: Atmospheres*, *128*(18), e2023JD039309. https://doi.org/10.1029/2023JD039309

Tryner, J., L'Orange, C., Mehaffy, J., Miller-Lionberg, D., Hofstetter, J. C., Wilson, A., & Volckens, J. (2020). Laboratory evaluation of low-cost PurpleAir PM monitors and in-field correction using co-located portable filter samplers. *Atmospheric Environment*, *220*, 117067. https://doi.org/10.1016/j.atmosenv.2019.117067

Tunby, P., Nichols, J., Kaphle, A., Khandelwal, A. S., Van Horn, D. J., & González-Pinzón, R. (2023). Development of a general protocol for rapid response research on water quality disturbances and its application for monitoring the largest wildfire recorded in New Mexico, USA. *Frontiers in Water*, *5*. Retrieved from https://www.frontiersin.org/articles/10.3389/frwa.2023.1223338

US Census Bureau. (2010). TIGER/Line Shapefiles. Retrieved May 30, 2024, from https://www.census.gov/geographies/mapping-files/time-series/geo/tiger-line-file.html

US Census Bureau. (2023, June 15). American Community Survey 5-Year Data (2009-2021). Retrieved January 6, 2023, from https://www.census.gov/data/developers/data-sets/acs-5year.html

U.S. Census Bureau. (2024). U.S. Census Bureau QuickFacts: New Mexico. Retrieved May 22, 2025, from https://www.census.gov/quickfacts/fact/table/NM/PST045223

US EPA. (2021). Wildfire Smoke: A Guide for Public Health Officials. Retrieved July 10, 2024, from https://www.airnow.gov/publications/wildfire-smoke-guide/wildfire-smoke-a-guide-for-public-health-officials/

US EPA. (2024a). Final Updates to the Air Quality Index (AQI) for Particulate Matter - Fact Sheet and Common Questions.

US EPA. (2024b, December 19). 40 CFR Parts 50 and 58. Retrieved July 1, 2025, from https://www.federalregister.gov/documents/2024/12/19/2024-29223/reconsideration-of-the-national-ambient-air-quality-standards-for-particulate-matter-correction

US EPA, O. (2017, June 30). 2017 National Emissions Inventory (NEI) Data [Other Policies and Guidance]. Retrieved November 27, 2022, from https://www.epa.gov/air-emissions-inventories/2017-national-emissions-inventory-nei-data

US EPA, O. (2020). 2020 National Emissions Inventory (NEI) Data [Other Policies and Guidance]. Retrieved August 23, 2023, from https://www.epa.gov/air-emissions-inventories/2020-national-emissions-inventory-nei-data

USDA. (2025, January 7). Sugar and Sweeteners - Background | Economic Research Service. Retrieved July 31, 2025, from https://www.ers.usda.gov/topics/crops/sugar-and-sweeteners/background

Vargo, J., Lappe, B., Mirabelli, M. C., & Conlon, K. C. (2023, June 7). Social Vulnerability in US Communities Affected by Wildfire Smoke, 2011 to 2021 [research-article]. https://doi.org/10.2105/AJPH.2023.307286

Volckens, J. (2024). Summertime Trends in U.S. Population Exposure to Fine Particulate Air Pollution (PM2.5) from Wildfire Smoke. *Environmental Science & Technology Letters*, *11*(11), 1182–1186. https://doi.org/10.1021/acs.estlett.4c00770

Wallace, L. A., Zhao, T., & Klepeis, N. E. (2022). Indoor contribution to PM2.5 exposure using all PurpleAir sites in Washington, Oregon, and California. *Indoor Air*, *32*(9), e13105. https://doi.org/10.1111/ina.13105

Wen, J., Heft-Neal, S., Baylis, P., Boomhower, J., & Burke, M. (2023). Quantifying fire-specific smoke exposure and health impacts. *Proceedings of the National Academy of Sciences*, *120*(51), e2309325120. https://doi.org/10.1073/pnas.2309325120

Westerling, A. L. (2016). Increasing western US forest wildfire activity: sensitivity to changes in the timing of spring. *Philosophical Transactions of the Royal Society B: Biological Sciences*, *371*(1696), 20150178. https://doi.org/10.1098/rstb.2015.0178

Yu, M., Zhang, S., Ning, H., Li, Z., & Zhang, K. (2024). Assessing the 2023 Canadian wildfire smoke impact in Northeastern US: Air quality, exposure and environmental justice. *Science of The Total Environment*, *926*, 171853. https://doi.org/10.1016/j.scitotenv.2024.171853

Zhang, B., Weuve, J., Langa, K. M., D’Souza, J., Szpiro, A., Faul, J., et al. (2023). Comparison of Particulate Air Pollution From Different Emission Sources and Incident Dementia in the US. *JAMA Internal Medicine*, *183*(10), 1080–1089. https://doi.org/10.1001/jamainternmed.2023.3300

Zhang, Q., Wang, Y., Xiao, Q., Geng, G., Davis, S. J., Liu, X., et al. (2025). Long-range PM2.5 pollution and health impacts from the 2023 Canadian wildfires. *Nature*, *645*(8081), 672–678. https://doi.org/10.1038/s41586-025-09482-1

Zhu, C., Kobayashi, H., Kanaya, Y., & Saito, M. (2017). Size-dependent validation of MODIS MCD64A1 burned area over six vegetation types in boreal Eurasia: Large underestimation in croplands. *Scientific Reports*, *7*(1), 4181. https://doi.org/10.1038/s41598-017-03739-0

APPENDIX A1

SUPPLEMENTAL INFORMATION FOR CHAPTER 2

Introduction

This supplemental material provides additional context and details essential for a comprehensive understanding of various aspects related to our findings. It details the pre-deployment quality checks of PurpleAir monitors (Figures A1.1-1.3) comparison of correction factors applied to PurpleAir field data (Figure A1.4, the timing, locations, and area burned for open burned authorizations (Figures A1.5-1.7), text (Text A1.1) and a figure (Figure A1.8) describing a specific smoke day example to further support our methods, cloud fraction from MODIS (Figure A1.9), a flowchart of our methods (Figure A1.10), matrices comparing monitor days in the “HMS alone” category to the ground-based threshold designation methods (Table A1.1.) figures from the main text plotted for other designation methods (Figures A1.11-1.15), the diurnal cycle of smoke and fires (Figure A1.17), tracking of HYSPLIT trajectory and monthly comparisons (Figures A1.18 – 1.19, Text A1.2), and a comparison of PurpleAir and regulatory monitor $PM_{2.5}$ measurements (Figure A1.20). Overall, this supplemental material aims to offer a transparent view of the research done in this project along with providing additional context.

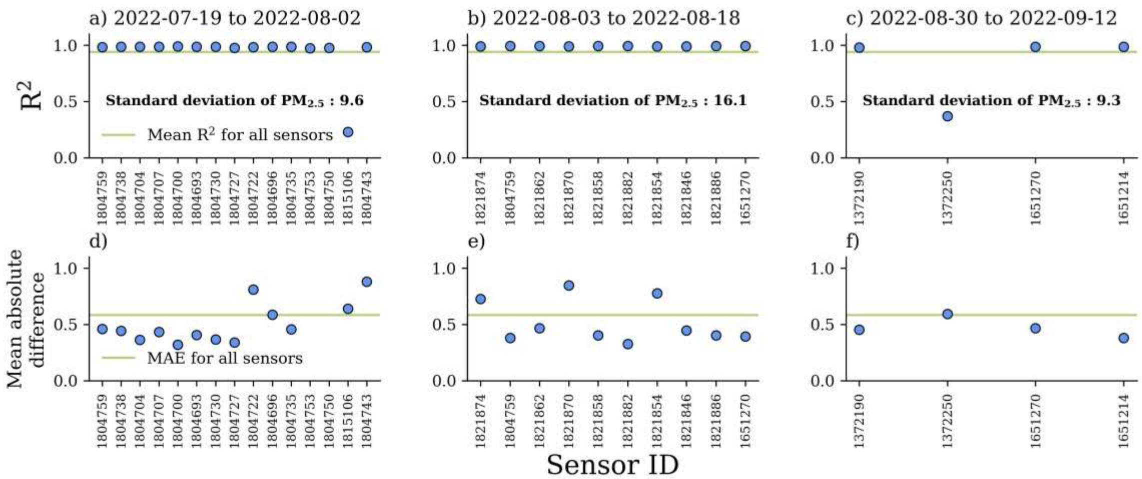

Figure A1.1. Pearson correlation between corrected PurpleAir channel A and channel B in comparison to the average correlation of all sensor channels (horizontal green line) for testing period 1 from 2022-07-19 to 2022-08-02 (a), testing period 2 from 2022-08-03 to 2022-08-18 (b), and testing period 3 from 2022-08-30 to 2022-09-12 (c). The mean absolute difference between channels is also provided for each testing period.

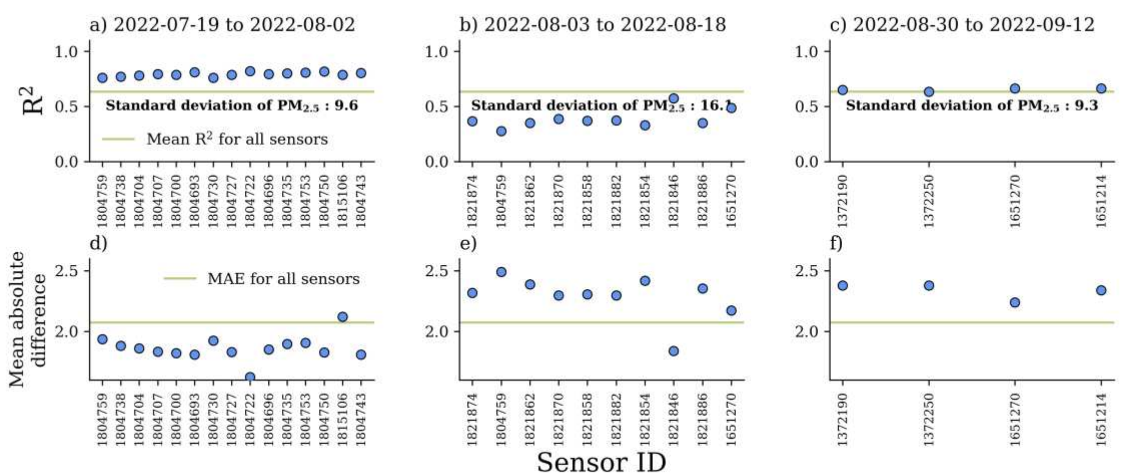

Figure A1.2. Pearson correlation between corrected 10-minute averages of PurpleAir sensors and the GRIMM monitor in comparison to the average correlation of all sensors (horizontal green line) and the GRIMM testing period 1 from 2022-07-19 to 2022-08-02 (a), testing period 2 from 2022-08-03 to 2022-08-18 (b), and testing period 3 from 2022-08-30 to 2022-09-12 (c). The mean absolute difference between channels is also provided for each testing period.

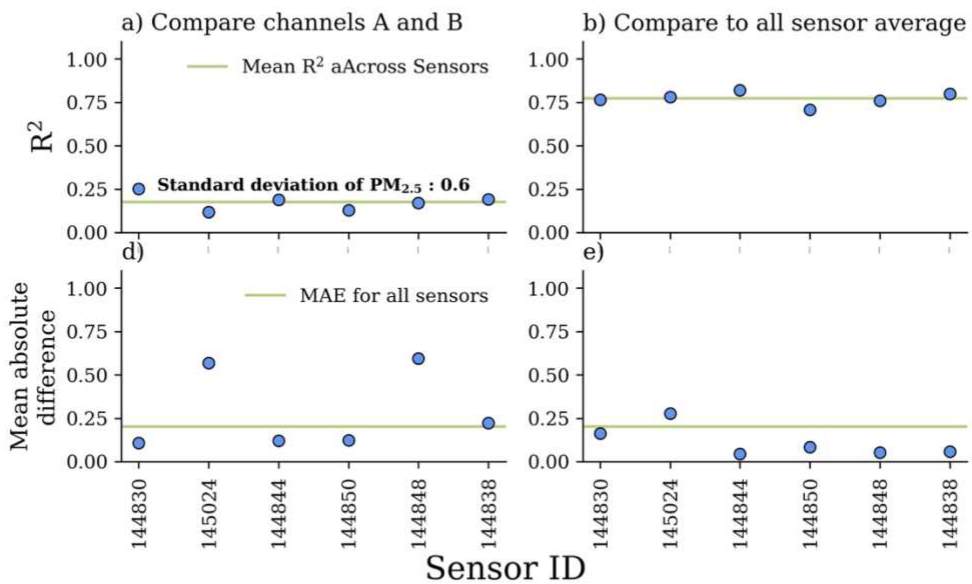

Figure A1.3. Pearson correlation for brief testing (1 day) between 10-minute averages of the corrected PurpleAir sensor channels (a) and between the individual sensor channel average and the overall monitor average (b). The average correlation of all sensors for each test is represented by the green horizontal line. The mean absolute difference between channels (c) and the average (d) is also provided.

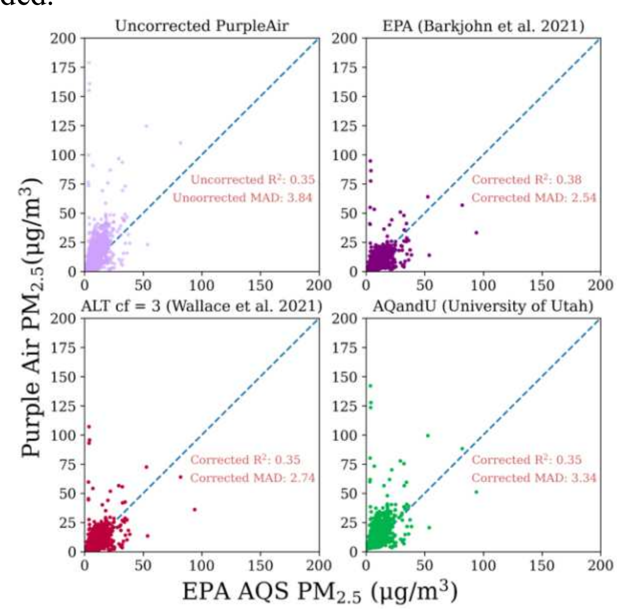

Figure A1.4. Comparison of the hourly average of 14 Belle Glade PurpleAir monitors deployed by CSU and the EPA regulatory monitor in Belle Glade (AQS Site ID: 12-099-0008) with uncorrected PurpleAir data, Purple Air data with the Barkjohn et al. (2021) correction factor, the ALT [cf = 3] correction factor (Wallace et al. 2021), and the AQandU correction factor (Kelly et al., 2017; Sayahi et al., 2019). The Pearson correlation (R^2) and mean absolute difference (MAD) is displayed in each figure for the corresponding data.

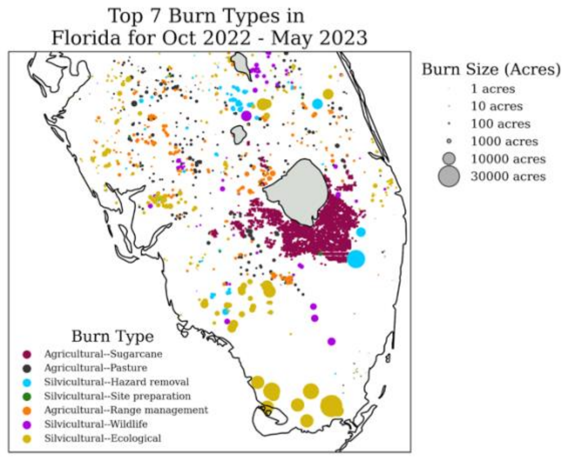

Figure A1.5. Map of study region including only the seven burn types with the most acreage burned from the Florida Fire Service Open Burn Authorizations. Markers are colored by burn type and sized by the acreage burned for October 2022 - May 2023.

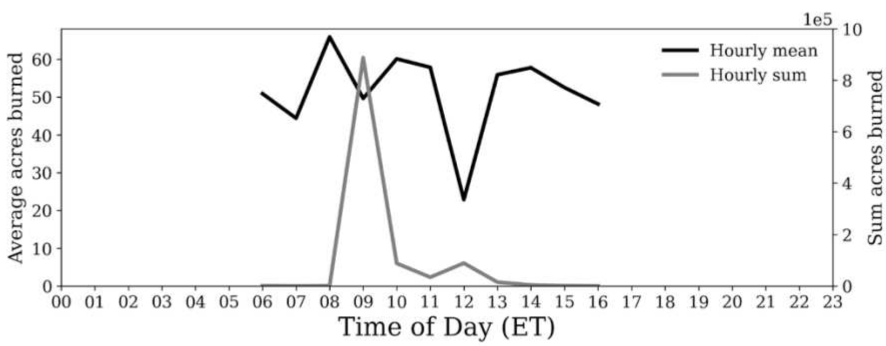

Figure A1.6. Hourly average acres burned (black) and hourly sum of acres burned (gray) from Florida Fire Service Open Burn Authorizations of sugarcane agricultural burning in the study region (≤ 27.5°) for October 2020 - May 2023.

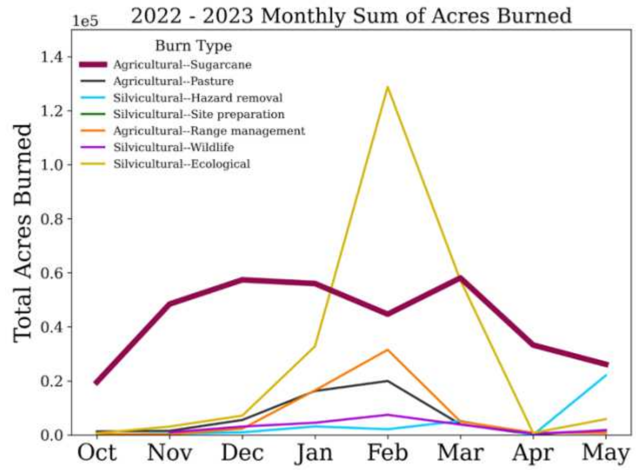

Figure A1.7. Monthly acres burned from sugarcane-agricultural fires from the Florida Fire Service Open Burned Authorizations for October 2022 - May 2023 in the study region (< 27.5° N).

Text A1.1.

While other studies have relied solely on the HMS product to designate smoke, the limitations of HMS smoke plumes in the study region made it unreliable for consistently identifying smoke from agricultural fires in Florida. For example, on October 6, 2022, there were no HMS smoke plumes reported, although the increased $PM_{2.5}$ concentrations in Belle Glade and HMS fire hotspots suggest the presence of smoke from agricultural fires (Figure A1.8). The average inland-monitor $PM_{2.5}$ concentrations across all monitors increased from a minimum of 3.5 µg m^{-3} at 02:00 ET to 58.6 µg m^{-3} at 04:00. There was not a corresponding increase in $PM_{2.5}$ measured at coastal monitors on this day, with the minimum average across all coastal monitors occurring at 00:00 (2.2 µg m^{-3}) and the maximum occurring at 23:00 (5.2 µg m^{-3}). There was some variability between monitors in each region, with a maximum $PM_{2.5}$ for an individual inland monitor of 133.7 µg m^{-3} at 07:00 EST; however, the increase in $PM_{2.5}$ overnight is also present in the inland monitor average. We have confidence there was smoke on October 6, 2022, due to the short-lived increase in $PM_{2.5}$ observed with the inland monitors. The daily average of monitors in the city of Belle Glade, within the EAA, (inset in Figure A1.8) was 22.3 µg m^{-3} versus 5.9 µg m^{-3} for all other monitors on this day. Smoke plumes were not reported by HMS, likely because smoke occurred overnight when satellite observations were not available. If we relied on HMS smoke plumes to designate smoke impact, this day would be considered smoke-free.

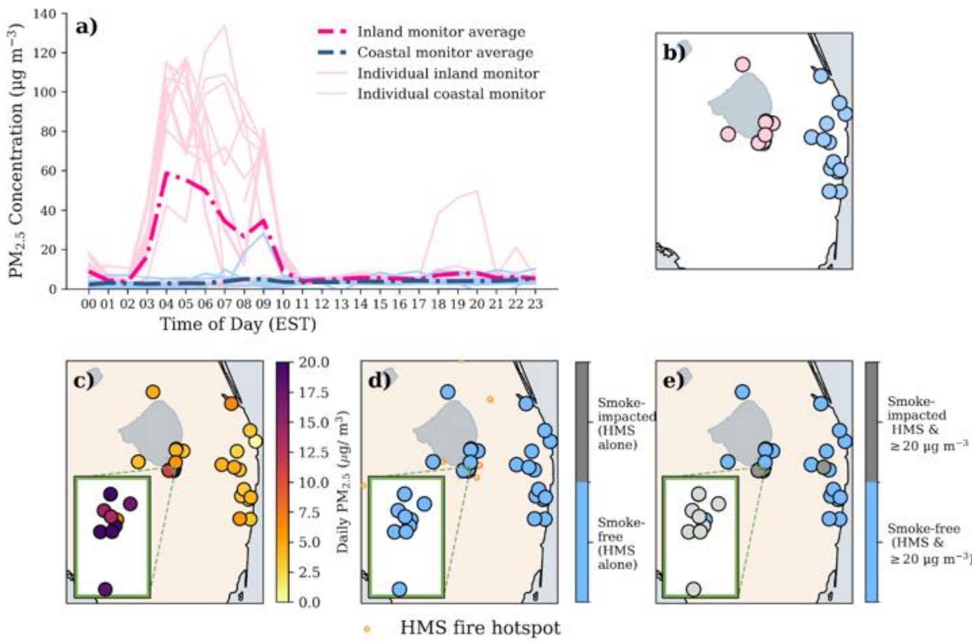

Figure A1.8. a) Hourly averages of individual inland monitors (light pink) and the average of all inland monitors (dark pink) on 6 October 2022 compared to hourly averages of individual coastal monitors (light blue) and the average of all coastal monitors (navy). We categorized monitors as coastal (<30 km from the coastline) or inland (>50 km from the coastline), with the inland monitors being closest to the EAA. b) Map showing the monitor separation (inland versus coastal), c) 24-hr average $PM_{2.5}$ concentrations with an enlarged area of the monitors clustered in a small area (7.5 km^2) near the city of Belle Glade, d) HMS fire hotspots are shown, while HMS smoke plumes are not available. c) our own smoke designation as described in Section 2.4 of the main text.

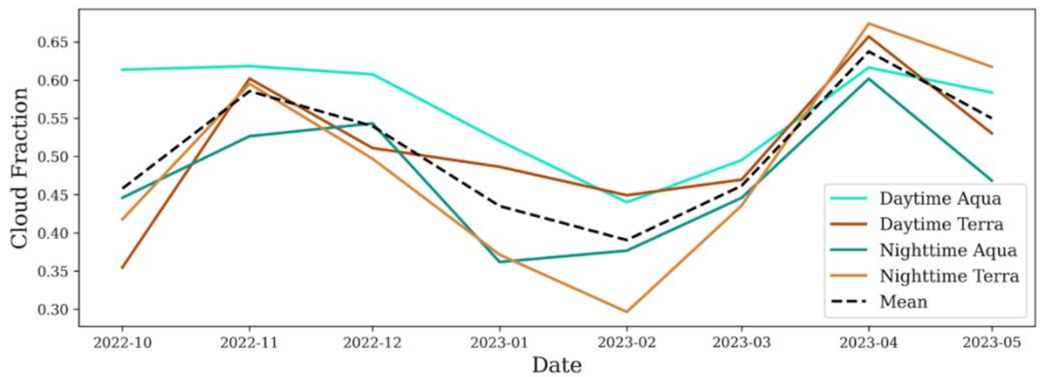

Figure A1.9. Time series from October 2022 - May 2023 of the cloud fraction from the day and nighttime MODIS product for Aqua and Terra. This is an area average of southeastern Florida which considers the region within longitudes 81°W to 80°W and latitudes 25°N to 27°N. The average of all 4 datasets is represented by the black dashed line.

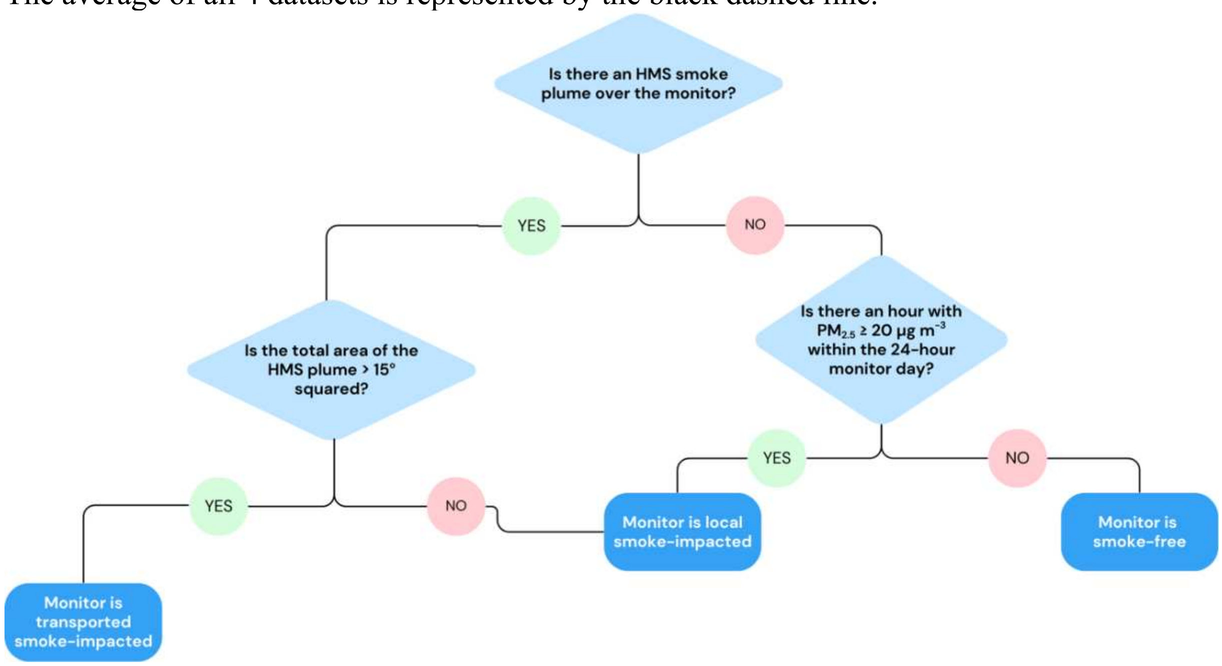

Figure A1.10. Flowchart detailing the “20 µg m^{-3} or HMS” smoke designation category.

Table A1.11. Matrices comparing the "HMS alone" category, where we use the presence on the NOAA Hazard Mapping System smoke plume over each monitor to determine smoke presence, to the ground-based observation thresholds (30 µg m^{-3}; 20 µg m^{-3}; 15 µg m^{-3}). The values in each cell represent monitor days in the categories

Was there an HMS smoke plume over the monitor?

30 µg m^{-3}

One hour above 30 µg m^{-3}?	yes	no
yes	43	105
no	756	3584

20 µg m^{-3}

One hour above 20 µg m^{-3}?	yes	no
yes	128	264
no	671	3425

15 µg m^{-3}

One hour above 15 µg m^{-3}?	yes	no
yes	253	490
no	546	3199

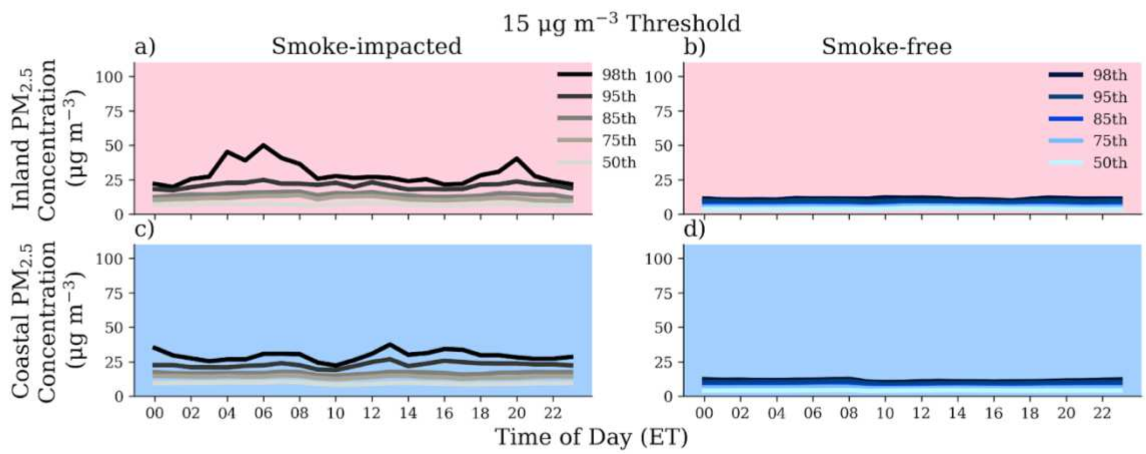

Figure A1.11. Hourly 50th, 75th, 85th, 95th, and 98th percentile PM$_{2.5}$ concentrations during October 2022 - May 2023 for a) inland monitors (> 50 km from the coastline; pink) on smoke-impacted days (classified using criteria of an hourly average PM$_{2.5}$ concentration ≥ 15 µg m^{-3}), b) inland monitor on smoke-free days, c) coastal monitors (<30 km from coastline; blue) on smoke-impacted days, and d) inland monitors on smoke-free days.

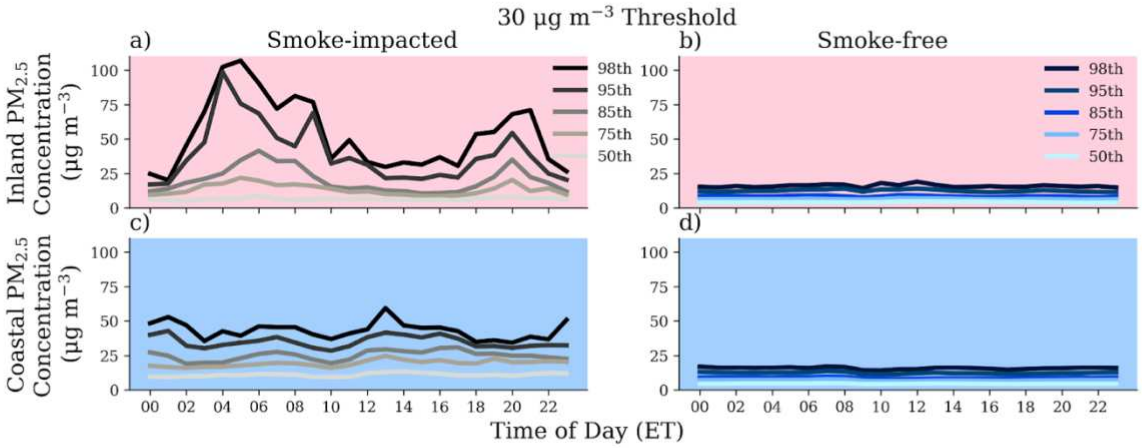

Figure A1.12. Hourly 50th, 75th, 85th, 95th, and 98th percentile $PM_{2.5}$ concentrations during October 2022 - May 2023 for a) inland monitors (> 50 km from the coastline; pink) on smoke-impacted days (classified using criteria of an hourly average $PM_{2.5}$ concentration ≥ 30 µg m^{-3}), b) inland monitor on smoke-free days, c) coastal monitors (<30 km from coastline; blue) on smoke-impacted days, and d) inland monitors on smoke-free days.

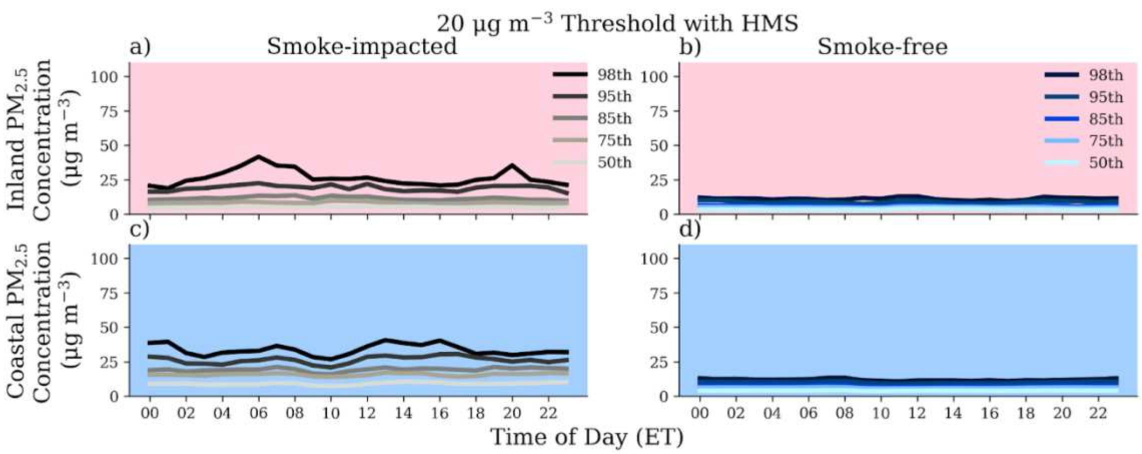

Figure A1.13. Hourly 50th, 75th, 85th, 95th, and 98th percentile $PM_{2.5}$ concentrations during October 2022 - May 2023 for a) inland monitors (> 50 km from the coastline; pink) on smoke-impacted days (classified using criteria of an hourly average $PM_{2.5}$ concentration ≥ 20 µg m^{-3} and HMS), b) inland monitor on smoke-free days, c) coastal monitors (<30 km from coastline; blue) on smoke-impacted days, and d) inland monitors on smoke-free days.

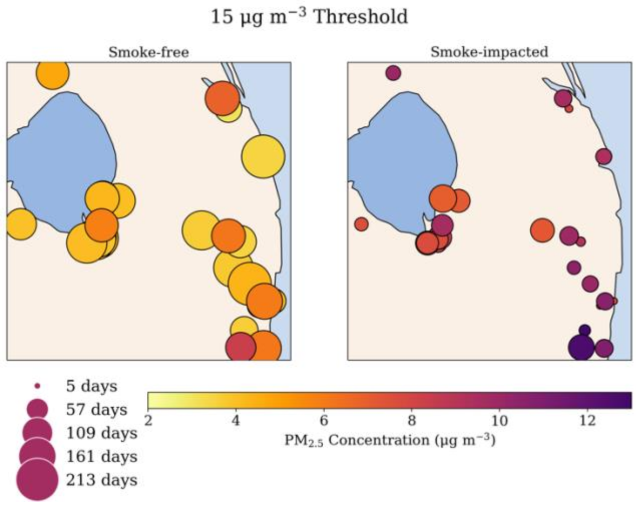

Figure A1.14. Maps of median $PM_{2.5}$ concentrations at each monitor for the ≥ 15 μg m^{-3} designation method on smoke-free (left) and smoke-impacted days (right). Markers are sized by the corresponding number of monitor days. Map regions are shaded by inland versus coastal. Note: the color bar is initiated at 2 μg m^{-3}.

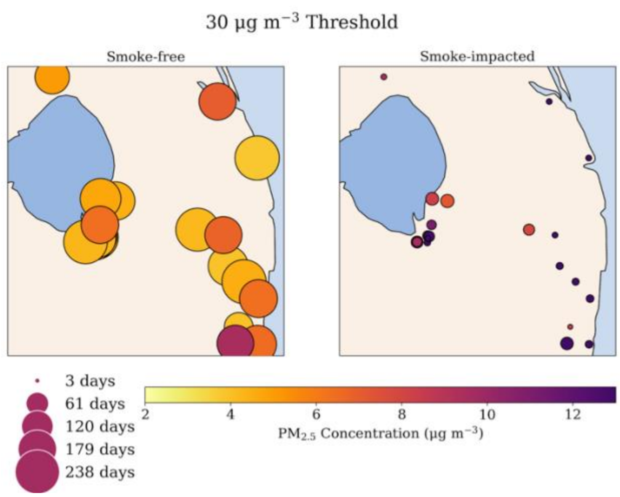

Figure A1.15. Maps of median $PM_{2.5}$ concentrations at each monitor for the ≥ 30 μg m^{-3} designation method on smoke-free (left) and smoke-impacted days (right). Markers are sized by the corresponding number of monitor days. Map regions are shaded by inland versus coastal. Note: the color bar is initiated at 2 μg m^{-3}.

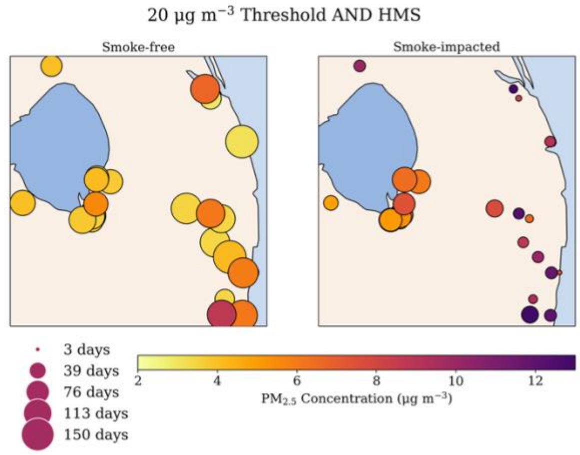

Figure A1.16. Maps of median $PM_{2.5}$ concentrations at each monitor for the ≥ 20 µg m^{-3} and HMS designation method on smoke-free (left) and smoke-impacted days (right). Markers are sized by the corresponding number of monitor days. Map regions are shaded by inland versus coastal. Note: the color bar is initiated at 2 µg m^{-3}.

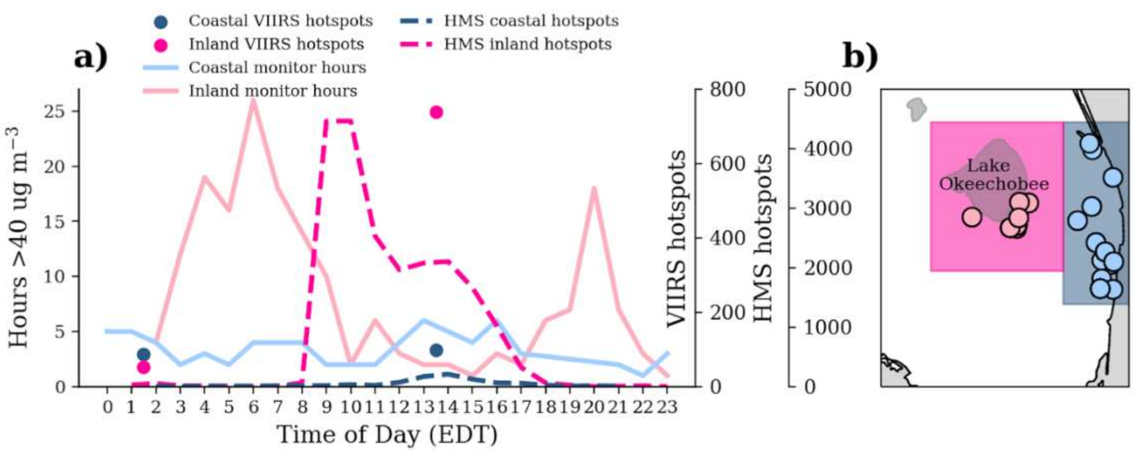

Figure A1.17. Hourly averages of the number of HMS hotspots detected in the inland region and within the pink shaded region on the map (dark pink), and hotspots detected near the coast and within the blue shaded region on the map (navy). Hourly averages of the count of monitors that exceed 40 µg m^{-3} in the inland region (light pink) and near the coast (light blue). The monitor locations are colored by region on the map.

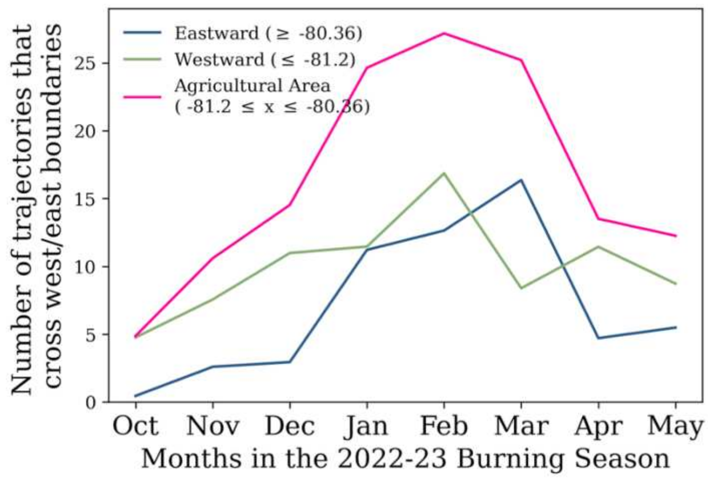

Figure A1.18. Number of HYSPLIT trajectories initiated from every HMS hotspot in southern Florida that moves eastward, with a longitude greater than or equal to -80.36° W (blue), that moves westward, with a longitude less than or equal to -81.2° W (green), or that stays in the agricultural area close to the EAA (-81.2° ≤ x ≤ -80.36°W) (pink) for October- May of 2022-23. Trajectories that cross the boundaries multiple times are only counted once.

Text S2.

From October-December, February, and April-May, more HYSPLIT trajectories moved westward (Figure A1.18). During March, when there was the greatest number of monthly detected hotspots (25), more trajectories moved eastward than westward (2106 versus 902). This suggests that in most months, smoke from agricultural burning primarily impacts regions to the west, potentially reducing smoke exposure along Florida's eastern coastline. However, the significant eastward transport during March, shows variability and complexity in smoke transport.

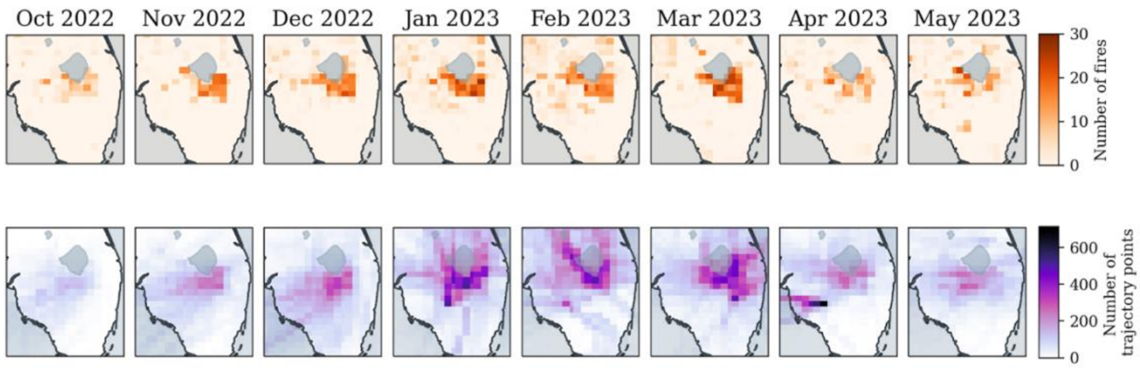

Figure A1.19. Gridded HMS fire hotspots for the 2022-23 burning season and 10-min interpolated 12-hour forward trajectories run from each HMS fire hotspot from the NOAA HYSPLIT model.

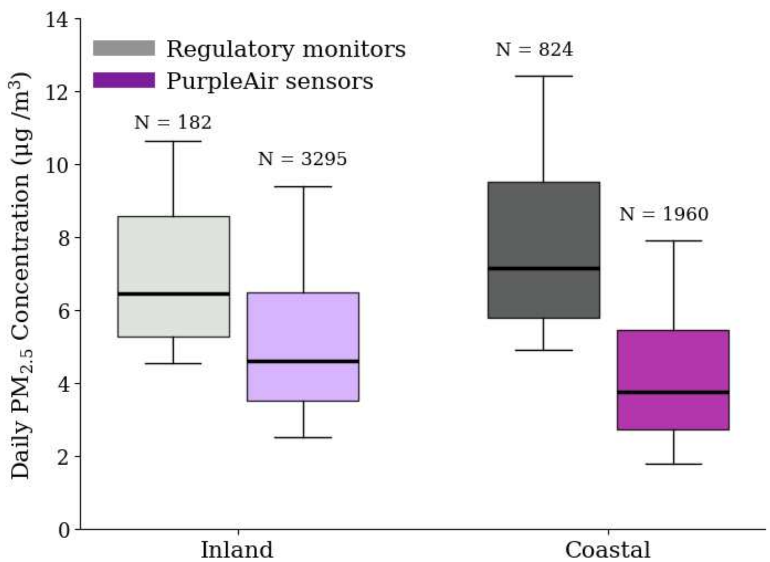

Figure A1.20. Daily average $PM_{2.5}$ for inland monitors versus coastal monitors days. The distributions are separated by regulatory monitors from the EPA AQS (grays) and PurpleAir sensors from the study deployment and public sensors (purples). Outliers have been excluded and the bold line represents the median for each category. The edges of the box represent the 1st and 3rd quartiles. The whiskers are 10th and 90th percentiles.

APPENDIX A2

SUPPLEMENTAL INFORMATION FOR CHAPTER 3

Introduction

This supplemental material provides additional context and details essential for a comprehensive understanding of various aspects related to our findings. It details results using different variogram ordinary kriging parameters (i.e., sill, range, nugget) for smoke product that uses measurements from the Environmental Protection Agency Air Quality System (EPA AQS) and low-cost PurpleAir sensors (Figure A.2.1). We also provide a comparison of the four gridded smoke product estimates ($PM_{2.5}$ from the EPA regulatory-grade monitors; $PM_{2.5}$ from both the EPA regulatory-grade monitors and low-cost PurpleAir observations; modeled 24-hour average wildfire smoke $PM_{2.5}$ from the Community Multiscale Air Quality Modeling System (CMAQ); CMAQ daily 1-hour maximum wildfire smoke $PM_{2.5}$) to the corresponding in situ measurements (Figure A2.2). A table detailing the ICD-10-CM codes for each health outcome is also given in this document (Table A2.1). Additionally, we provide a table to summarize cardiorespiratory-related Emergency Department (ED) visits in NM during April 6 – August 22, 2022, which was during the Calf Canyon/Hermit’s Peak fire (Table A2.2). To give context for the monitors most impacted by smoke, we showed the percentage of days with a NOAA Hazard Mapping System (HMS) smoke plume during the Calf Canyon/Hermit's Peak wildfire. Lastly, we provide results for all health outcomes using the two different referent periods and the two smoke exposure products the use in situ measurements (Figure A2.3). Overall, this supplement should be used to supplement understanding of the results and method used in the manuscript.

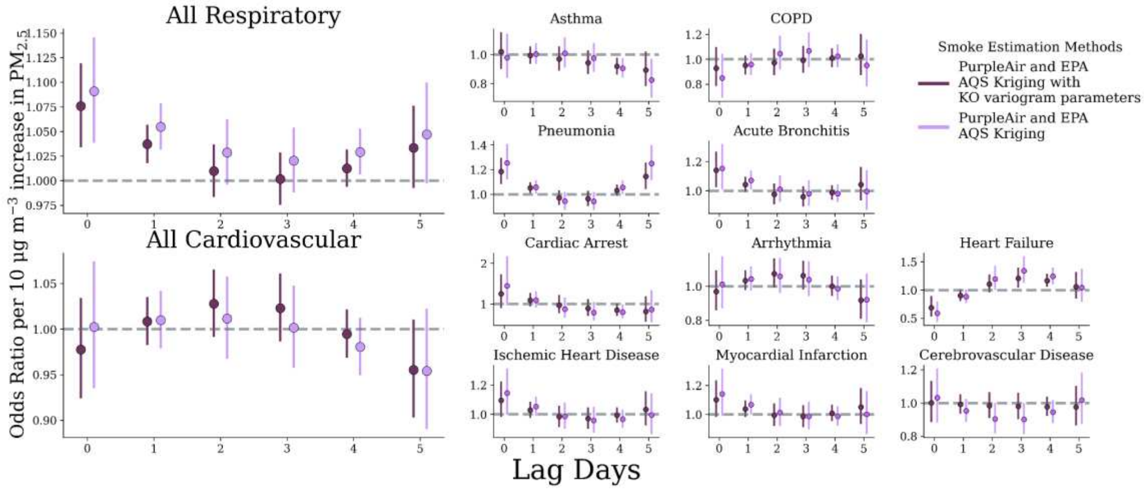

Figure A2.1. Distributed lag results for April 1 - September 30, 2022, ED visits and the Regulatory + PA smoke product with the same variogram parameters as the O'Dell et al. (2019) smoke product (light purple) and the Regulatory + PA smoke product with optimized variogram parameters (dark purple).

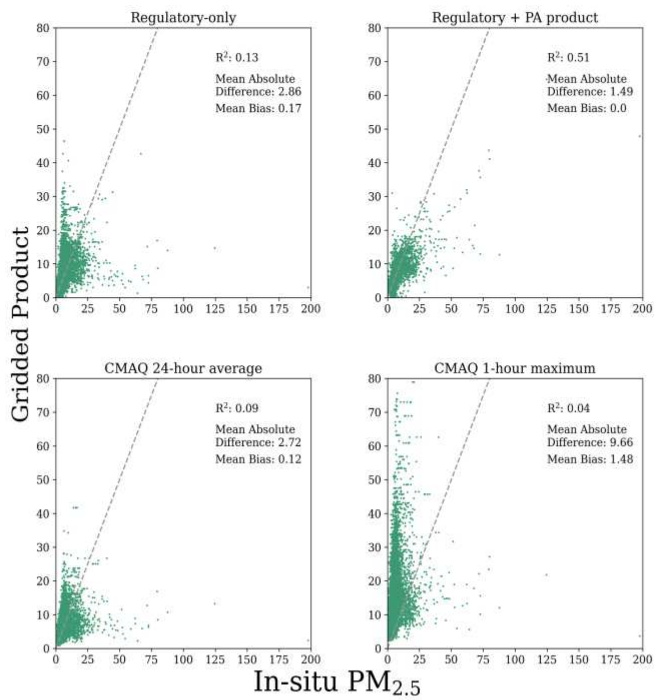

Figure A2.2. Comparison of 24-hour in situ measurements from PurpleAir and the regulatory monitors to the corresponding grid of total $PM_{2.5}$ product/model from April 6 - August 22, 2022. The Pearson correlation ("R^2"), mean absolute difference ($\mu g\ m^{-3}$), and mean bias (%) are displayed on the corresponding subplot. The gray dashed line is the 1-1 linne.

Table A2.1. Emergency department ICD-10 codes per diagnosis

Diagnosis	ICD-10-CM codes
All Respiratory	J00-J98
Asthma	J45
COPD	J44
Pneumonia	J12-J18
Bronchitis	J20-J22
All cardiovascular	I00-I78
Cardiac arrest	I46
Arrhythmia	I47-I49
Heart failure	I50
Ischemic heart disease	I20-I22, I24-I25
Myocardial infarction	I21, I22
Cerebrovascular disease	I60-I163, I65-I69, G45, I23

Table A2.2 Summary of cardiorespiratory-related Emergency Department (ED) visits in New Mexico between April 6 - August 22, 2022. American Indian/Alaskan Native is abbreviated as AIAN, and Asian/Native Hawaiian/Pacific Islander is abbreviated as AANHPI.

		Age Category			Sex		Race/Ethnicity					
Health Outcomes	**Cases(n)**	**<15 (%)**	**15 to 65 (%)**	**>65 (%)**	**Male (%)**	**Female (%)**	**AIAN (%)**	**AANPHI (%)**	**Black (%)**	**Hispanic (%)**	**White (%)**	**Unknown (%)**
All respiratory	21,223	29.8	48.4	21.8	46.4	53.6	9.3	0.6	2.6	49.0	34.3	4.2
Asthma	2,160	29.3	59.7	11.0	43.2	56.8	8.4	0.6	4.5	52.9	29.4	4.1
COPD	1,383	0.2	33.6	66.2	44.8	55.2	1.4	0.5	2.2	29.7	62.6	3.5
Pneumonia	3,789	14.2	41.1	44.7	50.8	49.2	6.2	0.5	2.4	42.2	45.3	3.4
Acute bronchitis	2,799	44.6	40.9	14.5	46.6	53.4	8.8	0.2	2.1	55.6	30.0	3.4
All Cardiovascular	11,651	0.3	41.0	58.7	54.0	46.0	3.9	0.8	2.5	36.9	51.5	4.4
Cardiac Arrest	373	3.2	44.2	51.5	59.2	40.8	5.1	1.1	4.0	38.6	38.9	12.3
Arrhythmia	2,329	0.2	34.4	65.4	52.7	47.3	3.3	0.9	0.9	25.3	64.7	4.9
Heart Failure	656	–	38.9	61.1	55.0	45.0	4.0	0.9	1.8	37.2	52.6	3.5
Ischemic Heart Disease	2,689	–	43.9	56.1	36.4	38.7	2.8	0.9	2.1	40.6	49.8	3.9
Myocardial Infarction	2,380	–	44.4	55.6	64.1	35.9	2.6	1.0	2.1	41.3	49.0	4.0
Cerebrovascular Disease	2,395	0.3	32.8	66.8	51.0	49.0	5.4	1.0	2.0	37.4	50.5	3.7
TOTAL	**33,266**	**6,357**	**15,152**	**11,753**	**16,308**	**16,955**	**2,442**	**233**	**838**	**4,832**	**13,498**	**1,423**

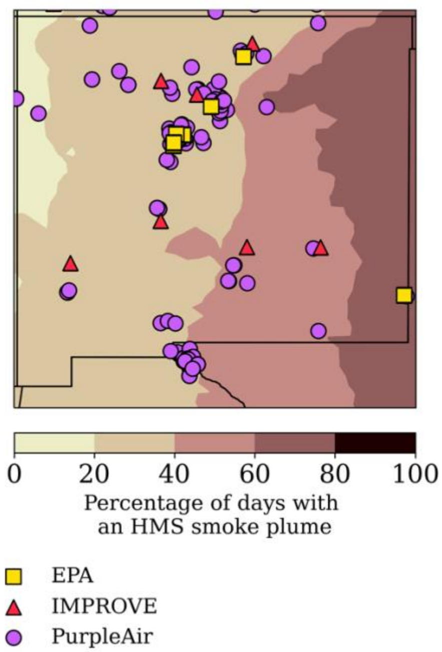

Figure A2.3. Percentage of days with a NOAA Hazard Mapping System (HMS) smoke plume during the Calf Canyon/Hermit's Peak wildfire (April 6 - August 22, 2022). Note: HMS is not a surface-based product; therefore, the smoke plumes used in this figure may be aloft and not contributing to ground $PM_{2.5}$ concentrations. Ground-based $PM_{2.5}$ sensors are maps, including the Environmental Protection Agency Air Quality System (EPA AQS) (yellow squares), the Interagency Monitoring of PROtected Visual Environments (IMPROVE) monitors (red triangles), and the PurpleAir sensors (purple circles).

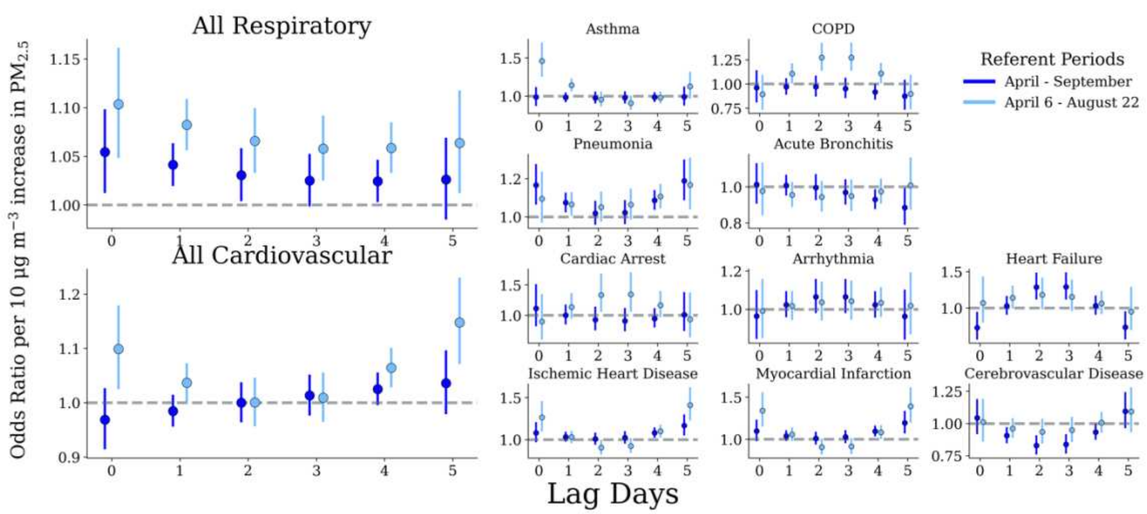

Figure A2.4. Distributed lag effects of a 10 μg m^{-3} increase in wildfire smoke $PM_{2.5}$ on likelihood of all cardiorespiratory-related emergency department visits during April - September

2022 (dark blue) and April 6 - August 22, 2022 (light blue) for the Regulatory-only smoke product.

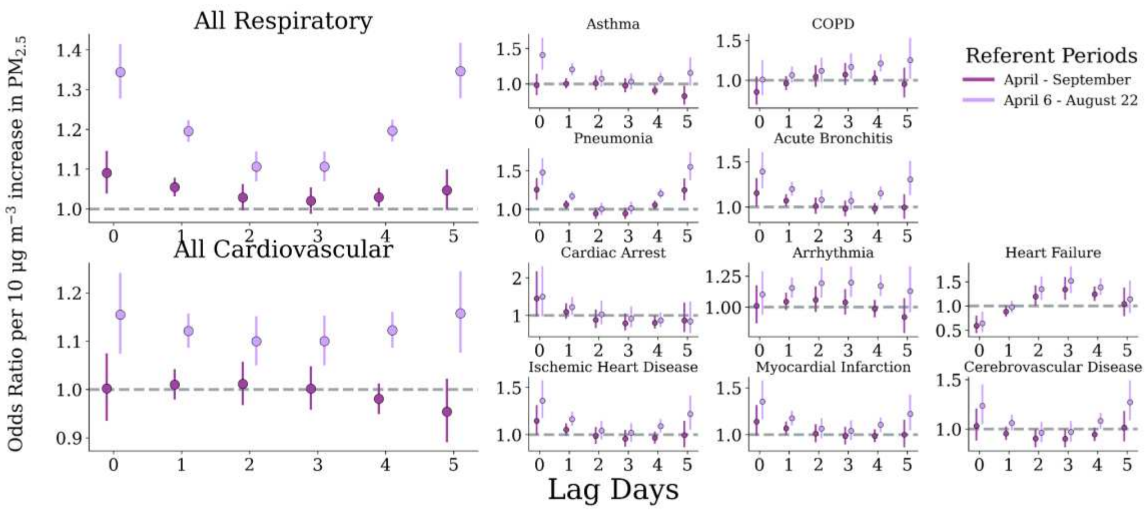

Figure A2.5. Distributed lag effects of a 10 μg m^{-3} increase in wildfire smoke $PM_{2.5}$ on likelihood of all cardiorespiratory-related emergency department visits during April - September 2022 (dark purple) and April 6 - August 22, 2022 (light purple) for the Regulatory + PA smoke product.

APPENDIX A3

SUPPLEMENTAL INFORMATION FOR CHAPTER 4

Introduction

This supplemental information provides more context for Chapter 4. We provide the ICD-10 codes for Emergency Department (ED) visit health outcomes (Table A3.1) and the query definitions for the Syndromic Surveillance (SS) data (Text A3.1). To show the disruptions in the health data caused by COVID-19 and confirm that our SS offline criterion reliably distinguished between online and offline periods, we included all-cause ED visits and SS reports from two hospitals and their offline/online SS periods (Figure A3.1). A time-series of state-wide average smoke $PM_{2.5}$ concentrations from the O'Dell product and COVID-19 rates is also given to show that both were changing over the study period (Figure A3.2). Figure A3.3 shows the epidemiological study results of all respiratory-related ED visits and SS reports for each year in our study individually. We provide ZIP code average smoke $PM_{2.5}$ estimates for 2016-2018 in Figure A.3.4. The O'Dell smoke product lacks accuracy where there are no regulatory monitors, which is shown in Figure A.3.5. Lastly, we show epidemiological results for all respiratory-related ED visits for 2016-2018.

Table A3.1 Emergency Department ICD-10 codes per diagnosis

Diagnosis	ICD-10-CM codes
All Respiratory	J00-J98
Asthma	J45
COPD	J44
Pneumonia	J12-J18
Bronchitis	J20-J22
All cardiovascular	I00-I78
Cardiac arrest	I46
Arrhythmia	I47-I49
Heart failure	I50
Ischemic heart disease	I20-I22, I24-I25
Myocardial infarction	I21-I22
Cerebrovascular disease	I60-I163, I65-I69, G45, I23

Text A3.1

Syndromic Surveillance query definition

Broad Acute Respiratory DD v1
Definition (query syntax):
Search Discharge Diagnosis Field:
^[;/]A22.1^,or,^[;/]A221^,or,^[;/]A37^,or,^[;/]A48.1^,or,^[;/]A481^,or,^[;/]B25.0^,or,^[;/]B250^,or,^[;/]B34.[29]^,or,^[;/]B34[29]^,or,^[;/]B44.[09]^,or,^[;/]B44[09]^,or,^[;/]B44.81^,or,^[;/]B4481^,or,^[;/]B97.[24]^,or,^[;/]B97[24]^,or,^[;/]J0[0-69]^,or,^[;/]J1[0-8]^,or,^[;/]J2[012]^,or,^[;/]J39.8^,or,^[;/]J398^,or,^[;/]J40^,or,^[;/]J47.9^,or,^[;/]J479^,or,^[;/]J80^,or,^[;/]J85.1^,or,^[;/]J851^,or,^[;/]J95.821^,or,^[;/]J95821^,or,^[;/]J96.[02]^,or,^[;/]J96[02]^,or,^[;/]J96.91^,or,^[;/]J9691^,or,^[;/]J98.8^,or,^[;/]J988^,or,^[;/]R05^,or,(,^[;/]R06.0[02]^,or,^[;/]R060[02]^,),AND,(,^[;/]R50.9^,or,^[;/]R509^,),or,^[;/]R06.03^,or,^[;/]R0603^,or,^[;/]R09.02^,or,^[;/]R0902^,or,^[;/]R09.2^,or,^[;/]R092^,or,^[;/]R43.[012]^,or,^[;/]R43[012]^,or,^[;/]U07.[12]^,or,^[;/]U07[12]^,or,^[;/]022.1^,or,^[;/]0221[;/]^,or,^[;/]034.0^,or,^[;/]0340[;/]^,or,^[;/]041.5^,or,^[;/]0415[;/]^,or,^[;/]041.81^,or,^[;/]04181[;/]^,or,^[;/]079.[1236]^,or,^[;/]079[1236][;/]^,or,^[;/]079.8[29]^,or,^[;/]0798[29][;/]^,or,^[;/]079.99^,or,^[;/]07999[;/]^,or,^[;/]117.3^,or,^[;/]1173[;/]^,or,^[;/]46[0-6][;/]^,or,^[;/]461.[0-9]^,or,^[;/]461[0-9][;/]^,or,^[;/]46[1456].[0-9]^,or,^[;/]46[1456][0-9][;/]^,or,^[;/]46[1456][0-9][019][;/]^,or,^[;/]478.9^,or,^[;/]4789[;/]^,or,^[;/]48[0-8][;/]^,or,^[;/]48[023478].[0-9]^,or,^[;/]48[023478][0-9][;/]^,or,^[;/]48[28][0-9][0-9][;/]^,or,^[;/]490[;/]^,or,^[;/]494.1^,or,^[;/]4941[;/

]^,or,^[;/]517.1^,or,^[;/]5171[;/]^,or,^[;/]518.5[13]^,or,^[;/]5185[13][;/]^,or,^[;/]518.6^,or,^[;/]5186[;/]^,or,^[;/
]518.8[124]^,or,^[;/]5188[124][;/]^,or,^[;/]519.8^,or,^[;/]5198[;/]^,or,^[;/]073.0^,or,^[;/]0730[;/]^,or,^[;/
]781.1^,or,^[;/]7811[;/]^,or,^[;/]786.2^,or,^[;/]7862[;/]^,or,^[;/]799.02^,or,^[;/]79902[;/]^,or,^[;/]799.1^,or,^[;/
]7991[;/]^,or,^[;/]033[;/]^,or,^[;/]033.[0-9]^,or,^[;/]033[0-9][;/]^,or,(,^[;/]780.60^,or,^[;/]78060[;/
]^,),AND,(,^[;/]786.0[59]^,or,^[;/]7860[59][;/]^,)

All cardiovascular
This was done in the “advanced query” option and includes the following parameters:
PatientState = NM [patient listed a NM address as their residence]
HasBeenEmergency = Yes [patient visited an emergency room]
DischargeDiagnosis = I00-I78 [note this is anywhere in the discharge diagnosis list; we do not have a way to distinguish primary diagnosis from non-primary within ESSENCE]

Asthma – NM definition which builds off of the “CDC Asthma CCDD v1” definition
CDC Asthma CCDD v1
Definition (Query Syntax):
Search CC and DD Field:
(,^asthma^,or,^[;/]asma^,or,asma^,or,^asthama^,or,^asthma^,or,^asthmia^,or,^bronchospasm^,or,(,(,(,^Airw
ay^,or,^Disease^,),AND,^Reactive^,),or,(,^Airway^,AND,^Disease^,),),or,^J45^,or,^[;/]281239006^,or,^[;/
]195967001^,or,^[;/]708038006^,or,^[;/]405944004^,or,^[;/]708090002^,or,^[;/]56018004^,or,^[;/]304527002^,or,^[;/
]1751000119100^,or,^[;/]401000119107^,or,^[;/]426979002^,or,^[;/]409663006^,or,^[;/]266364000^,or,^[;/
]31387002^,or,^[;/]389145006^,or,^[;/]442025000^,or,^[;/]708093000^,or,^[;/]135171000119106^,or,^[;/
]99031000119107^,or,^[;/]135181000119109^,or,^[;/]425969006^,or,^[;/]370218001^,or,^[;/]57546000^,or,^[;/
]312453004^,or,^[;/]707446004^,or,^[;/]427295004^,or,^[;/]370219009^,or,^[;/]233678006^,or,^[;/
]195949008^,or,^[;/]707447008^,or,^[;/]707445000^,or,^[;/]233683003^,or,^[;/]708094006^,or,^[;/]55570000^,or,^[;/
]426656000^,or,^[;/]707980005^,or,^[;/]390798007^,or,^[;/]5281000124103^,or,^[;/]370221004^,),ANDNOT,^not
asthma^

NM modifications to make it more true asthma visits:

([DISCHARGEDIAGNOSISCOMBOFREETEXT="*asthma with acute*"] OR
[DISCHARGEDIAGNOSISCOMBOFREETEXT="*asthma with (acute)*"] OR
[DISCHARGEDIAGNOSISCOMBOFREETEXT="*exacerbation*"] OR
[DISCHARGEDIAGNOSISCOMBOFREETEXT="*bronchospasm*"] OR
[DISCHARGEDIAGNOSISCOMBOFREETEXT="*asthmaticus*"] OR
[CHIEFCOMPLAINTCOMBOFREETEXT="*asthma*"] OR
[CHIEFCOMPLAINTCOMBOFREETEXT="*ashtma*"] OR
[CHIEFCOMPLAINTCOMBOFREETEXT="*asma*"] OR
[CHIEFCOMPLAINTCOMBOFREETEXT="*shortness of breath*"] OR
[CHIEFCOMPLAINTCOMBOFREETEXT="*sob*"] OR [CHIEFCOMPLAINTCOMBOFREETEXT="*wheez*"]
AND [CHIEFCOMPLAINTCOMBOFREETEXT<>"*covid*"] AND
[DISCHARGEDIAGNOSISCOMBOFREETEXT<>"*covid*"] AND
[DISCHARGEDIAGNOSISCOMBOFREETEXT<>"*j45909*"] AND
[DISCHARGEDIAGNOSISCOMBOFREETEXT<>"*j45.909*"])))))

*** this weeds out covid or J45.909 (asthma unspecified) visits ***

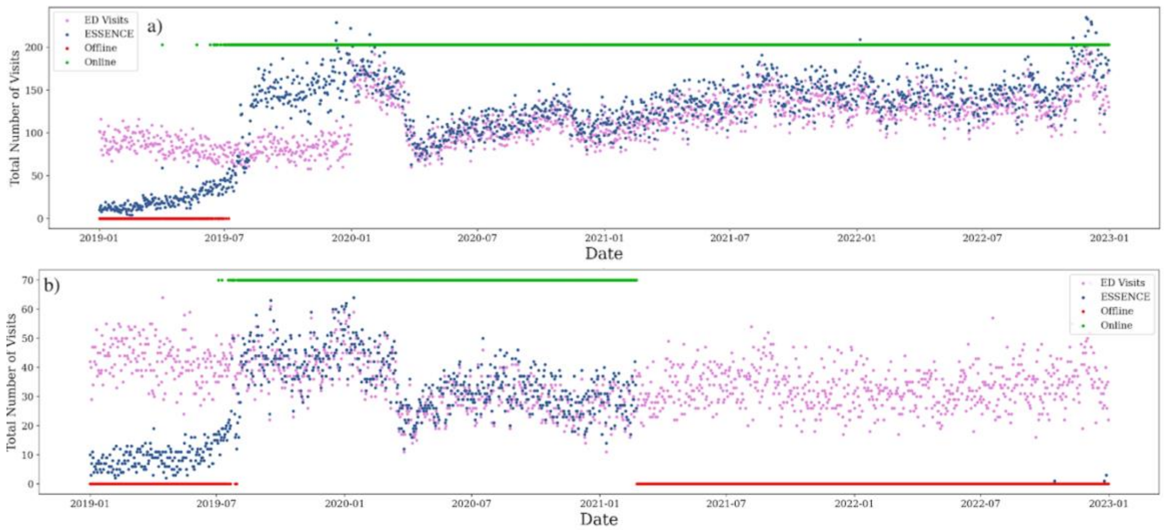

Figure A3.1. Total all-cause emergency department visits (pink) and syndromic surveillance reports (blue) with the offline (red) and online (green) periods noted for the syndromic surveillance systems for two hospitals in NM.

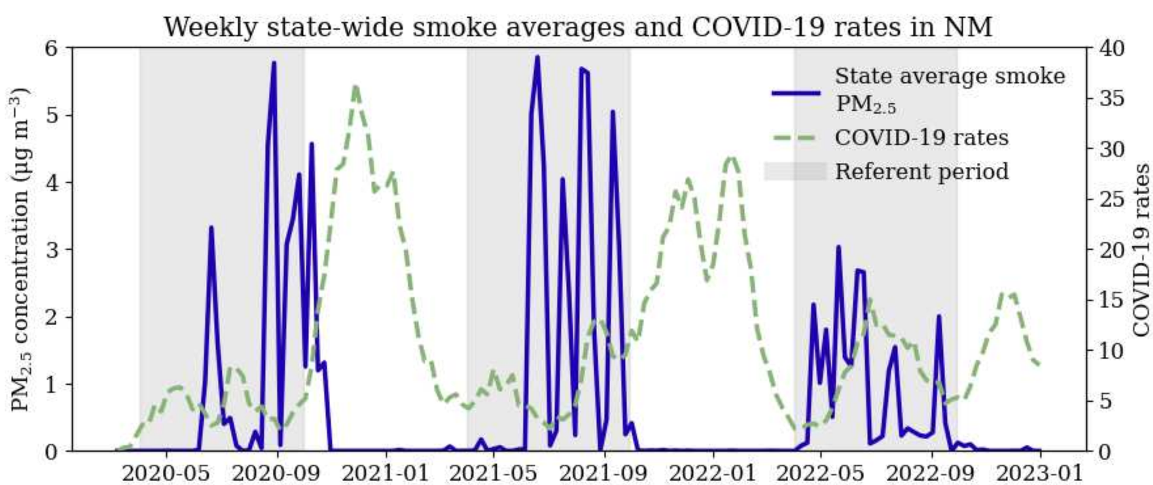

Figure A3.2. State-wide average smoke $PM_{2.5}$ concentrations from the O'Dell product (blue solid line; left y-axis) and COVID-19 rates (dashed green line; right y-axis) for NM from 2 March 2020 - 31 December 2023(CDC, 2025). Referent periods used in our study are shaded in gray.

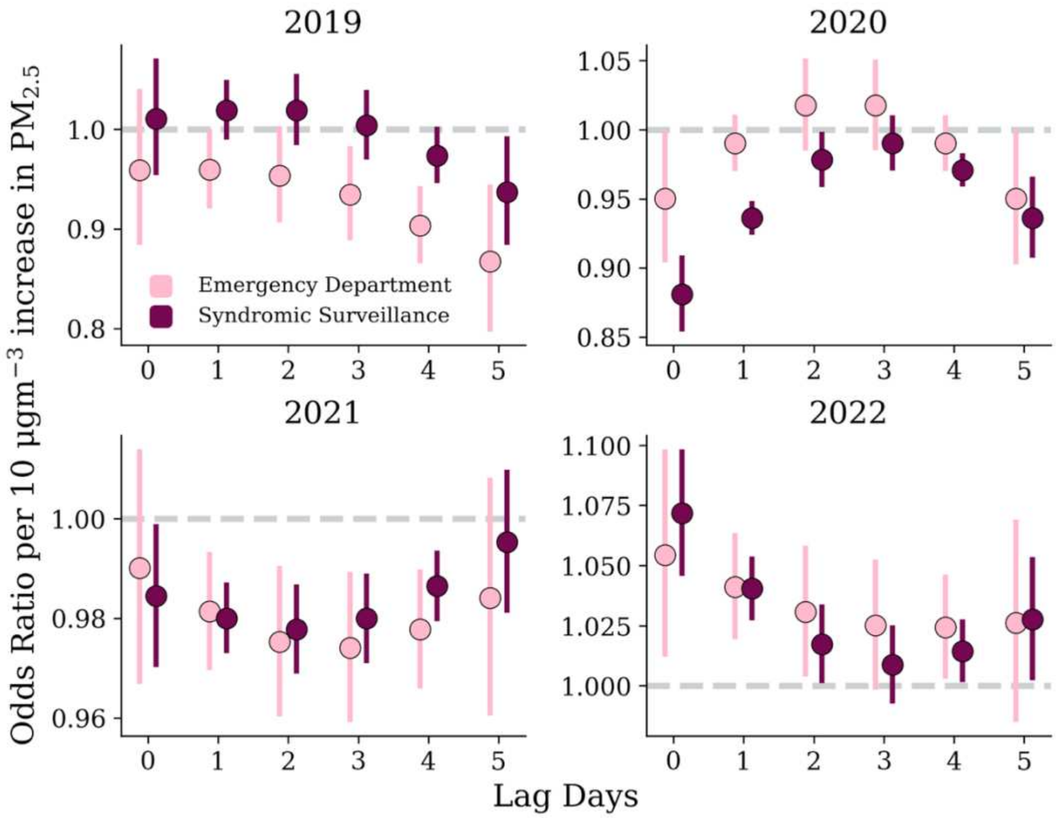

Figure A3.3. Distributed lag effects of a 10 µg m^{-3} increase of wildfire smoke $PM_{2.5}$ on likelihood of all respiratory-related emergency department visits (light pink) and broad-respiratory syndromic surveillance reports (dark red) for April - September for the years of 2019 - 2022.

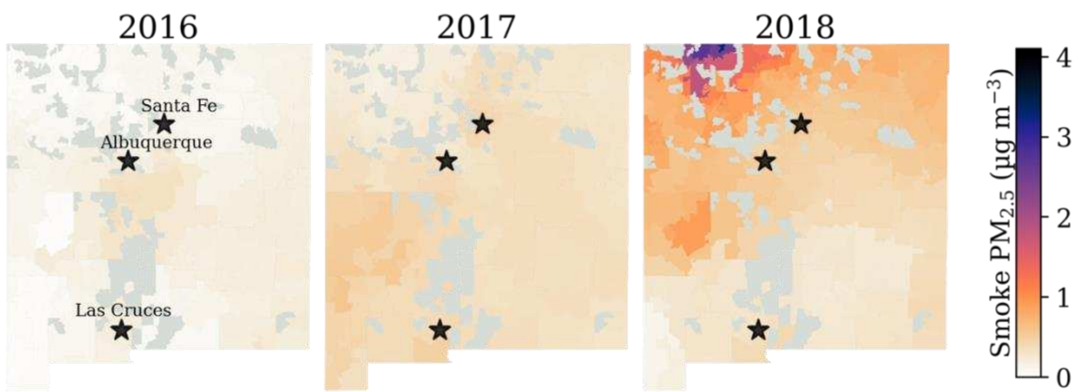

Figure A3.4. ZIP code average smoke $PM_{2.5}$ in New Mexico from 2016 - 2018 for April - September. Gray regions do not have a ZCTA code.

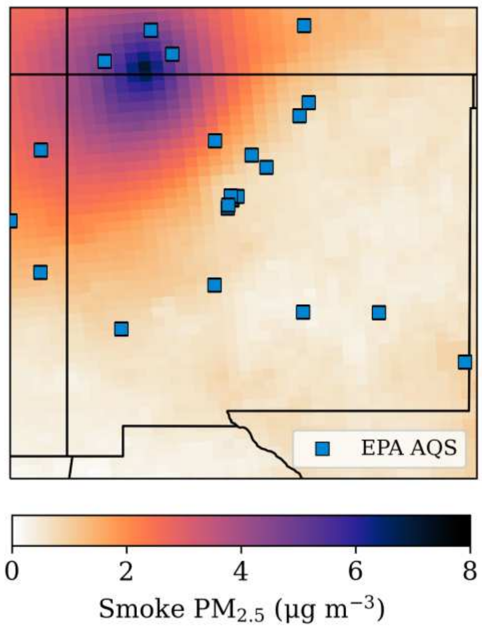

Figure A3.5. Gridded average smoke $PM_{2.5}$ in New Mexico for April - September 2018. $PM_{2.5}$ monitoring locations are represented by blue squares.

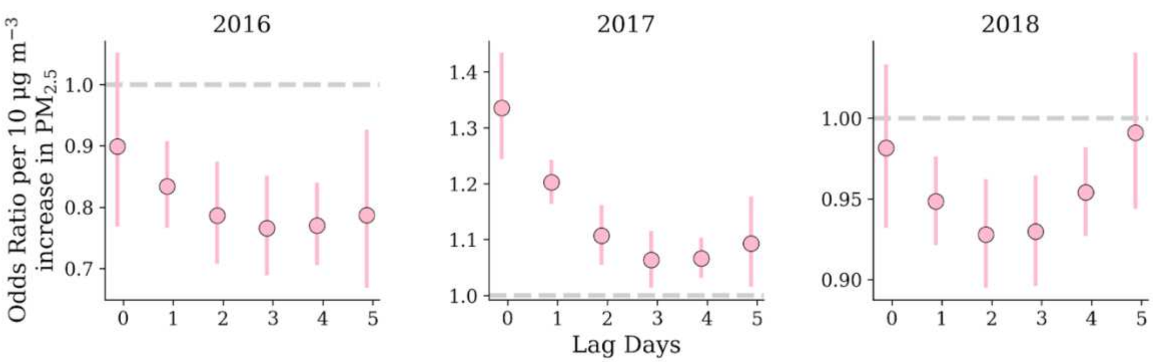

Figure A3.6. Distributed lag effects of a 10 µg m^{-3} increase of wildfire smoke $PM_{2.5}$ on likelihood of all respiratory-related emergency department visits for April - September of 2016-2018.